Vibration and capacitance coupling method for electrical contact evaluation

Schreiner, Zeljko

Award date:
2004

Awarding institution:
University of Bath

Vibration and Capacitance Coupling Method for Electrical Contact Evaluation

Submitted by

Željko Schreiner

for the degree of

Doctor of Philosophy in Electrical and Electronic Engineering

The University of Bath, UK
2004

Author's signature: 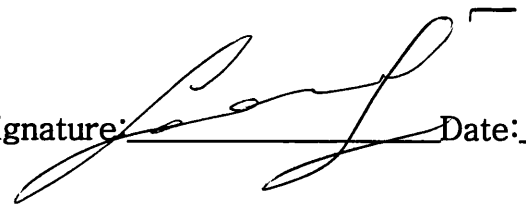 Date:_____

ProQuest LLC
789 East Eisenhower Parkway
P.O. Box 1346
Ann Arbor, MI 48106-1346

The University of Bath, UK

Abstract

VIBRATION AND CAPACITANCE COUPLING METHOD FOR ELECTRICAL CONTACTS EVALUATION

By Željko Schreiner

This thesis describes a new technique for electrical contact evaluation by which this method analyses broken or weak contact phenomena. By using capacitance coupling and measurement of the current change as detection of the contact states, this show the possibility to evaluate the contact states without using direct electrical contact measurement. This work is motivated by practical problems in the power utilities, concerned with weak or broken contacts, and with inappropriate tools for troubleshooting. In an endeavour to alleviate troubleshooting in electrical contact problems a proto-type diagnostic system has been developed. This prototype will be the base for the future product development. OMICRON electronics Company, the world leading advanced test equipment manufacturer for power utilities, will take the oportunity for the future product development.

Table of Contents

List of Symbols and Abbreviations

$C_{KG}(\rho F)$	Mutual Capacitance : Generator coupling electrode – Conductor
$C_{KM}(\rho F)$	Mutual Capacitance : Sensor – Conductor
$C_{KS}(\rho F)$	Mutual Capacitance : Screen – Conductor
$C_{GM}(\rho F)$	Mutual Capacitance: Sensor – Generator coupling electrode
$C_{SG}(\rho F)$	Mutual Capacitance: Screen – Generator coupling electrode
$C_{SM}(\rho F)$	Mutual Capacitance: Sensor – Screen
$V_G(V)$	Generator – Voltage
$I_M(A)$	Measured current
$\overline{Z}(\Omega)$	Contact Impedance
$C'_K = C_k / m$	Capacitance per meter length
$V_{AB}(V)$	Measured voltage
a(m)	Distance between conductor and generator coupler electrode
r(m)	Radius from cylindrical conductor
α(°)	Generator coupler electrode pitch
D(m)	Distance between generator coupler electrode and sensor
d(m)	Width of the screen
$r_i(m)$	Conductor radius

$r_a(m)$	Generator coupler electrode radius
DP	Delta peak
SF	Sensitivity factor
DPV	Delta peak value
PV	Peak value
DDS	Direct digital synthesis
HW	Hardware

* Hereafter, the term "coupler" will refer collectively to the generator coupler electrode and the sensor.

List of Figures

List of Equations

List of Tables

List of Appendices A

ACKNOWLEDGMENTS

I would like to express my sincere appreciation to Dr. Philip J. Moore for his supervision, professional support, advices and assistances in the preparation of this manuscript.

Additionally I would like to thank my wife Lela, for all her support and understanding.

Chapter 1

1. Introduction

Critical nodes in power systems are electrical substations. Whether they are generation, transmission or distribution substations, the basic tasks are always similar ie. controlling the energy flow, metering, measuring and protecting from electrical, mechanical and thermal faults.

Each electrical substation in a power system can be divided into two major parts: the primary part and the secondary part. The primary part is the body and the secondary part is the nerves of the electrical substation. The primary part is everything that is connected to the primary voltage level. The primary voltage level is the nominal power system voltage, which is usually standardised for each country (eg. 700 kV, 500 kV, 400 kV, 220 kV, 110 kV etc.)

Equipment that is working at the primary voltage level must be both mechanically and electrically constructed for this use. It will likely be prohibitively expensive or nearly impossible to

make all the substation equipment work only at the primary voltage level. This was the reason for the transformation of the primary values to lower levels using current and voltage transformers (CT & VT) and for the connection of measurement and protection equipment to this level. Furthermore, auxiliary (almost always DC from a separate battery) voltage for controlling, signalling and power supply is used in order to keep these important functions independent of the power system conditions.

The secondary part is understood to be everything that is working on the AC transformed side (secondary of CT/VT) or on the DC auxiliary side.

All secondary equipment is inter-connected using secondary terminals. In each electrical substation there are hundreds or even thousands of such terminals. Some of the standard secondary terminals are shown in the following figures:

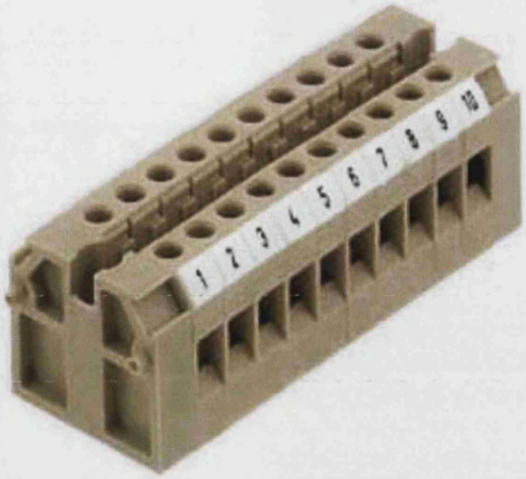

Figure 1 – Secondary terminals

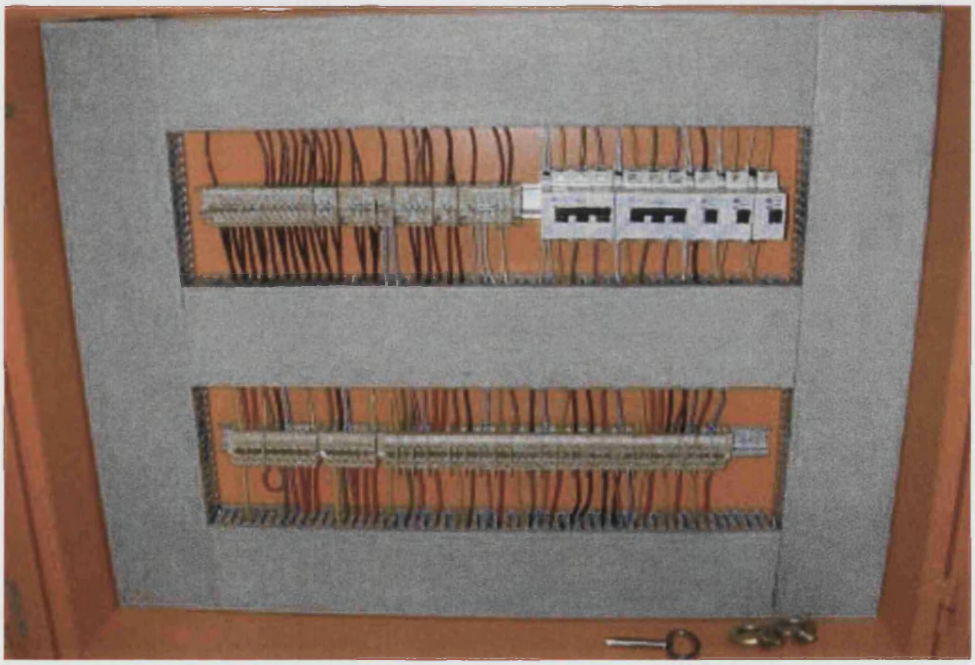

Figure 2 – Example of secondary terminals in the electrical switchgear

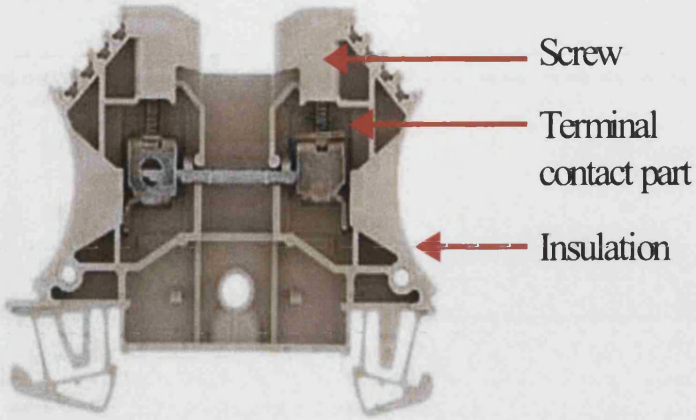

Figure 3 - Major parts of the secondary terminals

From the author's personal experience and the experience of colleagues, the single most common cause of operational problems is due to secondary terminals. A commonly heard phrase is "If something is not working, first have a look at the secondary terminals".

This problem was the original impetus to start thinking about a solution to help engineers troubleshoot secondary terminals.

1.1 Problem Description

If some equipment is not working in the electrical substation during commissioning, it is usually one of three major problems with secondary terminals:

1. Incorrect wiring (functional problems caused by incorrectly connected secondary terminals)
2. Broken contact (no contact at all)
3. Weak contact (random contact)

1.1.1 Incorrect Wiring

Incorrect wiring can be caused by two typical mistakes:

- The wiring work is done according to the connection plan but the connection plan is wrong
- The connection plan is correct, but there is a mistake in the wiring work

The following figure shows one example of incorrectly connected secondary terminals where "+" and "−" potential are exchanged.

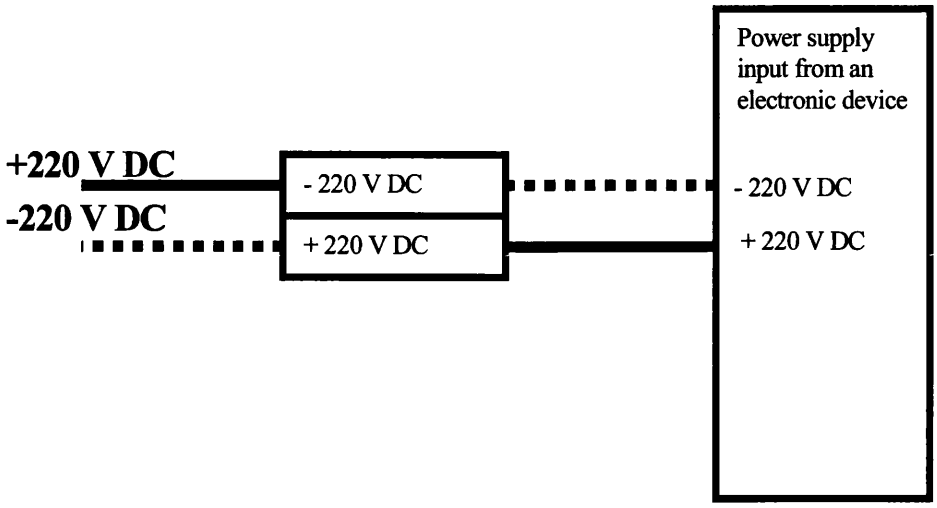

Figure 4 – Example of the incorrectly connected secondary terminal

As a consequence of the mixed/incorrect wiring at the secondary terminals, the connected electric device will not work and it may be damaged because the wrong polarity protection is missing.

Furthermore, if some logic circuits are incorrectly wired, the consequence will be wrong functionality, for example, interlocking logic in a case of an interlocking circuits in a substation.

1.1.2 Broken contacts

Broken contacts at the secondary terminals occur when the electrical contact between two conductors connected in the

terminal is missing. In the following figure, some of the reasons for broken contacts occurring in practice are presented.

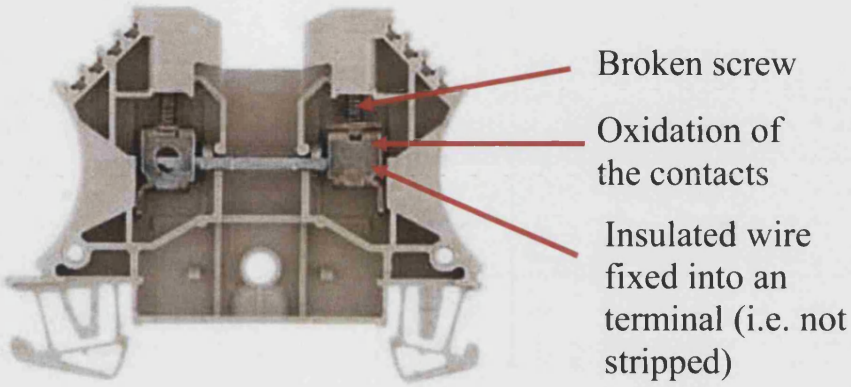

Figure 5 - Reasons for broken contacts

The most frequent practical cases where this error occurs are:

1. Production failures [1]
2. Insulated wire fixed in the terminal
3. Broken terminal screw
4. Broken cable-end connector
5. Incorrectly tightened terminal length bridge
6. Contact corrosion and tarnishing
7. Fretting and fretting corrosion
8. Contact aging

Practically broken contacts can be classified into two groups:

1. Broken contacts (contact failures) caused by human errors:

a. Production failures [1]

b. Insulated wire fixed in the terminal

c. Broken terminal screw

d. Broken cable-end connector

e. Incorrectly tightened terminal length bridge

2. Broken contacts (contact failures) caused by natural events:

a. Contact corrosion and tarnishing

b. Fretting and fretting corrosion

c. Contact aging

Contact failures caused by human error are well known problems to the operative people, but broken contacts caused by natural events require some better explanations.

1.1.3 Contact Corrosion and Tarnishing

Contact corrosion is one of the very serious reasons for contacts failure [2 - 7].

The closed electric contact has to perform its function of passing electric current reliably and with no change in its

contact resistance (R_c) for the duration of its life. The contacts have to perform this function even though the ambient atmosphere in which they reside contains pollutants which can cause the contact to tarnish or corrode.

The clean surfaces of many metals exposed to air oxidize quickly. The initial rapid reaction rate decreases as protective films are formed. The usual tarnish films formed in air at ambient temperatures are mostly composed of mixtures of oxides, sulphides, and chlorides as well as carbonates and sulphates. The majority of these films are insulating.

According to the literature [2, 3, 4] different types of corrosion and tarnishing phenomena exist:

- **Dry Corrosion**: occurs when a metal is exposed to an "oxidizing gas" such as oxygen or sulphur dioxide, no water film is necessary for this to take place.
- **Galvanic corrosion**: occurs when a thin layer of water is involved on the contact surface. This film can give rise to a phenomenon known as galvanic corrosion. Thin water film creates an electrolyte.

- **Pore Corrosion:** of connectors, using a thin layer of gold which is nearly always porous. If a thin layer of water in which ionisable dissolved gas is present, the galvanic cell results. The corrosion products are transported from the reactive base through a hole in plating to the contact surface.
- **Creep Corrosion:** occurs when a reactive substrate metal like silver or copper is in physical contact with a noble metal e.g. gold. The substrate metal corrosion products creep over the noble metal surface.
- **Electromigration:** phenomena that involve the transport of a metal across a non-metallic medium under the influence of an electric field. According to the reference [5] there are several kind of elctromigration:
    - **Metalic Electromigration**
    - **Electrolytic Electromigration**
    - **Dry Elctromigration**
    - **Humid Electromigration**

It may be questioned whether the term "corrosion" is most appropriate for the subject under discussion. This is due to the fact that this term often invokes images of strong visual effects; e.g. rusting of steel. This is dramatically different than the relevance of corrosion in the contact field which often involves the formation of thin, surface films

It is well established that thin films, even at thickness on the order of $< 1\times10^{-12}$ m may be virtually insulating. Corrosion films in this range are well below the limits of visual detection which may be in the range of $3-4\times10^{-12}$ m. In this case the user may often not perceive a corrosion problem.[4]

The corrosion of electrical contacts is driven by complex interaction of interacting variables [6, 7]:

- relative humidity
- reactive chlorides
- reduced sulphides (H_2S)
- air exchange rate
- humidity cycling
- linear velocity
- oxidizers (NO_2, O_3)
- sulphur dioxide

- temperature

Variable are listed in approximate order of decreasing importance.

1.1.4 Fretting (fretting corrosion) of Tarnish Films

Fretting corrosion is one of the most important failure mechanism for tin plated contacts and has been discussed in many publications [8 -18]. Many of these publications describe the mechanism of accumulation of oxidation products at the contact spot caused by so-called micro motions. This results in resistance spikes during motion as well as in an uncontrolled increase of the contact resistance in the longer term. [8]

Application of the contacts that are exposed to high vibratory and shock stress (i.e. automotive or sliding contacts) require the use of fretting protected connectors. Fretting corrosion is caused by a relative motion of mated contacts surfaces and results in contact failures.

Such contact applications can be found in industry switchgears and in power plants. Rotating machines (generators, electrical motors) produce mechanical vibration which is transmitted to

the contact systems and supports the development of fretting corrosion. Other example are automotive and railway applications.

Wiring connections are often made without previously liberating the contacting wires from their tarnish films, although these may be visible as a colour that is slightly different from the colour of the clean metal. According to the conventional experience it is taken for granted that these films, which actually are insulators when coherent, do not essentially disturb the conduction through the contact. However, the experienced conduction is not due to a proper quality of films but to the fact that they either become mechanically ruptured in some spots at contact make or are electrically broken down when enough voltage is applied. The breakdown considered is called *fretting*.[3]

Fretting is a kind of electrical breakdown different from the breakdown that operates with electron avalanches. When pure fretting appears in contact films, these are too thin for any form of avalanche breakdown. In an avalanche an electron must move through several volts (up to 10 V) between two opportunities to ionize. Fretting of previously insulating films has been observed at total contact voltage of one volt.

According to literature [9, 10] parameters that are significant influencing fretting corrosion are:

A: Fretting vibration frequency: at lower frequency, a fewer cycles are required to attain a given increase in contact resisatnce.

B: Wipe Distance/Slip Amplitude: Increasing of the wipe distance or slip amplitude results in a rapid escalation in the contact resistance which reduces connector life.

C: Normal Load: Higher contact load lengthens the period of stable and relatively low electrical resistance. A higher load reduces fretting sliding motions amplitudes and increase contact areas. However, severe wear and deformations may result if load is too high.

Fretting amplitude and contact force are dominant factors governing cycles to failure. [16]

Decreasing contact force and increasing fretting amplitude produce increasing contact degradation.

D: Electrical Load: Passage of current at low voltage during fretting has little effect on film formation and contact resistance. Contact resistance can be reduced if the voltage is sufficiently high to cause fretting of surface films.

E: Underplate , Substrate and Plating: protective plantings shield connector substrate metals from corrosive attacks and lengthen connector life.

F: Lubricants: can significantly improve the contact resistance of fretted electrical contacts by reducing rate of wear, dispersing frictional polymers, and shielding, the surface from the air, thereby retarding the formation of corrosive products.

G: Fretting Coefficient: can change according to the number of cycles.

Combination effects of fretting and corrosion greatly aggravates connection performance. According to the literature [11, 15] reduction of the contact compression force causes fretting at the contact interface. Tarnish films are contaminating contact surface. Consequently connection resistance increases and corrosion is accelerated. This finally causes failure of the contact. Reduced contact force (i.e due vibration) can accelerate fretting effects and corrosion that cause contact failure.

Fretting corrosion is widely known as a degradation mechanism in base metal contacts. The discovery of this as

a serious failure mechanism in metal contact systems dates back to 1911. [13]

1.1.5 Contact Aging

According to reference [19 - 22] the contact surfaces age from exposure to a variety of environmental conditions. Generally temperature, humidity and the concentration of corrosive substances promote the growth of non-conductive films on contact surfaces. In the reference [19] the Monte Carlo Method is the method used for simulating contact degradation. A Monte Carlo simulation of aged crossed rod copper contacts was conducted to evaluate the effects from a number of variables such as film thickness, contact force, micro hardness and geometry.

The deterioration and failure of an electrical contact in which good contact has been established usually involves a gradual reduction in the area of metallic contact at its interface. Eventually, this reduction can increase the constriction resistance and thus raise the local temperature in the contact region. This temperature rise accelerates the metallurgical and chemical deterioration processes, and further increases the

resistance and hence the local temperature. This leads to accelerate failure mechanism.

A broken terminal can be represented by the following figure:

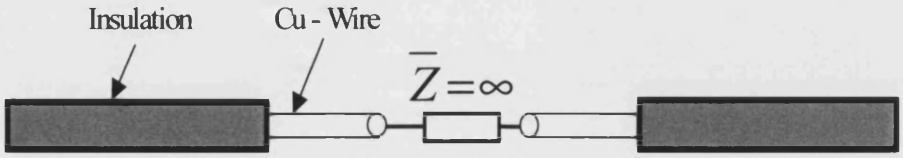

Figure 6 - Broken terminal

1.1.6 Weak Terminal Contacts

A special problematic case of terminal error is weak contacts. Weak contacts are random functions and are dependent on many different parameters. Temperature changes, mechanical pressure, mechanical resonance, and vibrations, etc., can cause one weak contact to change randomly between being conducting and to being insulating.

The following figure will show the most common practical reasons for weak contacts:

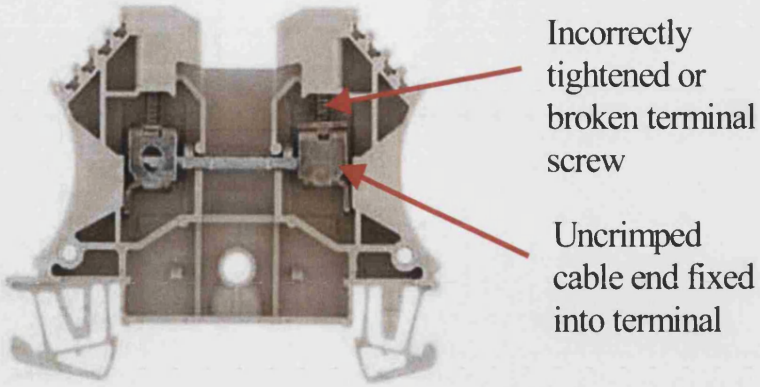

Figure 7 - Reasons for weak terminal connections

The most frequent practical cases where weak terminal contact can occur are:

- Production failures
- Incorrectly tightened terminal screw
- Broken terminal screw
- Uncrimped cable end fixed into terminal

1.2 Problem Analysis and Conclusions

Incorrect wiring is a problem that can be solved only by using manual investigation (trouble-shooting) of the connected circuits and this will not be part of the research.

The research will concentrate on the investigation of two other cases: broken contact and weak contact. Phenomena such as

contact corrosion or tarnishing will be investigated only in terms of causing broken contacts. A testing method that can be used without disconnecting the terminals will be a significant asset.

1.2.1 Problems Caused with Incorrect Terminals

Secondary electrical terminals connect many different circuits within electrical substations. Some of the typical functions include:

- Current circuits
- Voltage circuits
- Trip circuits
- Control circuits
- Interlocking circuits
- Signalling circuits
- Alarming circuits
- Information circuits
- Auxiliary circuits
- Power supply circuits, etc.

The loss of electrical contacts or weak contacts at the secondary terminals can be the cause of many problems and can be the cause of failures in the electrical substations.

For example, a broken contact in the current circuit (open-current circuits) can cause very high voltages to occur in the secondary terminals, which can be very dangerous for the personnel.

Some terminals are only in operation during some events, e.g., trip circuits. If the trip circuit fails, then the circuit breaker (CB) will not operate.

Many of the functions will not be in operation for several years (e.g., some signalling or alarm functions) but they are very important in case they are needed.

Usually many of the failures associated with broken or weak contacts at the secondary terminals will be found after failures or malfunctions (e.g., if no CB trips after protection is switched off). Such failures can cause power cuts which could implicate large economic losses.

Usually maintenance engineers detect such failures during troubleshooting. The problem is very simple: no contact through a secondary terminal or weak contact at the secondary terminal.

1.3 Scope of the Work

This work will focus on the secondary terminals in the electrical substations.

The research will concentrate on the investigation to find a testing method to detect broken or weak terminal contact without disconnecting the terminals, and without using direct contact electrical measurement. This will be a significant asset for faster troubleshooting in the electrical power system wiring.

The basic work will concentrate on finding theoretical methods that can be used for detection of broken or weak contacts at electrical terminals without disconnecting them. Furthermore this method will be the basis for designing small portable test devices, which will be used by the substations operational people for detection of the terminal contact problems. To design the test device, the following practical considerations must be taken into account:

- Simple use
- Light weight

- Low costs

The thesis will describe the research work as following:

CHAPTER 2: Investigation and description of the existing testing methods and published researches

---

CHAPTER 3: Presenting the idea of the thesis

CHAPTER 4: Theoretical investigations

CHAPTER 5: Mathematical modelling of the theoretical investigations

---

CHAPTER 6: Practical considerations – Theoretical MATLAB simulations

---

CHAPTER 7: Design of the experimental hardware solution

CHAPTER 8: Improvement of the experimental hardware solution

CHAPTER 9: Experimental work. Research of the testing method using practical measurements with a developed experimental hardware

---

CHAPTER 10: Further work and additional applications

CHAPTER 11: Conclusions

References Chapter 1

1. Effects of Manufacturing Processes on Contact Surfaces and Resistance; H.A. Francisco, K. Koeneke and J. Wallace; Conference on Electrical Contacts, 1990., Proceedings of the Thirty-Sixth IEEE Holm Conference,20-24 Aug. 1990; Pages:376 - 394.

2. "Electrical Contacts - Principles and Applications": Paul G. Slade; 1999; Marcel Dekker AG.

3. "ELECTRIC CONTACTS Theory and Applications"; R.Holm Fourth Edition; 2000; Springler-Verlag Berlin.

4. The Effect of Power on Low Frequency Fretting Corrosion; N. Stennett, J. Swingler; Conference on Electrical Contacts, 1993., Proceedings of the Thirty-Ninth IEEE Holm Conference, 27-29 Sept. 1993; Pages:205 - 210.

5. Metallic Elektromigration Phenomena; S.J.Krumbein; IEEE Transactions on Components, Hybrids, and Manufacturing Technology,;Volume: 11, Issue: 1, Year: Mar 1988; Page(s): 5-15.

6. A possible degeneration mechanism in stationary electrical contacts; R.S.Timsit; IEEE Transactions on Components, Hybrids, and Manufacturing Technology,; Volume: 13, Issue: 1, Year: Mar 1990; Page(s): 65-68.

7. Materials, Environment, Motion and Electrical contact Failure mechanism; W.H.Abbott; Conference on Electrical Contacts, 1989., Proceedings of the Thirty Fifth Meeting of the IEEE Holm Conference ,18-20 Sept. 1989.; Pages:3 - 11.

8. A Design Solution for Fretting Corrosion; P. van Dijk and F. van Meijl; Conference on Electrical Contacts, 1996., Proceedings of the Forty-Second IEEE Holm Conference; Joint with the 18th International Conference on Electrical Contacts, 16-20 Sept. 1996.; Pages:375 - 382.

9. Resistance Buildup in Electrical Connectors Due to Fretting Corrosion of Rough Surfaces; M. Bryant; Conference on Electrical Contacts, 1993., Proceedings of the Thirty-Ninth IEEE Holm Conference ,27-29 Sept. 1993.; Pages:178 - 190.

10. Assessment of Fretting Failure Models of Electrical Connectors; M.D. Bryant; Conference on Electrical Contacts, 1994., Proceedings of the Fortieth IEEE Holm Conference, October 17-19, 1994.; Pages:167 - 175.

11.Combination Effect of Fretting and Corrosion on Bolt_Type Power Connectors; Guo-Ping Luo, Liang-Jun Xu, Ji-Gao Zhang; Conference on Electrical Contacts, 2000. Proceedings of the Forty-Sixth IEEE Holm Conference , 25-27 Sept. 2000.; Pages:60 - 66.

12.Fretting Corrosion Degradation, Threshold Behaviour and Contact Instability; Robert D. Malucci; Conference on Electrical Contacts, 2003. Proceedings of the Forty-Ninth IEEE Holm Conference , 8-10 Sept. 2003.; Pages:2 - 15.

13.E.M. Eden W.N.Rose and F.L. Cunningham, Proc. Instn. Mech.Engrs. 1911.; 4 page 839.

14.Fretting corrosion of tin at elevated temperatures; A. Lee, A. Mao, and M. S. Mamrick; Conference on Electrical Contacts, 1988., Proceedings of the Thirty Fourth Meeting of the IEEE Holm Conference , 26-29 Sept. 1988.; Pages:87 - 91.

15.Effect of fretting on the contact resistance of aluminium with different contact materials; M.Braunovic; IEEE Transactions on Components, Hybrids, and Manufacturing Technology, [see also IEEE Trans. on Components, Packaging, and Manufacturing Technology, Part A, B, C] , Volume: 2 , Issue: 1 , Mar 1979.; Pages:25 - 31.

16.Impact of Fretting Parameters on Contact Degradation; R. Malucci; Conference on Electrical Contacts, 1996., Proceedings of the Forty-Second IEEE Holm Conference, Joint with the 18th International Conference on Electrical Contacts , 16-20 Sept. 1996.; Pages:395 - 403.

17.Intermittence Detection in Fretting Corrosion Studies of Electric Contacts; S. Murrell,S. L. McCarthy; Conference on Electrical Contacts, 1997., Proceedings of the Forty-Third IEEE Holm Conference on , 20-22 Oct. 1997.; Pages:1 - 6.

18.Corrosion Processes in the Development of Thin Tarnish Films; J.H. Payer; Conference on Electrical Contacts, 1990., Proceedings of the Thirty-Sixth IEEE Holm Conference and the Fifteenth International Conference on Electrical Contacts , 20-24 Aug. 1990.; Pages:203 - 211.

19.Making Contact to Aged Surfaces; R.D. Malucci; Conference on Electrical Contacts, 1992., Proceedings of the Thirty-Eighth IEEE Holm Conference, 18-21 Oct. 1992.; Pages:237 - 248.

20.The Ageing Physics of Electrical Contacts Subjected to DC Current; A. Oberg, R. Gustafson, O. Saksvvk, H. Stomberg, K.-E Olsson; Conference on Electrical Contacts, 1996., Proceedings of the Forty-Second IEEE Holm Conference Joint with the 18th International Conference on Electrical Contacts , 16-20 Sept. 1996.; Pages:189 - 194.

21.A Possible Degeneration Mechanism in Stationary Electrical Contacts; R. S. Timsit; Conference on Electrical Contacts, 1989., Proceedings of the Thirty Fifth Meeting of the IEEE Holm Conference, 18-20 Sept. 1989.; Pages:201 - 203.

22.Computer Modeling of Contact Degradation by Intermetallic Growth; A. Oberg,K. Olsson; Conference on Electrical Contacts, 1997., Proceedings of the Forty-Third IEEE Holm Conference, 20-22 Oct. 1997.; Pages:41 - 45.

Chapter 2

2. Existing Measuring Methods and Publications

The following chapter contains a literature research about existing measuring methods and publications. The literature research has focussed on following sources :

- Standard methods specific for power system applications
- IEEE Holm Conference on electrical contacts
- Journals
- Patent researches

2.1 Existing Technologies in Power System Applications

The most common technologies for contact evaluation in the described application include:

- Resistive method for contact resistance measurement [1-4]
- Contact thermal screening [5-9]

- Circuit monitoring systems [10-13]

2.1.1 Resistive Method for the Contact Resistance Measurement

One of the most commonly used methods for primary contact resistance measuring is the microohm Meter method (Pure Ohm's law method) [1-4]. The electron current that flows through any conductor is directly proportional to the potential difference between terminals.

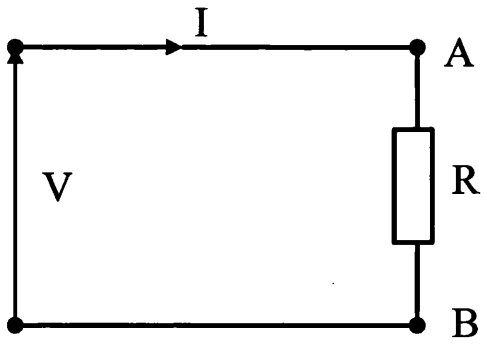

Figure 8- Ohm's law

$$V = R \times I \qquad I = \frac{V}{R} \qquad [1]$$

Equation 1- Ohms' law - Voltage-Current

The resistance of the conductor depends only upon the dimensions and the material of the wire and its temperature. It is entirely independent of V and I. This holds equally well whether the entire circuit is considered or if only a portion of the circuit is considered. When applied to a single conductor AB, the law states that the current flowing through the conductor is equal to the fall of potential between A and B divided by the resistance of this part of the circuit.

This elementary law is basic to the most used method for primary contact resistance measuring (Microohm meter test method). Applying DC current through the resistance (contact) and measuring the voltage drop, the result is calculated directly as:

$$R = \frac{V}{I} \qquad [1\text{-}3]$$

Equation 2- Ohms law - Resistance

From a practical point of view, this simple and traditional method is useless [2,3]. There is no practical possibility to apply DC current through the secondary contact and measure voltage. The measurement must be done during the standard

operational conditions of the terminals, and the wiring insulation must not be removed or destroyed (see figure below).

Additionally there are several hundreds, or even thousands, of terminals in the substation and testing would require an impossible length of time.

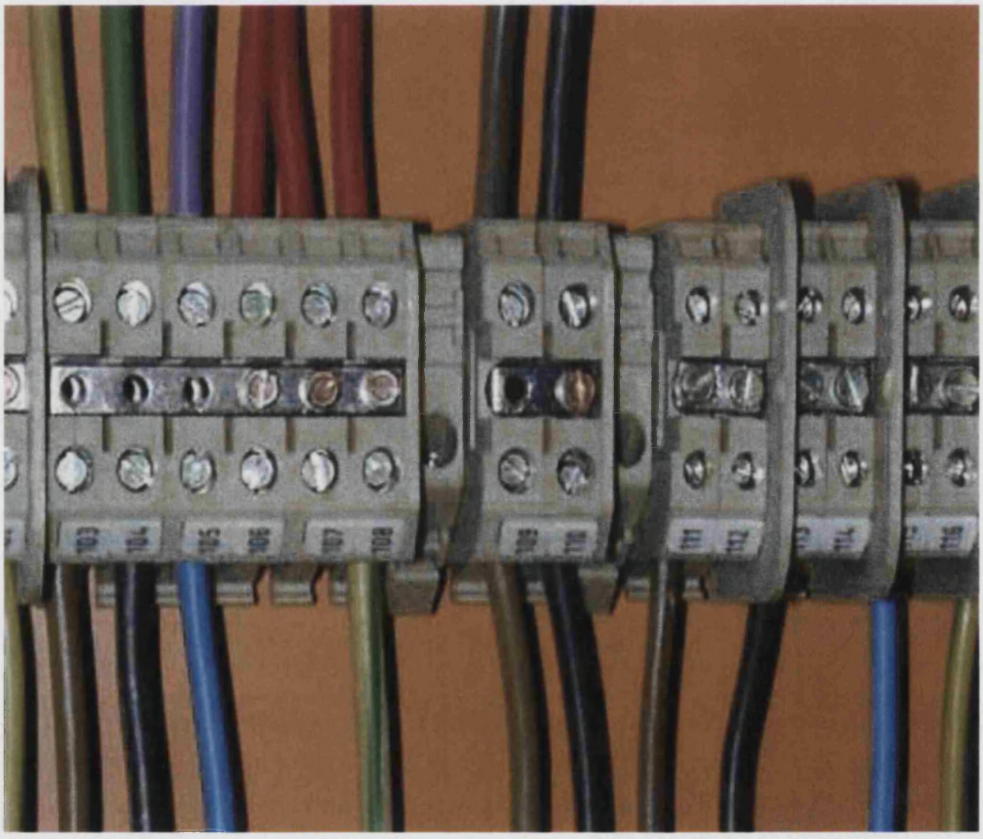

Figure 9 - Practical application problem for standard microohm meter method

2.1.2 Kelvin 4-Wire Resistance Measurement

A further often used test method for accurate contact resistance measurement is the Kelvin (4-wire) measurement method. This method is commonly used today for small resistance measurement [4] of primary contacts (ie. CB contacts).

The Kelvin method is used if the measurement of some resistance takes place a significant distance away from the ohmmeter. In this case the ohmmeter will measure all resistances in the circuit loop which includes the resistances of the wires. Such measurement is shown in the figure below:

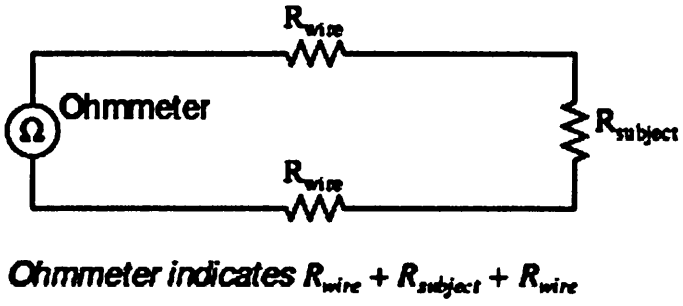

Figure 10 – resistance measuring with significant long measuring wires

Usually the wire resistance is very small but for the cases where $R_{SUBJECT}$ is very small the measurement error introduced by wire resistance will be substantial.

$R_{SUBJECT}$ as explained in the paragraph above (Ohm's law) can be measured in the following way:

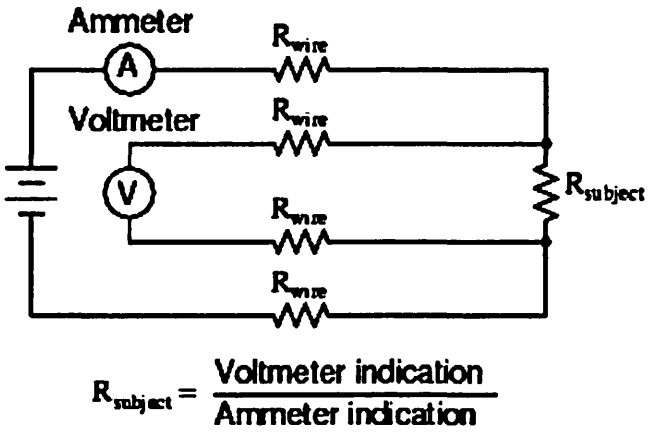

Figure 11-Kelvin 4-wire resistance measuring method

Special connecting clips called "Kelvin Clips" are made to facilitate this kind of connections across a subject resistance:

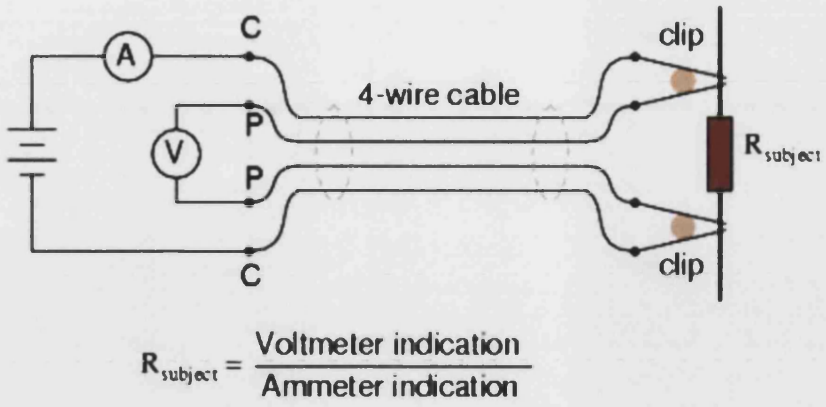

$$R_{subject} = \frac{\text{Voltmeter indication}}{\text{Ammeter indication}}$$

Figure 12: Kelvin Clips

In Kelvin Clips, the jaw halves are insulated from each other at the hinge points, only contacting at the tips where they clasp the wire or terminal of the subject being measured.

This described method can not be used for the application which is the topic of this research. The reason is the same as described before with the simple Ohm method: there is no easy possibility to connect the measuring apparatus to the measured resistance.

2.1.3 Infrared Screening Method - Thermography

One of the often used methods for electrical primary contact evaluation is infrared, screening. - thermography [5-9]. Thermography is the use of an infrared imaging and measurement camera to "see" and "measure " thermal energy emitted from an object. Infrared thermography cameras produce images of invisible infrared or "heat" radiation and provide precise non-contact temperature measurement capabilities. An infrared camera is a non-contact device that detects infrared energy (heat) and converts it into an electronic signal, which is then processed to produce a thermal image on a video monitor and perform temperature calculations.

Sir William Herschel, an astronomer, discovered infrared in 1800. He built his own telescopes and was therefore very familiar with lenses and mirrors. Herschel wanted to find out which colour(s) were responsible for heating objects. He devised an experiment using a prism, paperboard, and thermometers with blackened bulbs where he measured the temperatures of the different colours. Herschel observed an increase in temperature as he moved the thermometer from

violet to red in the rainbow created by sunlight passing through the prism. He found that the hottest temperature was actually beyond red light. The radiation causing this heating was not visible; Herschel termed this invisible radiation "calorific rays." Today, we know it as infrared.

The infrared screening method uses thermographic measurement of the contact over-temperature to detect contact problems. In the case of weak contacts the contact resistance increases, causing extra power dissipation and an increase in temperature.

This efficient testing method has very big limitations for the application on the secondary terminals in the electrical substations. The majority of the conductors in the terminals are potential-free (i.e., no current and no thermal radiation). Thermography testing (measuring) method is limited to the secondary terminals on the secondary circuits under load conditions only.

2.1.4 Circuit Monitoring Systems

For some very important functions, such as trip circuits, there exist special monitoring systems such as “Trip Circuit

Supervision". Trip Circuit Supervision is a monitoring system of the trip circuit based on the resistive method [10-13].

Such monitoring systems are controlled from the Trip Circuit Supervision Relays.

Some of the typical "Trip Circuit Supervision" schemes are shown in the figures below:

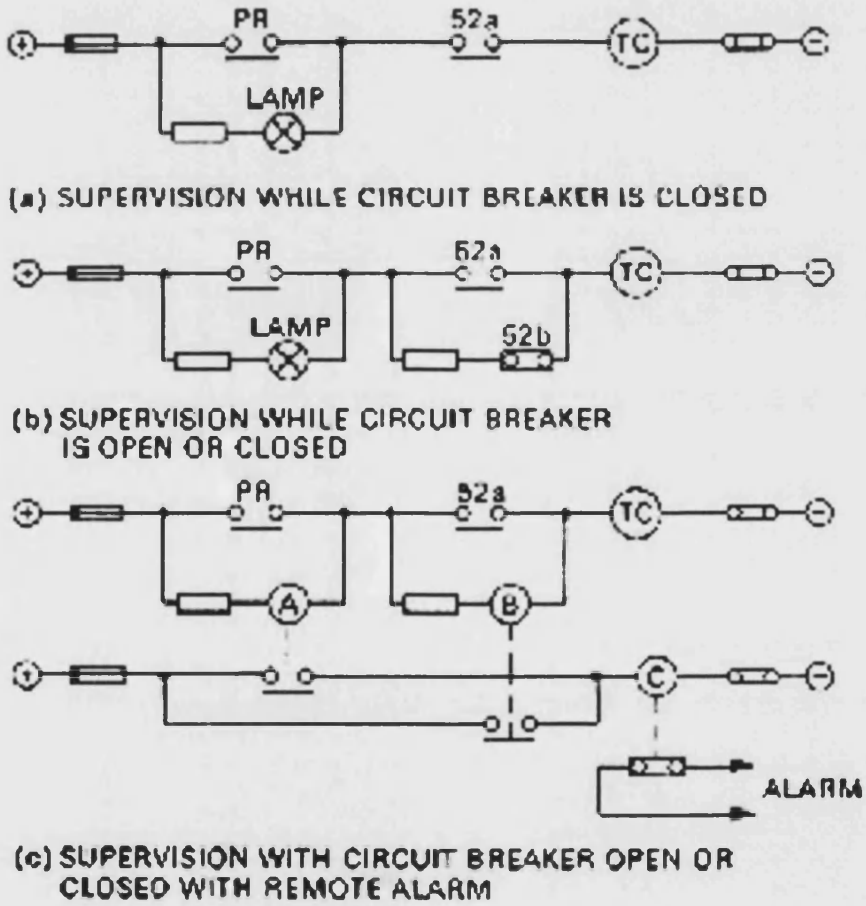

Figure 13: Trip Circuit Supervision – Basic schema [10]

The trip circuit extends beyond the relay through a considerable amount of circuit wiring with intermediate terminal boards.

The simplest arrangement contains a healthy trip lamp, as shown in Figure 13 (a). This provides supervision while circuit breaker is closed.

Figure 13 (b) shows how, by the addition of a normally closed auxiliary switch and a resistance unit, supervision can be obtained while the breaker is both open and closed.

Both schemes described above are suitable for locally controlled installations, but when control is exercised from a distance it is necessary to use the relay system which is shown in the Figure 13 (c).

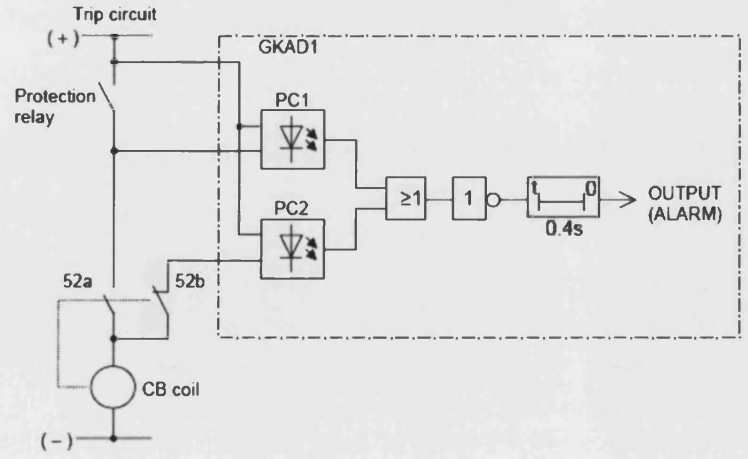

Figure 14: Trip Circuit Supervision – Example [11]

In the example presented in the Figure 14 the relay GKAD1 monitors continuity of the trip circuit including CB coil. When the trip circuit is complete, a small current flows in photo-couplers PC1 and/or PC2, the circuit breaker auxiliary contacts and the trip coil. This current flows for both the breaker open and closed conditions. If the trip circuit supply is lost or if connection becomes open circuit then the relay GKAD1 issues a "Trip Circuit Fail Alarm" [11].

Such monitoring systems are very expensive and they are not common solutions for all substation functions other than circuit breakers. A further disadvantage of these monitoring systems is that they are not detecting what (or who) caused problem, they are just detecting that there is a problem in the circuit (broken circuit).

A second disadvantage of these monitoring systems is very difficult detection of the weak contacts. A circuit monitoring system does not give reliable results with the weak contact phenomena.

2.2 Holm Conference

The internationally recognised association for the phenomena of electrical contacts is the Holm Conference [14]. Since 1953 about 2600 conference papers have been published.

The Holm Conference began in 1953 as a forum for the discussion of electrical contact phenomena and related fields. In 1968, the conference was named the Holm Conference in honour of Dr. Ragnar Holm. Dr. Holm, whose contributions to the field of electrical contacts spanned 50 years and form the foundation of the electrical contacts field, was the inspiration and guide of the Conference from its inception until his death in 1970. In 1985, IEEE society started sponsoring the conference as recognition of its importance in the field of electrical engineering. In addition to the Annual Conference, the Conference Organization regularly conducts an intensive one-week course on contacts and participates in the biannual International Conference on Electrical Contacts [14].

Usually the conference proceedings are grouping publications on the different technical directions and themes including:

- High current
- Low current

- Relays
- Automotive
- Degradation
- Fundamentals
- High frequency
- Connectors
- Power connectors
- Sliding contacts
- Others

Beside fundamental research, the majority of the publications are investigating applications in electronic and microelectronic contacts. The majority of the references from the Holm Conference are related to laboratory research. The theme of contact resistance measurement is a widely researched topic in several publications within the Holm Conference.

2.2.1 Holm Conference – Contact Resistance

Contact resistance belongs to the most important phenomena in the field of electrical contacts. Measurement of the contact

resistance and research of finding new methods for determination is the topic in many of the papers on the Holm Conference. In this section several interesting publications on contact resistance have been analysed [15-20]. The applicability of these references are more related to the general understanding of the complexity of the contact resistances phenomena. The methods and technologies presented in the references [15 - 20] are all related to laboratory research.

Basically three different resistance phenomena are analysed in these references:

- Static Resistance/Conductance
- Dynamic resistance
- Constriction resistance

Static resistance is generally used to measure the states of the electrical contacts. This is the value of the contact resistance without time or other variable dependency.

Contact phenomena are dependent on several dynamic conditions, i.e. environmental or weak contact phenomena. Such phenomena require analysis of the dynamic behaviour of the contacts (dynamic contact resistance). Such analyses are

presented in several references [16 – 18]. Dynamic contact is the topic which is widely investigated in the relay contacts. As the main topic of this thesis is evaluation of the terminal contacts, an understanding of dynamic contact resistance is important within the investigation of the weak contact phenomena.

The measurement of electrical resistance is performed in order to characterize the interface between two metallic bodies. The resistance can be expressed as the following sum, when contact interface films (surface of the contact area) are ruled out [19,20]:

$$R_m = R_b + R_c \qquad [19]$$

Equation 3: Interface resistance

R_b - Corresponds to the region of the constant current density

R_c - Corresponds to the region of the region of the variable current density

R_c is called the constriction resistance. Constriction resistance gives information about contacting surface of the multi-spot contacts. Constriction resistance arises in electrical interfaces because contact is made as discrete spots as defined by the

surface roughness and contact pressure. Holm [3] developed the following expression of the constriction resistance between two conducting half-spaces separated by a circular constriction:

$$R_c = \frac{\rho}{2a} \qquad [3]$$

Equation 4: Constriction resistance

$\rho(\Omega m)$ - Electrical resistivity of two conductors

$a(m)$ - Constriction radius

It maybe be questioned why the equitation [4] contains the factor $1/a$ instead of $1/a^2$. The following simple consideration gives the answer. An electric resistance varies in proportion to a length and in inverse proportion to a cross-section. The dominating part of the constriction resistance is found in the neighbourhood of the contact surface. The order of magnitude is for its length a and for the cross-section a^2; thus the factor in the equitation is: $a/a^2 = 1/a$ [3]

Expression was derived under the assumption of the DC current.

As was stated before the analyses and explanations above are used for better understanding of the complexity of the contact

resistance phenomena. The usage of the references in terms of the application which is topic of this thesis is very limited.

2.2.2 Holm Conference – Noise analyses

Some research groups have investigated contact phenomena by the use of noise analysis which is one of the interesting methods for detection of the contact failures [21-23]. In these references, it is cliamed that current noise measurement can be used as new technique for predicting time to failure. It is further claimed [22] that the main advantage of the noise measurements are that the tests are less destructive, faster and more sensitive than DC measurements. Such a technique is most used in the "accelerated life tests" and in the contact reliability analyses [22].

One of the interesting references which uses noise spectral analysis is the work from the University of Florence, Italy [23]. This application is focused on electronic connectors.

Testing methods can be meaningfully viewed from the electronic perspective, treating the connector as “black box”.

In this sense, a research has been developed based on the contact resistance measurements and spectral analyses of the voltage drops while passing d.c. current when the contact is activated in its typical working condition and is subjected to mechanical vibrations and to thermal fatigue. The research analyses the phenomena of contact resistance increase due to thermal fatigues, humidity, oxidation and vibration influences. This is especially true with the circuits which are handling low voltage analogue signals that are very sensitive to even slightest increase of the contact resistance. A special focus of this work is investigating the mechanical vibrations influence on the contact quality. The comparison of the contact resistance in static and dynamic condition defines the technique of evaluating the electrical functionality of a connector in dynamic condition by means of noise measurement based on experimental verifications.

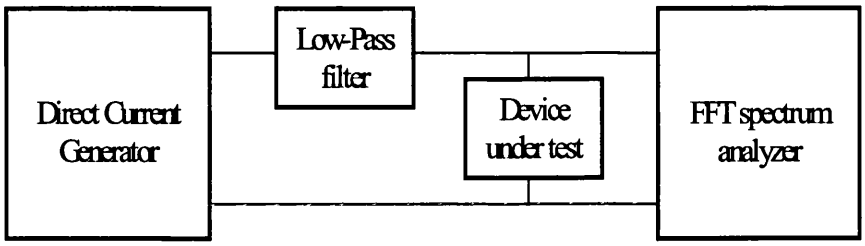

Figure 15 – Measuring circuit – Noise spectral analyses

Spectral analysis of contact voltage drop while passing d.c. current during the application of sinusoidal vibration provides a sensitive method of contact damage detection and evaluation.

As can be seen, this method covers testing of the contact pattern damaging and it is not focused on the broken or weak contact phenomena.

The described research work investigates electronic modules and connectors as test objects. For such type of test objects accessibility to the electric contact does not present any problem, but the method can not be used for this specific application of the secondary terminals.

2.2.3 Holm Conference – Testing of the contact reliability and stability – Ultrasonic method

Ultrasonic describes mechanical waves propagated through matter at frequencies above the upper limit for the human ear, that is, above 16000 Hz. Ultrasonic is the technique which is used in non-destructive testing and quality control of bonds in electrical contact assemblies [24]. This method is used often in the process of the contact manufacturing. Basically two test methods (technique) are used:

- Pulse-echo or reflection technique
- Through-transmission technique

In both these methods, a beam of ultrasonic energy is directed into the test object. In the pulse-echo technique, the flaw or discontinuity in the test object is indicated by the energy reflected back to the receiving transducer. In the through-transmission technique, the discontinuity or flaw is detected by the attenuation or decrease in the transmitted energy caused by the discontinuity in the test object. Of these two methods, pulse-echo technology is most common widely used [24].

Since the ultrasonic method is relative, very careful calibration (fingerprint) of the test equipment using known reference standard defects is essential. Usually some other confirmatory tests (destructive methods) must be used for verification of ultrasonic data. For this reason the described methods have only limited use in the application which is the topic of this thesis.

2.3 Methods based on contactless capacitive coupling

Within all the literature research, the most useful references have been found in the patent documentations (United States Patent).

In several patent publications the need for a contactless measuring method was stated [25 - 32]. These show that an electromagnetic field can be used to inject the measuring signal, without metallic contact, into the tested material.

The following two patent documentations have been selected as the references which are most interesting for this thesis:

- Process for Contactless Measurement of the Electrical Resistance of a Test Material [31]
- System and Method for Accurate Contactless Measurement of the Resistivity of a Test Material [32]

2.3.1 Process for Contactless Measurement of the Electrical Resistance of a Test Material [31]

This paper describes a very interesting method (system) which claims to accurately measure the resistivity of a material via capacitive coupling without contact with material. This invention generally relates to a system and method for contactless measurement of the electrical resistivity ρ (resistivity per unit area of material (Ω/m^2); inverse of conductivity) of any material encapsulated, contained, or otherwise isolated by a substantially dielectric material via capacitive coupling using RF electromagnetic energy. Basically the invention came about to measure characteristic of commercial product performance. As examples, there is detection of contamination level of industrial fluids, water, liquid lubricants, and solvents, determination the amount of one

substance within another, such as the quantity of fat, salt, or water, in food. In the following figure the principle of the described system is presented:

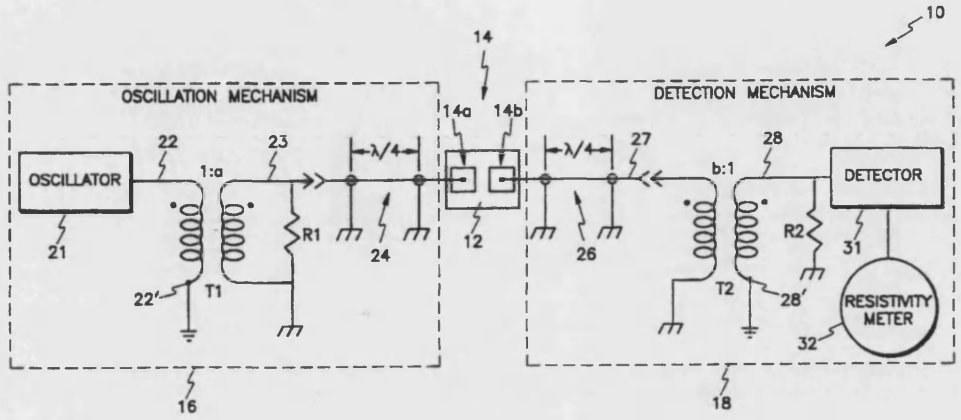

Figure 16: System and method for contactless mesurement of the resistivity of a test material [31]

- 10 – System
- 18 - Detection mechanism
- 16 – Oscillation mechanism
- 21 - Oscillator
- 12 – Measured material
- 14a – Transmission electrode
- 14b – Reception electrode
- T1 - Transformer
- 24 – Quarter-wavelength stub in oscillation section
- 26 - Quarter-wavelength stub in detection section

- 22 – Periodic signal
- 31 – Detector
- R1 – Termination resistor
- R2 - Termination resistor

The system 10 comprises an oscillation mechanism 16 connected to the transmission electrode 14a, and detection mechanism 18 connected to the reception electrode 14b. The oscillation mechanism 16 has an oscillator 21 for providing sinusoidal signal 22, having predetermined frequency f to the transformer T1. Quarter-wavelength stub ($\lambda/4$)is connected between transformer T1 and the transmission electrode.

The detection mechanism 18 has a quarter-wavelength stub ($\lambda/4$)connected between transformer T2 and reception electrode. A detector 31 receives the resistivity RF signal 28 and rectifies or detects the envelope of the RF signal and produces a DC level that is directly proportional to the resistivity. It is claimed that the accuracy of the resistivity measurement of 5% can be reached.

A basic capacitance technique is used to transmit and receive energy to and from material. The capacitance coupling is performed with the VHF (very high frequency) signal range

approximately 155.5 MHz. VHF signal is selected because they readily penetrate through dielectric materials.

As can be seen in this reference focus was on measurement of the resistivity per unit area of the material (Ω/m^2). This interesting measurement method can not be used for the application which is topic of this thesis for the following reasons:

The method uses one transmission and one receiving coupler (electrodes). Using this method together with the application which is the topic of this thesis the following will occur:

- 16 – VHF generator
- 18 – Detector
- 12 – Material under test
- 14a – Generator electrode
- 14b – Detector electrode

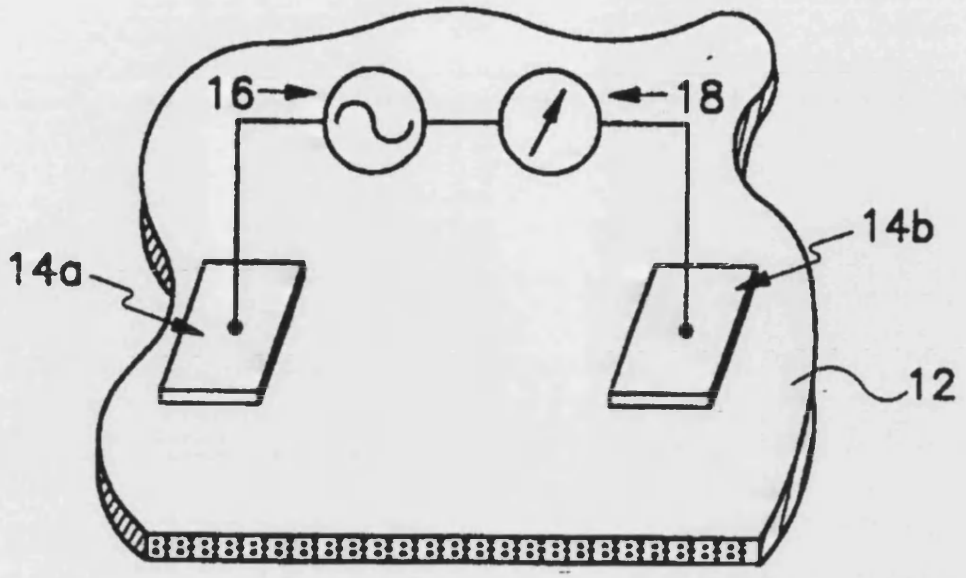

Figure 17: Basic principal of the measurements of resistivity per unit area of material using high frequency (155.5 MHz) signal

Using the described principle is possible to measure resistivity per area unit of the material using VHF signal and capacitive coupling.

Further the measurement of the terminal contact resistance can be approximate with following figure:

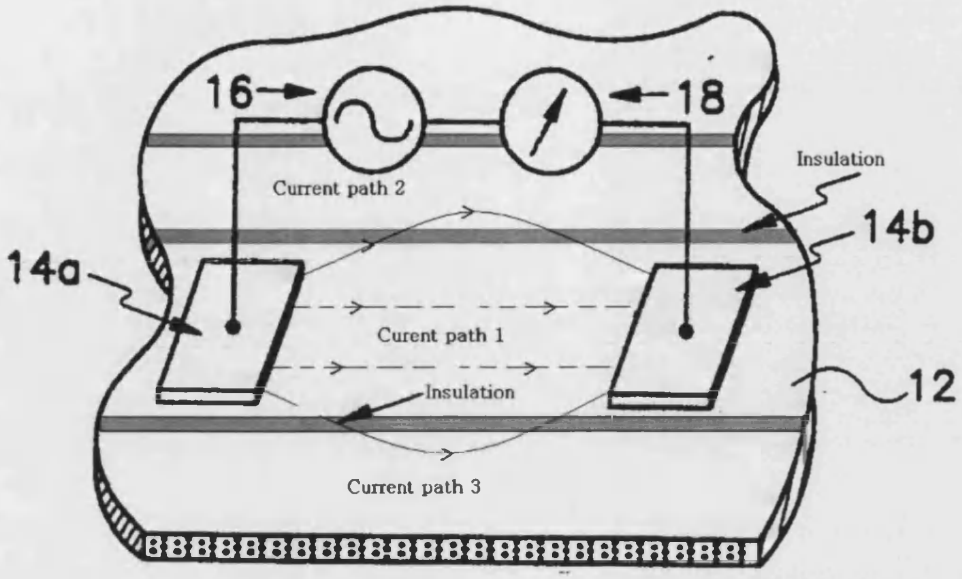

Figure 18: Approximation of the solid contact resistance measurement with conductors placed close to each other

As can be seen in the figure above with presented system, the resistance per area of the test material (Ω/m^2) will be measured but, it will not be possible to measure the resistance in "Current path 1" only (bordered with insulation) (Approximation of several conductors which are placed close to each other).

Broken contact condition can be approximated within following figure:

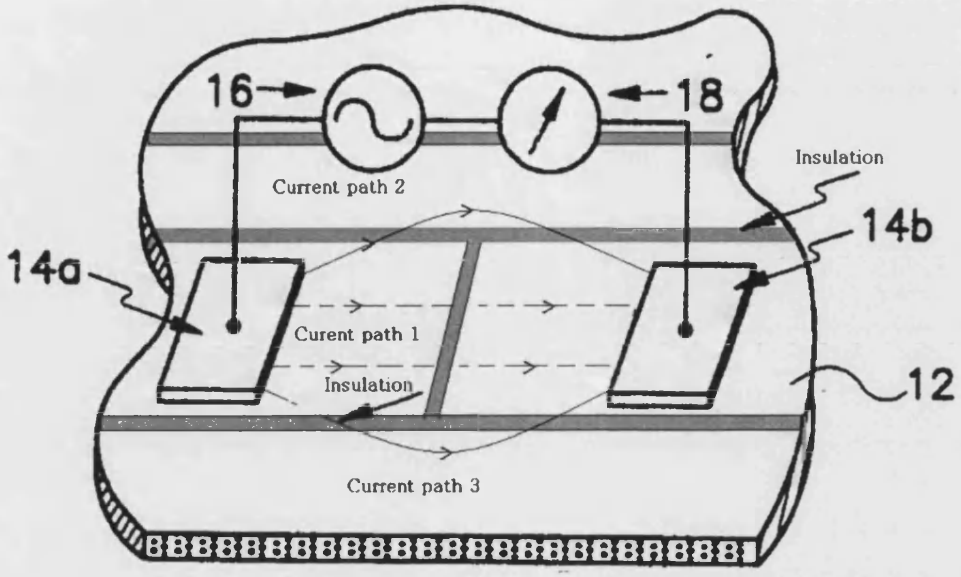

Figure 19:Aproximation of the broken contacts resistance resistance measurement with conductors placed close to each other

Using a frequency of 155.5 MHz the generated signal will penetrate through insulation from neighbouring conductors, through the metal plate below the conductors or through very small insulation level (distance) of the broken contacts. Current will, as known, select the path of least resistance and distinguish between the cases shown on the Figure 18 and 19 will not be possible with this system.

Although this method looks very similar to the topic of this thesis, the methodology and technology used are quite different.

A system which is capable of measurements in the application of solid and broken / weak contacts must have the following improvements:

- Used frequency in the method was 155.5 MHz. Such VHF frequency will readily penetrate through dielectric material and the ohmic path will be closed through neighbouring terminals. A lower frequency must be selected to avoid influence of the system (it is estimated that the frequency should be below 5MHz)
- Special shaped couplers for more focused capacitance coupling must be used
- Influence of the parallel load, next bay conductors or back metal plate will make this method useless. The use of one transmit and one receive electrode will cause problems if the contact is broken. The current will flow through other conductors or through other neighbouring terminals. Separate circuits for measurement (detector) and generator must be used. In a case of broken contact current will flow through measuring circuits (very low resistance) and not through the neighbouring conductors/terminals.

- The method measures resistance per unit of area of the material (Ω/m^2) and not resistance between two couplers and the method prefers the use of a flat material.

2.3.2 System and Method for Accurate Contactless Measurement of the Resistivity of a Test Material [32]

The reference [32] describes process for contactless measurement of the electrical resistance of preferable flat material in which an alternating current is capacitively coupled into the test material with the help of two electrodes. The total impedance is measured using at least three different frequencies, and from that measurement, the stray capacitance between two couplers and the test material, as well as the resistance of the test material is determined. This invention is focused on the application for controlling windshield wipers of a motor vehicle. The claim of this paper is that this method is more accurate as other methods for contactless resistance measurement.

The following figure shows the equivalent circuit diagram on which the process of measurement is based.

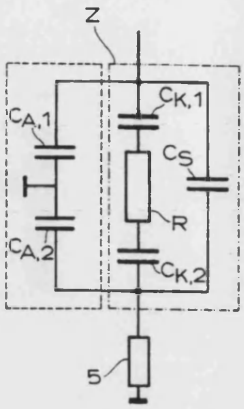

Figure 20: Equivalent diagram

- R – Electrical resistance of the test material
- C_K,1 & C_K,2 – Coupling capacitances between coupler and test material
- C_S – Stray capacitance between coupler electrodes
- C_A,1 & C_A,2 – Decoupling capacitances
- 5 – Measuring resistances

The following equations result from the above equivalent circuit diagram:

$$Z = \frac{\omega^2 R C_K^2 - j\omega(C_S + C_K + \omega^2 R^2 C_S C_K^2)}{\left(\omega^2 R C_S C_K\right)^2 + \omega^2 \left(C_S + C_K\right)^2} \quad [32]$$

Equation 5: Total impedance Z

Z - Total impedance

C_S - Stray capacitance

C_K - Coupling capacitance

R - Resistance

$$X_I = -\frac{C_S + C_K + \omega^2 R^2 C_S C_K^2}{\omega^3 R^2 C^2{}_S C^2{}_K + \omega(C_S + C_K)^2} \qquad [32]$$

Equation 6: Imaginary part of the total impedance

X_I - Imaginary part of the total impedance

$$X_R = \frac{RC_K^2}{(\omega R C_S C_K)^2 + (C_S + C_K)^2} \qquad [32]$$

Equation 7: Real part of the total impedance

X_R - Real part of the total impedance

According to the invention, in a first step the imaginary part X_I of the total impedance is measured with a high frequency (ω_1) alternating current and, from that measurement, the stray capacitance C_S is determined. In the second step, the imaginary part X_I of the total impedance is measured with a

low frequency alternating current from which the coupling capacitance C_K is determined. Finally, the real part X_R of the total impedance is measured with an alternating current of a frequency lying between the high and the low frequency. Further resistance R of a test material can be determined. Frequencies used in this method are in the range between 200 kHz and 5 MHz.

The following equations are used for the determination of the resistance. The equations are based on the assumption that $\omega_1 > \omega_2 > \omega_3$.

$$C_S \approx (\omega_1 X_I)^{-1} \qquad [32]$$

Equation 8: Approximation of the stray capacitance

$$C_K \approx \frac{1}{\omega_3 X_I} - C_S \qquad [32]$$

Equation 9: Approximation of the coupling capacitance

$$R \approx \frac{1}{2\omega_2^2 X_R C_S}\left(1-\sqrt{1-\left(\frac{2\omega_2 X_R C_S (C_S + C_K)}{C_K}\right)^2}\right) \qquad [32]$$

Equation 10:Aapproximation of the resistances

The main focus of the reference described above is the accuracy of the material resistance measurement. The application and method is suited to the measurement of the resistance of the flat test material. The reference is interesting for this thesis since it uses a contactless capacitive coupling method. The following disadvantages of described method relevant to the application which is topic of this thesis can be listed:

- Similarly to reference [31], the influence of the parallel load, next bay conductors or back metal plate will make this method useless. Using one transmit and one receive electrode will cause problems if the contact is broken. The current will flow through other conductors or through other neighbouring terminals. Separate circuits for measurement (detector) and generator must be used. Hence, in the case of a broken contact, current will flow through the measuring circuit (very low resistance) and not through the neighbouring conductors/terminals.
- The method/device is designed for measurement of the resistances of a flat material with three electrodes (for three frequencies). Such device can not be used for application of the conductors and terminals.

- The system is complex and mathematically intensive in that it requires measurement and analyses of three different frequencies, phase and stray capacitance.
- The system has limited applicability

2.4 Summary about Publications-Researches

During the literature research it was discovered how little was published about the application which is the topic of this thesis. Through investigation and studying of many papers and publications it was very difficult to find something that was focused on the same application problem. Most useful references have been found in the patent literature. The application problem about terminal contact evaluation has not been written about in any references, but some very useful information and experiences have been found in other application areas.

The literature research showed that the following problems related to the application of this thesis are not solved and require some new approaches:

- Economically acceptable, accurate contact condition evaluation
- Method which is supporting a simple, low cost, portable test device
- Weak contact phenomena can be very difficult to detect
- For referenced capacitive coupling methods, the use of only one electrode pair will be inadequate in this application

References Chapter 2

1. A. W. Smith & M. L. Wiedenbeck " Electrical Measurement" McGraw-Hill Book Company, Inc. New York, Toronto, London 1959

2. "Electrical Contacts - Principles and Applications": Paul G. Slade; 1999; Marcel Dekker AG.

3. Electric Contacts Theory and Applications; R.Holm Fourth Edition; Springler-Verlag Berlin 2000

4. "Kelvin (4-Wire) Resistance Measurement"; www.allaboutcircuits.com ; Accessed on 02.03.2004.

5. "Infrared Theory"; www.infra-red.hypermart.net ; Accessed on 02.03.2004

6. "How Thermal IR Imagers Work"; www.infra-red. hypermart .net; Accessed on 02.03.2004

7. "Infrared Thermography as a Diagnostic Tools in Power Engineering"; www.power-engineering.co.uk.com ; Accessed on 02.04.2004.

8. " Improving Electrical System Reliability With Infrared Thermography"; www.infraredelectrical.com; Accessed on 02.04.2004.

9. A Diagnostic System for Live Electrical Joints in Power Transmission Systems; R.-D. Rogler, H. Lobl; Conference on Electrical Contacts, 1996., Proceedings of the Forty-Second IEEE Holm Conference, Joint with the 18th International Conference on Electrical Contacts ,16-20 Sept. 1996.; Pages:173 - 179

10. "Protective Relays Application Guide";March 1995 GEC ALSTHOM T&D PROTECTION & CONTROL limited St.Leonards Works Stafford ST17 4LX England.

11.Trip Circuit Supervision, GKAD1 Relay; www.tmd-d.com; Accessed on 02.03.2004.

12.Trip Circuit Supervision, MRA1 Relay; www.tmd-d.com; Accessed on 02.03.2004.

13.Trip Circuit Supervision for M-family Relays; GE Publication No. GET-8465A

14.Holm Conference on Electrical Contacts; http://www.ewh.ieee.org/soc/cpmt/tc1/h2001int.html; Accessed on 18.03.2004;

15.A System for analyzing contact resistance; G.J.Russ; IEEE Transactions on Components, Hybrids, and Manufacturing Technology,[see also IEEE Trans. on Components, Packaging, and Manufacturing Technology, Part A, B, C] ,Volume: 2 ,Issue: 3 ,Sep 1979. Pages:317 - 320

16.A New Test Equipment For High Dynamic Real-Time Measuring of Contact Resistances. Frank Hübner-Obenland and Jürgen Minuth; Conference on Electrical Contacts, 1999., Proceedings of the Forty-Fifth IEEE Holm Conference,4-6 Oct. 1999 Pages:193 - 202

17.A Testing Instrument for Dynamic Contact Resistance; Li Wenhua, Li Zhigang; Electron Devices Meeting, 1999. Proceedings., 1999 IEEE Hong Kong ,26 June 1999 Pages:124 - 127

18.Study and Reliability Analyses on Testing Instrument for Dynamic Contact Resistance; Wen-hua Li, Cuo-jin Li; Conference on Electrical Contacts, 2000. Proceedings of the Forty-Sixth IEEE Holm Conference, 25-27 Sept. 2000 Pages:109 - 114

19.Constriction Resistance of a Multispot Contact: An Improved Analytical Expression; L. Boyer, S. Noel and F. Houze; Conference on Electrical Contacts, 1990., Proceedings of the Thirty-Sixth IEEE Holm Conference and the Fifteenth International Conference on Electrical Contacts ,20-24 Aug. 1990. Pages:646 - 650

20.Constriction Resistance at High Signal Frequency; J.D.Lavers, L.S.Timsit; Conference on Electrical Contacts, 2001. Proceedings of the Forty-Seventh IEEE Holm Conference, 10-12 Sept. 2001. Pages:167 - 174

21.Characterization of Probe Contact Noise for Probes Used in Wafer-Level Testing; A.M.Yassine, T.M.Chen, B.A.Beitman; IEEE Transactions on Electron Device Letters, Volume:12 ,Issue: 5 ,May 1991.; Pages:200 - 202

22.Noise as a Diagnostic Tool for Quality and Reliability of Electronic Devices; L.K.J.Vandamme; IEEE Transactions on Electron Devices, , Volume: 41 , Issue: 11 , Nov. 1994. Pages:2176 - 2187

23.Connector Reliability Testing: Noise spectral analyses M.Catelani, G.Luciano, A. Zanini Univerity of Florenz - Italy; Electro International, 1991 , April 16-18, 1991 Pages:636 - 641

24.Nondestructive Ultrasonic Inspection of Braze Bonds in High Current Electrical Contact Assemblies; R.I.Bukley, K.R. Komey, P.V.Popat; IEEE Transactions on Parts, Hybrids, and Packaging, , Volume: 8 ,Issue: 1 ,Mar 1972.; Pages:26 - 34

25.Contactless Facilities for Determining The Specific Resistance of the Test Sample; Milos Jurca; United States Patent Nr. 4,075,557, Oct 1 1976

26.Apparatus for Contactless Measurement of the Electrical Resistance of a Conductor; Robert E. Richardson ; united States Patent Nr. 5,923,175, Jul. 13, 1999

27.Electromagnetic Noncontacting Measuring Aparatus; Tex N. Yukl; United States Patent Nr. 4,234,844, Nov. 18, 1980

28.Device for the Contactless Measurement of the Resistance of Thin Layers of Material; Elliot Brian John; European Patent Nr. EP 0007408, 06.02.1980

29.Contactless Measurement of the Electrical Resistance per Length of Filaments; Gary S. Sapsford, Alan Robinson; United States Patent Nr. 5,083,090, Jan. 21, 1992

30.Contactless Resistivity Measurement Method and Apparatus; Artur Ballato, Gerald J. Iafrate; United States Patent Nr. 4,353,027, Oct. 5, 1982

31.Process for Contactless Measurement of The electrical resistance of a Test Material; Ulrich Pingel, Hans-Henning Nolte; United States Patent Nr. 5,210,500, May 11, 1993.

32.System And Method For Accurate Contactless Measurement of The Resistivity of a Test Material; Dennis R.Jones, James E.Lutz, Richard H.Campbell, Denys D.Overholser; United States Patent Nr. 5,386,196 Jan. 31, 1995.

Chapter 3

3. New Approach – Contact Evaluation Using Mutual Capacitance Coupling

3.1 Introduction

Secondary terminals in the electrical power substations are almost always connected with 1.5 – 2.5 mm^2 wire (sometimes 4 to 6 mm^2 for current circuits). Copper wires are insulated and insulation must not be destroyed for testing (See Figure 21 – Standard terminal connection). Wires are used for the transmission of measured values such as currents, voltages and for control and signalling circuits. The voltage value at the terminals is typically low (24 V< Voltage < 250 V AC or DC). The following figure shows a typical terminal connection where two wires are fixed into the terminal.

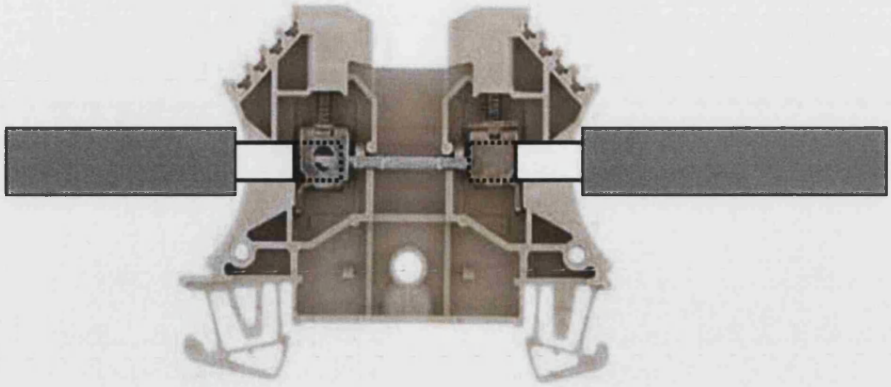

Figure 21 - Standard terminal connection

A secondary terminal is represented in the following diagram, where copper conductors are connected from both sides and the terminal contact is represented by impedance Z. Impedance Z is a complex value influenced by the terminal geometry and secondary signal frequency.

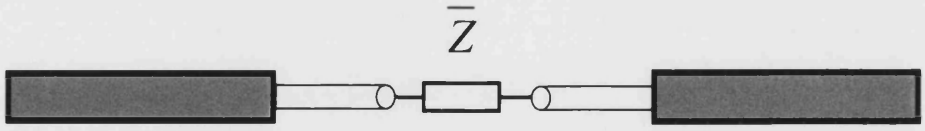

Figure 22 – Electrical replacement diagram for standard terminal

Ohm's law will be used to measure impedance. As described before, the problem is that insulation must not be destroyed while the measurement is performed.

3.2 Basic Research Idea

The idea is to use an injected high-frequency voltage signal for contact resistance measurement. Using mutual capacitive coupling a high frequency voltage signal is injected and by measuring the current through the terminal, the contact impedance can be calculated (this is the ideal case). The high frequency voltage is injected in the conductor using a generator electrode and capacitance coupling (mutual coupling). For the measurement of a resulting terminal current, a sensor working on the same mutual principle will be used. Separate sensor and generator circuits are the invention of this thesis (described in Chapter 2, section 2.3.1)

3.3 Mathematical Model

Contact resistance evaluation using mutual coupling is the basic principle of the researched method and a basic scheme is shown in the following equation model:

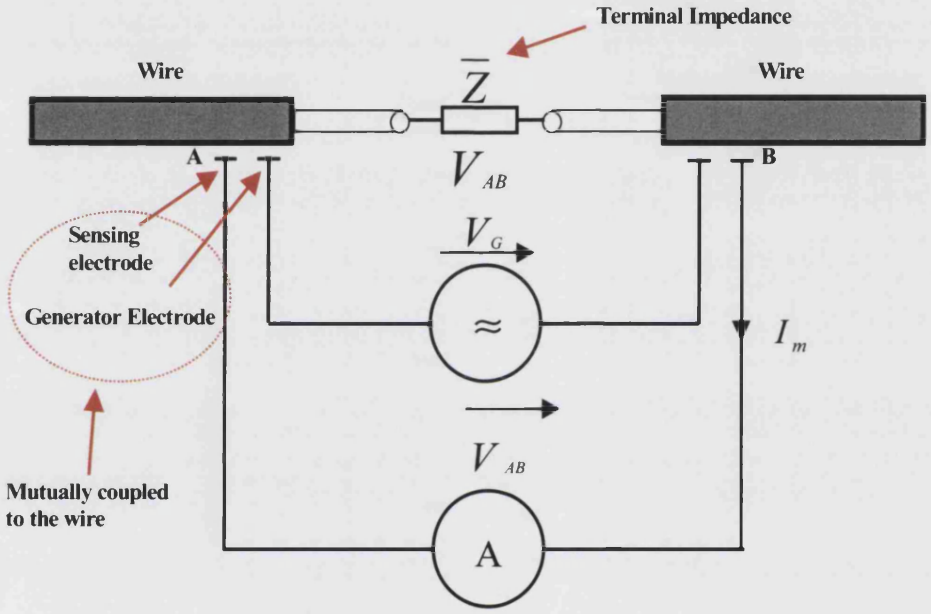

Figure 23 - Basic principle of a mutual coupling method for electrical contact evaluation

The impedance Z value can be measured using voltage V_{AB} ,and current I_m so the value of Z and its resistive part can be solved.

It can be seen in the figure above that separate circuits and couplers are used for generator electrodes and for the

measurement sensor. The use of separate sensing and generating electrodes is necessary because of the reasons described in Chapter 2, section 2.3.1 and the fact, that pure (ideal) voltage source (very low resistance) is used. Usage of such measurement is necessary because of the fact that expected value of the measured current is very low (in the level of several μA) and separate sensing is required.

In the case of a solid electrical contact, the contact resistance value is about one mΩ and a quantitative evaluation of Z will probably not be possible since the measured current will be too small.

- Case of solid electrical contact:

$$\text{IF} \quad \overline{Z} \to 0 \quad \text{THEN} \quad V_{AB} \to 0 \quad \& \quad I_m \to 0 \quad *$$

Equation 11– Case of solid contact

*If $\overline{Z} \to 0$ with a solid electrical contact then $V_{AB} \to 0$ and without voltage V_{AB} value of the current I_m through ammeter A will be $I_m \to 0$

In the case of a broken terminal contact, the resistance of about 1MΩ quantitative evaluation of Z will be possible.

- Case of broken contact:

$$\text{IF} \quad \overline{Z} \to \infty \quad \text{THEN} \quad V_{AB} \neq 0 \ \hat{} \ I_m \neq 0 \quad *$$

Equation 12– Case of broken contact

*If $\overline{Z} \to \infty$ for a broken electrical contact then V_{AB} exists and then the current I_m can be measured as well.

This is the basic principle of the research idea.

The main question to answer is in regards to the variation of the current I_m with impedance Z, which changes depending on the state of electrical contacts. It is therefore important to establish that measurements of I_m can be made accurately for different contact conditions.

The model (simulation) shown in the next figure will be used for electrical contact evaluation:

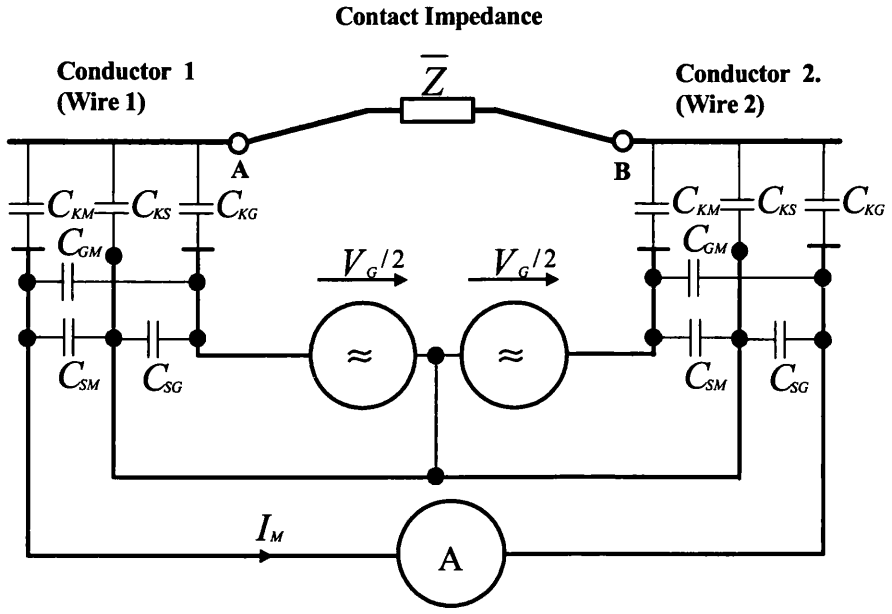

Figure 24- Electrical model of the basic principle of the capacitance coupling method for electrical contact evaluation

C_{KG} Mutual Capacitance : Generator coupling electrode – Conductor

C_{KM} Mutual Capacitance : Sensor – Conductor

C_{KS} Mutual Capacitance : Screen – Conductor

C_{GM} Mutual Capacitance: Sensor – Generator coupling electrode

C_{SG} Mutual Capacitance: Screen – Generator coupling electrode

C_{SM} Mutual Capacitance: Sensor – Screen

V_G Generator – Voltage

I_M Measured current

$\bar{Z}$ Contact Impedance

In order to develop this idea further, it is important to find values for mutual capacitance:

- C_{KG} Mutual Capacitance : Generator coupling electrode – Conductor
- C_{KM} Mutual Capacitance : Sensor – Conductor,
- C_{KS} Mutual Capacitance : Screen – Conductor

For more simple analysis $C_{KG} = C_{KM}$ will be used. For calculation of the values $C_{KG} = C_{KM}$ different capacitors will be analysed.

3.4 Possible Application Problems

With reference to the basic scheme shown in the Figure 24 , the following application problems can be expected:

- Problem of the parallel connected load to the broken contact
- Influence of adjacent terminal blocks

- Influence of the disturbance to the measurement technique of current/voltage signals in the measured conductors (contact)
- Influence of the earthed metal plate below the terminals

All these listed problems must be investigated through experimental measurements.

3.5 Summary about the Basic Idea

As can be seen, the basic idea is based on the simple Ohm's law. Ohm's law in the high frequency domain with capacitance mutual coupling is used as the elementary measuring method.

Measurements made without electric contact require a method where it will be possible to inject measuring signals (through the conductor insulation) and measure without touching conductors.

The elementary idea is using symmetry of the electric circuit where two generator electrodes are injecting high frequency

voltage signal and two electrodes are measuring the current which is flowing through the circuit in the case of broken electrical contacts. This simple method will give the possibility of evaluating terminal contact problems in terms of broken or weak contacts. For the case of broken contacts, some current must flow through the measuring circuit and for the case of solid contact, much lower currents must be measured. (Current is due to dissipation capacitances)

As a conclusion, it can be stated that research will investigate the changing of the electrical current as a function of changing contact impedance Z which changes depending on the state of electrical contacts.

Chapter 4

4. Research about Couplers

4.1 Introduction

It was explained in the introduction that no electrical contact is possible in this measuring application. The idea is to use a high frequency voltage signal mutually coupled to the wire and to receive this signal to determine the contact condition.
In further explanations, generator electrodes and measurement sensors will be referred to as “couplers”.

In the following sections the difference between the shape of couplers (e.g., concentrically cylinder segment, two parallel lines, etc.) will be analysed. The reason for this analysis is the practical realisation for the development of the coupler design. The influence that the shape of the couplers has on the measurements must be investigated.

This analysis has been made while ignoring the influence of the wire insulation and its permittivity. In later research, this

influence will be analysed using a developed hardware model. It can be expected that better results of the capacitance coupling will be achieved with higher permittivity of the wire insulation that will have positive influence on the measurement. [1, 2]

4.2 Analyses of the Coupler as a Concentrically Cylinder

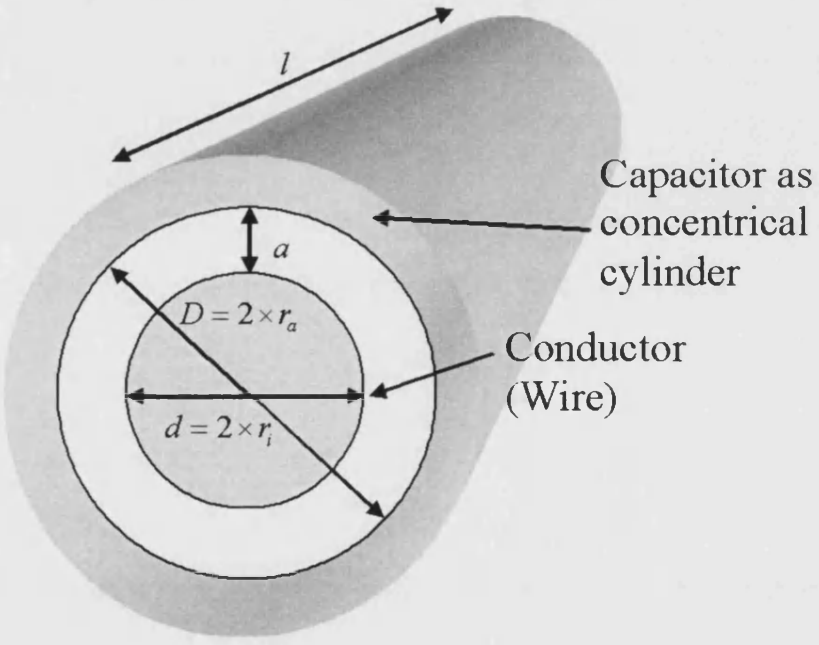

Figure 25 – Concentrical Cylinder Capacitor

The capacitance per meter length of a cylindrical capacitor can be calculated with the following equation:

$$C' = \frac{0.241 \times l}{\log 10\left(\frac{r_a}{r_i}\right)} \qquad \left(\frac{F}{m}\right) \qquad [2, 3, 4]$$

Equation 13– Capacitance of a cylindrical capacitor per length

l = length of cylinder

r_a = outside cylinder radius

r_i = inside cylinder radius

In the above figure, the pitch angle is 360°, which gives the best capacitance coupling (in comparison with cylinder segment capacitors), but makes the mechanical construction of the couplers and the measuring procedure difficult because of the clamp construction and arrangement.

With a coupler designed as a cylinder pitch segment or as a pure cylinder, the mechanical design will be inexpensive and much easier. Additionally, the influence of different pitch angles will be investigated. The target will be to find an

optimised and an inexpensive shape of the couplers which gives accurate results in the measuring method.

4.3 Analysis of the Coupler as a Concentrical Cylinder Segment

Initially, a coupler with the shape of a concentric cylinder segment will be used and the dependency of the distance between the electrode and the conductor will be analysed. Later on, the influence of a variable coupler pitch angle will be investigated.

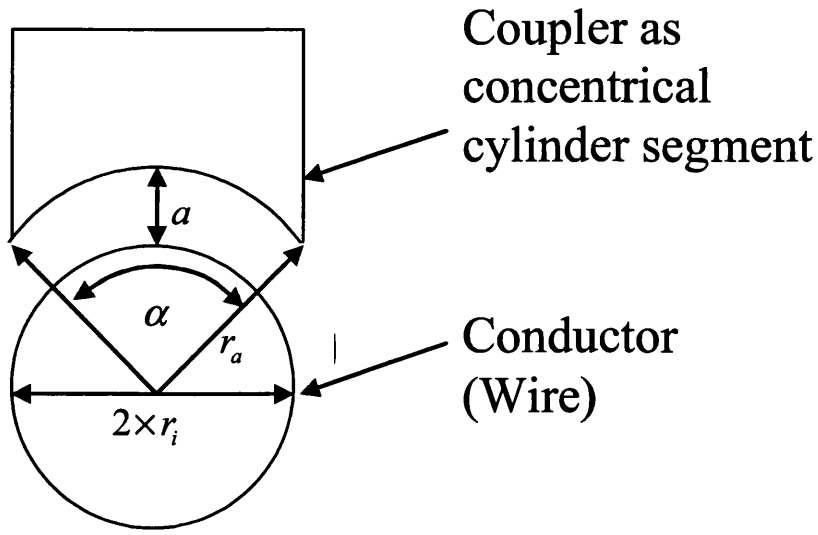

Figure 26 – Capacitor as Concentrically Cylinder Segment

a = distance between conductor and coupler

α =pitch angle

r_a =coupler radius

r_i =conductor radius

To obtain an approximate value, the following data for the calculation was used:

- Conductor: $1.5mm^2$
- r_i : $0.7mm$
- Coupler-pitch angle $\alpha = 45°$
- Distance between conductor and coupler $r_a - r_i = a$

The equation for the calculation of the concentric cylinder segment must take pitch into consideration:

$$C' = \left(\frac{\alpha}{360}\right) \times 100 \times \frac{0.241 \times 10^{-12}}{\log 10\left(\frac{r_a}{r_i}\right)} \qquad \left(\frac{F}{m}\right) \text{ [2, 3, 4]}$$

Equation 14- Capacitance of the concentric cylinder segment capacitor per length

In some literature (e.g. [2]) there is another representation of this equation available and that can be seen below:

$$C' = \left(\frac{\alpha}{360}\right) \times \frac{2 \times \pi \times e_0}{\ln\left(\frac{r_a}{r_i}\right)} \qquad \left(\frac{F}{m}\right) \quad [2]$$

- $e_0 = 8.8542 \times 10^{-12}$ – Air Permittivity

Equation 15- Capacitance of the concentric cylinder segment capacitor per length

Using a MATLAB simulation, the following dependency, capacitance versus distance "a"; $C' = f(a)$ can be shown: (See MATLAB script in Appendix 1):

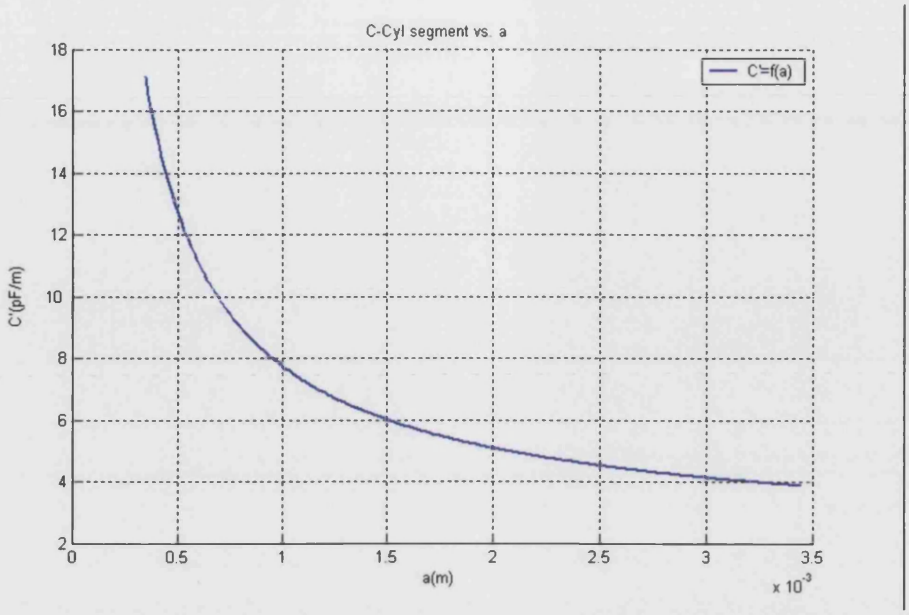

Figure 27 - $C' = f(a)$ Concentric cylinder segment capacitor with 45°pitch angle and variable distance "a"

The above figure shows the influence of distance "a" on the capacitance for this shape of the coupler. This relationship will be investigated further since it is important for the practical measurements.

4.3.1 Concentric Cylinder Segment Capacitor and influence of the Coupler Pitch Angle

The next analysis should show the influence of the pitch angle on the coupler capacitance. For the technical realisation of the capacitor, it is much easier to take a coupler with a small pitch

angle. The following simulation analyses the influence of the variable pitch angle on the capacitance value: (see MATLAB simulation in Appendix 2)

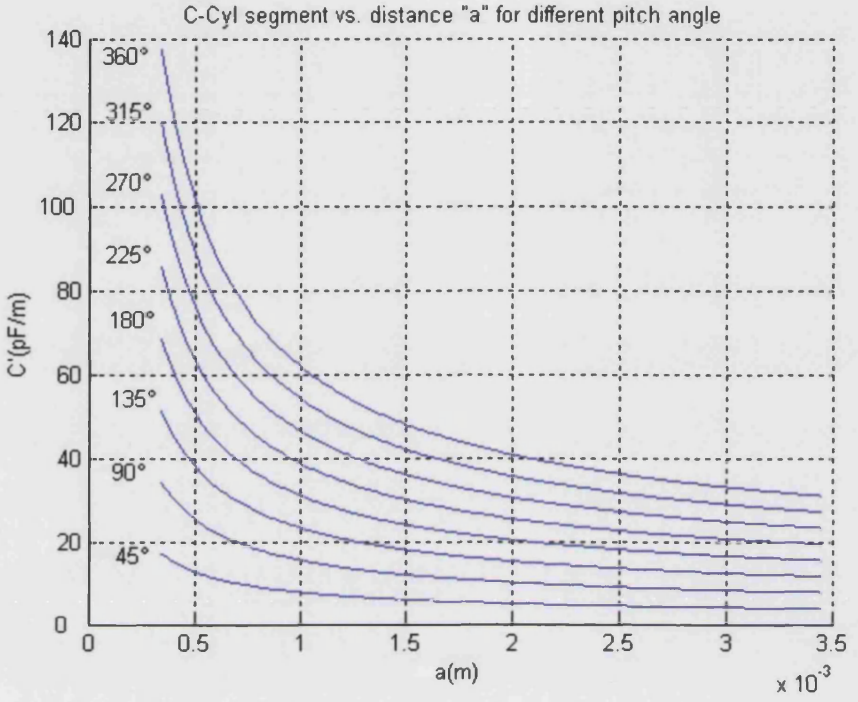

Figure 28 - Concentric cylinder segment capacitor and the influence of the variable pitch angle vs. distance a

In the figure above, the influence of the pitch angle on the capacitance is shown. The variable pitch angle from 45° - 360° with a 45° step is analysed (45°-90°-135°-180°-225°-270°-315°-360°). For the practical realisation of the couplers, a pitch angle greater than 180° will be difficult to realise because of the clamp construction. For the inexpensive coupler

mechanical construction, the pitch angle will be somewhere between 120 and 180°.

4.3.2 Concentric Cylinder Segment Capacitor and the Influence of the Variable Coupler Pitch Angle and Distance "a"

As can be seen in the analyses above, both variables, pitch angle and distance "a" can have a large influence on the capacitor. In practice, the value of distance "a" cannot be less than approximately $a = 1mm$ when insulated wires are used and all simulations must take this into consideration.

With the next MATLAB simulation, the change of the capacitance when the pitch angle α and distance "a" are changed are shown (see MATLAB simulation in Appendix 3)

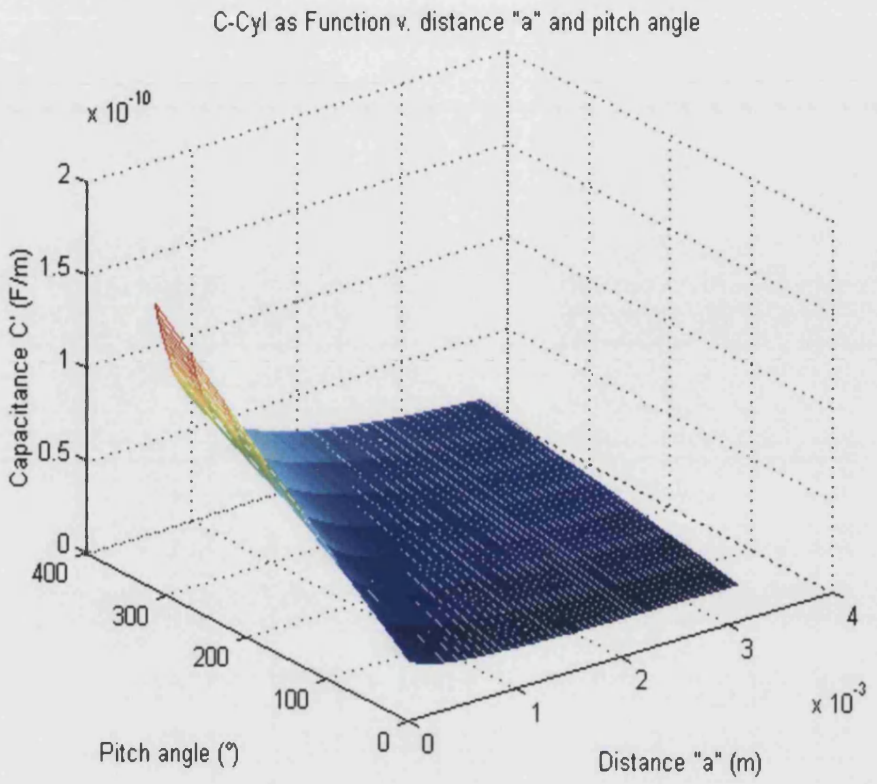

Figure 29 - 3D figure $C' = f(\alpha; a)$ Concentric Cylinder Segment Capacitor and Influence of variable Pitch Angle α and Distance "a"

The above figure shows that a smaller distance to the conductor and a larger pitch angle will increase the capacitance. Larger capacitance makes better mutual coupling and better coupling generates higher values of the current, which can be more easily measured. Later on, the dependency of the measured current on capacitance will be investigated.

4.4 Analyses of Coupler Made of Two Simple Cylinder Conductors

In the second analysis, a coupler in the shape of a simple cylindrical conductor is used to analyse the dependency (relationship) of the distance between the conductor and the capacitor coupler.

For a first approximation, the following data was used for the calculation:

- Conductor: $1.5mm^2$
- r_i: $0.7mm$
- Coupler-radius $r_i = r_a$

The distance "a" between the conductor and the coupler is variable.

C_k' = Capacity per meter of the coupler

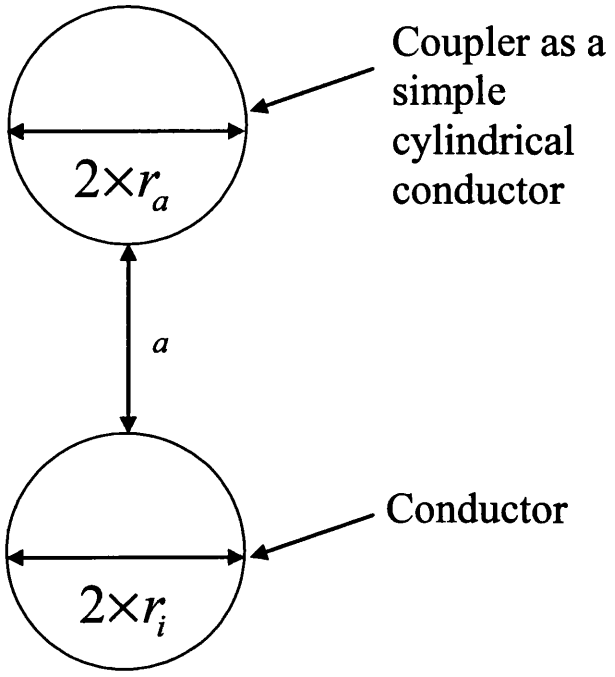

Figure 30 –Two parallel conductors as a capacitor

Using the following equations, it is possible to calculate the capacitance of the two parallel cylinders. In this case, this will mean that the conductor (wire) acts as one cylinder and the coupler acts as the other cylinder.

$$C' = 100 \times \frac{0.241 \times 10^{-12}}{\log 10\left(4 \times \frac{(a + r_a + r_i)^2}{r_i \times r_a}\right)} \quad \left(\frac{F}{m}\right) \text{ [2, 3, 4]}$$

Equation 16 – Capacitance of parallel cylindrical conductor capacitor

There is another representation of this equation available, in the literature [2] which is shown below:

$$C' = \frac{2 \times \pi \times e_0}{\ln\left(4 \times \frac{(a + r_a + r_i)^2}{r_i \times r_a}\right)} \quad \left(\frac{F}{m}\right) \quad [2, 3, 4]$$

- $e_0 = 8.8542 \times 10^{-12}$ –Air Permittivity

Equation 17 – Capacitance of parallel cylindrical conductor capacitor

In following figure the capacitance of two parallel conductors as function of the distance "a"" is presented as calculated from a MATLAB calculation in Appendix 4.

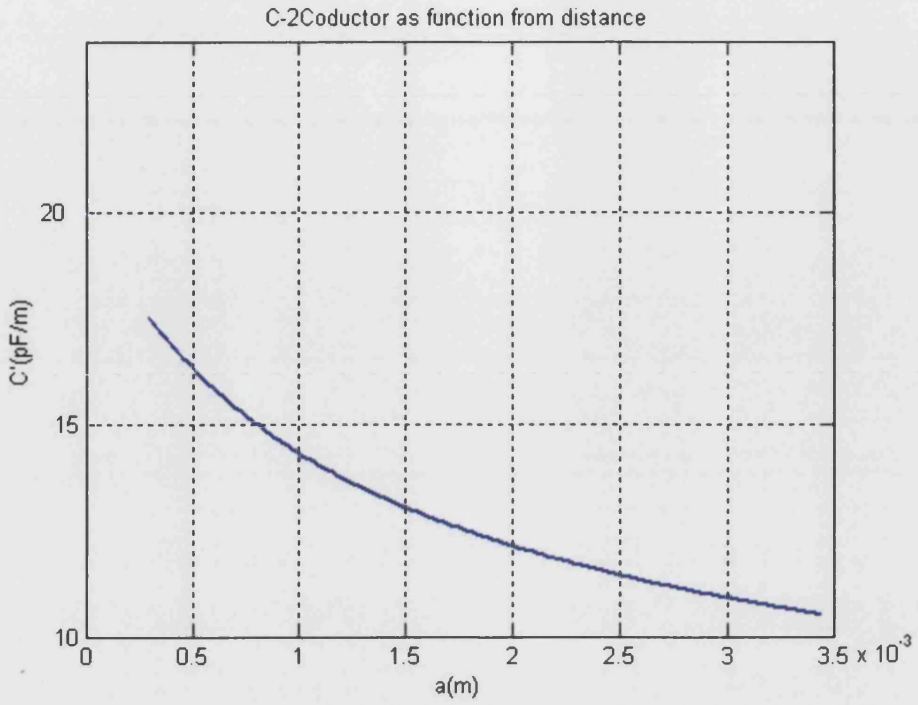

Figure 31 - $C' = f(a)$ Capacitance of two parallel conductors as function of distance "a"

The influence of distance "a" for "$a > 1mm$" for the above-analysed shape of the couplers is lower than shown in the case of the concentric cylinder segment coupler with pitch angle lower then 90° (lower slope).

4.5 Comparison of Two Different Shapes of Couplers

Displaying the simulations results for both types of couplers on the same diagram will show that concentric cylinder segment capacitors have better coupling properties when starting from a pitch angle of 135°.(See MATLAB script in Appendix 5)

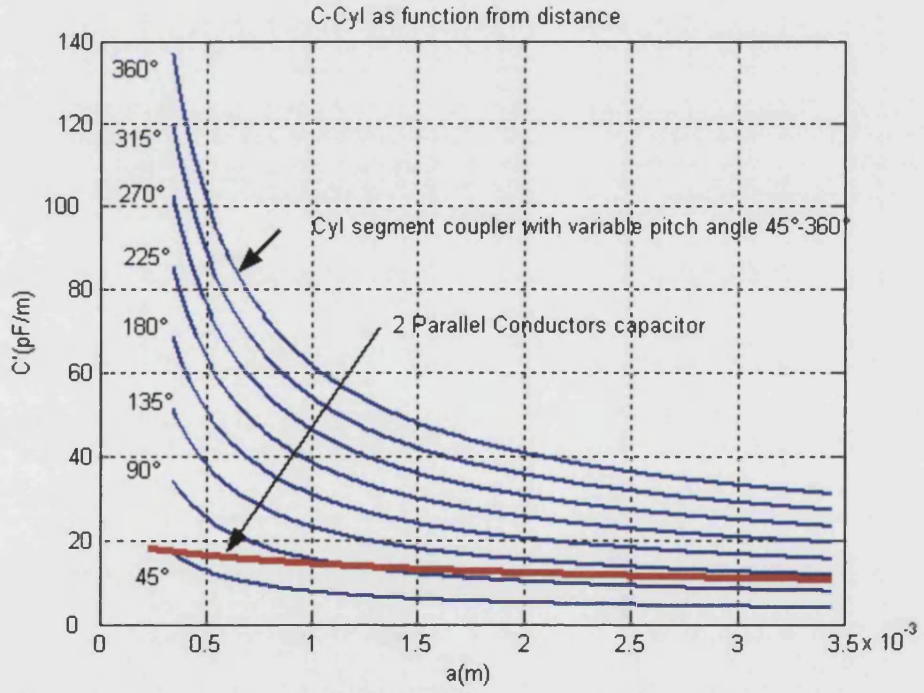

Figure 32 - Comparison of the capacitors as 2 parallel cylinder and the concentric cylinder segment

4.6 Summary about Couplers

In the analysis above, the influence of the coupler shape on the capacitance was investigated. The shape of the coupler is important for the mechanical realization of the hardware. It must not be forgotten that low cost is one of the limiting factors for the research as well.

Two different shapes were investigated: concentric cylinder segment and 2 parallel cylinders. The comparison of the two different shapes was done, with calculation and simulation of the capacitance in function of the distance "a" (Coupler to the conductor) and dependency from the pitch angle α for each individual capacitor shape. It was shown that concentric cylinder segment capacitor has better capacitive coupling for all pitch angle greater as 135°.

References Chapter 4

1. A. W. Smith & M. L. Wiedenbeck " Electrical Measurement" McGraw-Hill Book Company, Inc. New York, Toronto, London 1959

2. Dieter Nührmann " Das große Werkbuch Electronik ; Band 2" Franzis-Verlag München 1998

3. A. A. Zaky and R. Haveley " Fundamentals of Electromagnetic Fields Theory"George G. Harrap & Co. Ltd 182-184 High Holborn, London WC1V 7AX

4. Zahn Markus " Electromagnetic Field Theory" John Wiley Wiley & Sons, Inc.

Chapter 5

5. Capacitor Analyses – Mathematical Model

5.1 Introduction

The target of the following chapter will be to determine dependency : measured current versus impedance $I_m = f(Z)$. (as explained in the Chapter 3 ; section 3.3)

Before developing the hardware prototype, the feasibility of the method will be examined using MATLAB for simulation and theoretical investigations.(Chapter 6).

The mutual capacitive coupling measurement method causes the following dependency: the current I_m is dependent on, not only the contact impedance, but the mutual capacitances as well. For determination $I_m = f(Z)$ all mutual coupling capacitance must be calculated. Some of the mutual capacitances can be only estimated. In the following figure, it can be seen which values must be determined. $I_m = f(Z)$ all mutual coupler capacitance must be calculated.

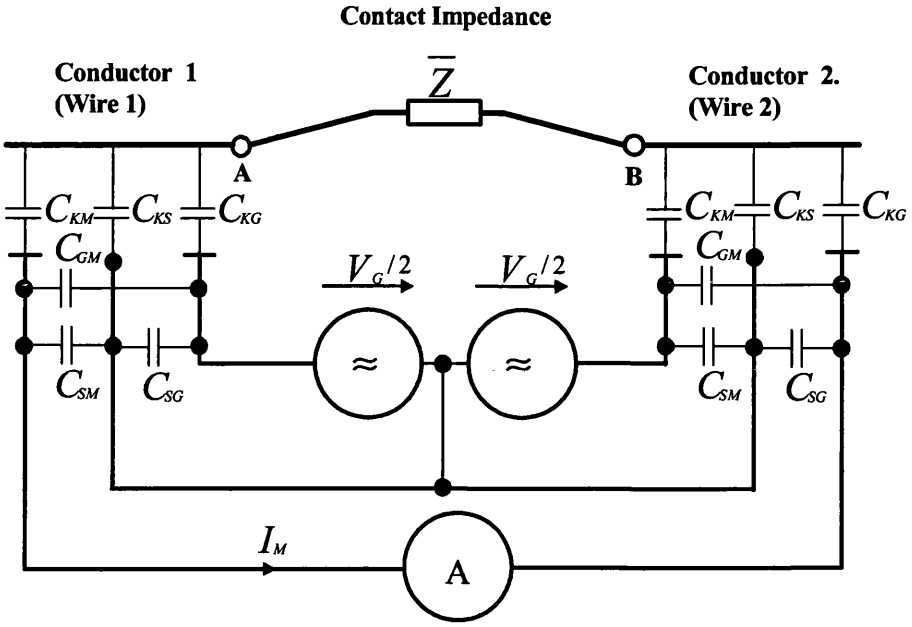

Figure 33 - Electrical model of the basic principle of the capacitance coupling method for electrical contact evaluation

C_{KG} Mutual Capacitance : Generator coupling electrode – Conductor

C_{KM} Mutual Capacitance : Sensor – Conductor

C_{KS} Mutual Capacitance : Screen – Conductor

C_{GM} Mutual Capacitance: Sensor - Generator coupling electrode

C_{SG} Mutual Capacitance: Screen – Generator coupling electrode

C_{SM} Mutual Capacitance: Sensor – Screen

All mutual capacitance values $C_{KG}, C_{KM}, C_{KS}, C_{GM}, C_{SG}, C_{SM}$ are determined in the following sections.

5.2 Determination of the Value of C_{KM} and C_{KG} – Mutual Couplers Capacitance

The value of the capacitance will be somewhere between the analyses of the two different types of couplers (Coupler as two parallel cylinders and coupler as concentrically cylinder segment as explained in Chapter 4 ;section 4.6).

The actual shape of the couplers has some influence on the gradient of the capacitance C_{KM} and C_{KG} over distance "a" for "$a > 1mm$",but as is shown in the Figure 32, this influence is not as big for a pitch angle that is smaller than 90°. For a pitch angle greater than 90°, the slope of the function $C' = f(a)$ becomes bigger (for "$a > 1mm$"). Values of the Capacitance for"$a < 1mm$" are not important for the practical realisation of the measurement because of the insulation thickness.

For the simplification of the analyses assume $C_{KM} = C_{KG} = C'_K$.

(C'_K is value of capacitance over distance "a", refer to Equation 14, Chapter 4, section 4.3)

To continue the analysis, the following approximated values are used as a basis for the simulation: value of the coupler capacitance which will be used for mathematical simulation will be somewhere between analyses made in the analysis of the concentric cylinder segment with a pitch angle of 135° and the two parallel cylindrical conductors as a capacitor. Because of the influence of the dissipation capacitances value of the capacitance will be lower as the capacitance value of the concentric cylinder segment with a pitch angle of 135° and will be greater than the capacitance value of the two parallel cylindrical conductors as a capacitor. Value will be will be approximated for a=1mm, a=2 mm and a=3 mm as average capacitance value between two different calculations. (Using MATLAB (see Appendix 6) the approximated values of the $C_k' = C_{KM} = C_{KG}$ will be calculated.

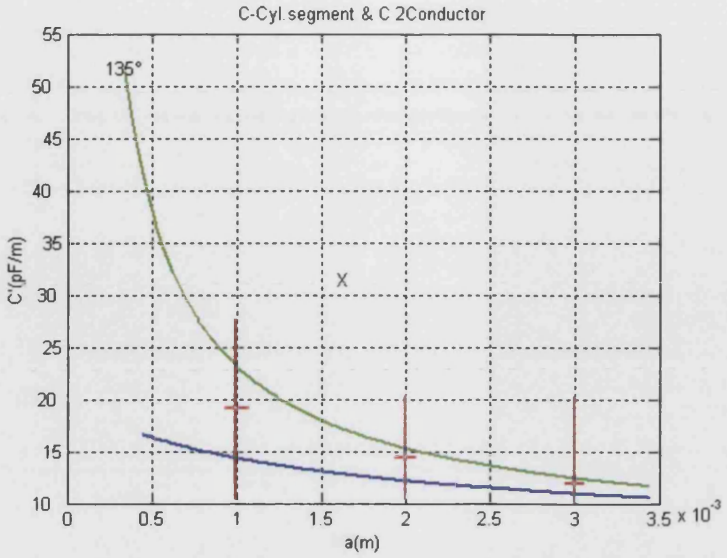

Figure 34 - Function of the capacitance

The following approximate values can be taken from the calculation and will be used for later calculation as mutual couplers capacitance:

$C_k' \approx 18\ pF/m\ at\ 1mm$

$C_k' \approx 14\ pF/m\ at\ 2mm$

$C_k' \approx 12\ pF/m\ at\ 3mm$

As stated in the introduction of this section, the following simplifying was done:

$$C_k' = C_{KM} = C_{KG}$$

5.3 The Determination of the Value of C_{GM} Mutual Capacitance between Two Couplers : Sensor–Generator Coupling Electrodes

After finding the values for the Mutual Coupler Capacitance, in the following analysis the value of dissipation (stray) capacitance C_{GM} between the two couplers is investigated, as is shown in the following figure:

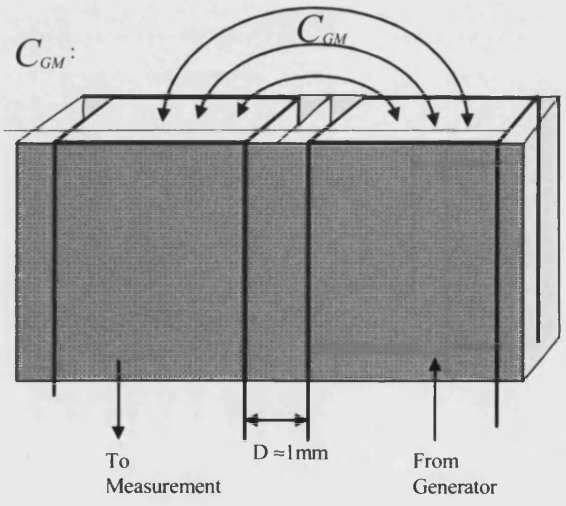

Figure 35- Influence of the mutual capacitance C_{GM} between couplers : sensor – generator

An example of two screened couplers will also be investigated. For the mutual capacitance between the two couplers, the experience table and Nuehrmann approximations will be used. [1]

Two couplers showed in the figure above can be approximated for rough estimation in the following case:

- Strongest electromagnetic field for the case shown in Figure 35 (above) will be on the side which is bordering to the next electrode (see next Figure 36)

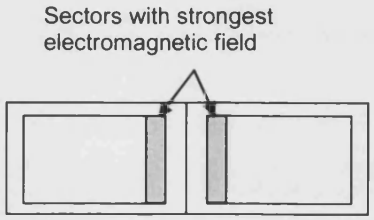

Figure 36: Sectors with strongest electromagnetic field

Coupler sectors shown in the figure above can be approximated with two Cylinders.

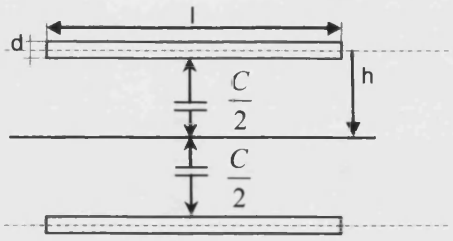

Figure 37: Approximation with two parallel cylindar

According the reference [1] capacitance of the case shown in the figure above can be calculated as:

$$C = \frac{1}{4} \times \frac{0.241 \times l}{\log 10\left[\frac{2h}{d}\left[1 + \sqrt{1 - \frac{1}{\left(\frac{2h}{d}\right)}}\right]\right]} \qquad (pF) \qquad [1,2,3]$$

Equation 18: Capacitance of the two horisontal cylindar

l - length

h - distance from screen

d - cylinder diameter

if $l > h > d$ following simplification can be used:

$$C = \frac{1}{4} \times \frac{0.241 \times l}{\log 10\left(\frac{4 \times h}{d}\right)} \qquad (\text{pF}) \qquad [1,2,3]$$

Equation 19: Simplified equiation about two horisontal cylinder capacitance

In the following (approximation) example for the two parallel cylinders, the capacitance between the two couplers is calculated as 0.2 pF. [1,2,3]

$$C = \frac{1}{4} \times \frac{0.241 \times l}{\log 10\left(\frac{4 \times h}{d}\right)} = \frac{1}{4} \times \frac{0.241 \times 1}{\log 10\left(\frac{4 \times 0.5}{1}\right)} = 0.2\,pF$$

Equation 20– Example of capacitance between two cylindrical couplers

For different shapes of couplers, the capacitance C_{GM} will have different values. Approximations made in the paragraph above had confirm estimations presented the literature [1,2,3,] that the value of the C_{GM} will be in the range between 0.1 and 0.5 pF.

For the coupler shaped as a concentric cylinder segment, C_{GM} is estimated as: average value:

$$C_{GM} \approx \frac{0.1+0.5}{2} = 0.3pF \quad [1]$$

For the coupler shaped as two parallel conductors, C_{GM} is estimated as :

$C_{GM} \approx 0.1pF$ Estimated according ref.[1]

Additionally, using of the hardware prototype value of the mutual capacitance C_{GM} : sensor-generator is constant because the same coupler shape is always used and this value can be calibrated. This value can be measured with the coupler in the air and afterwards this value can be calibrated (zero offset).

5.4 The determination of the Value of C_{KS} – Mutual Capacitance Screen – Conductor

To allow better capacitive coupling between the conductor and the sensors, a screen between the generator electrodes and measurement sensor must be used. (See Figure 38 and Figure 39)

In addition, the mutual capacitance between the conductor and the screen C_{KS} has to be evaluated. The following figure shows C_{KS} and the influence of the system geometry:

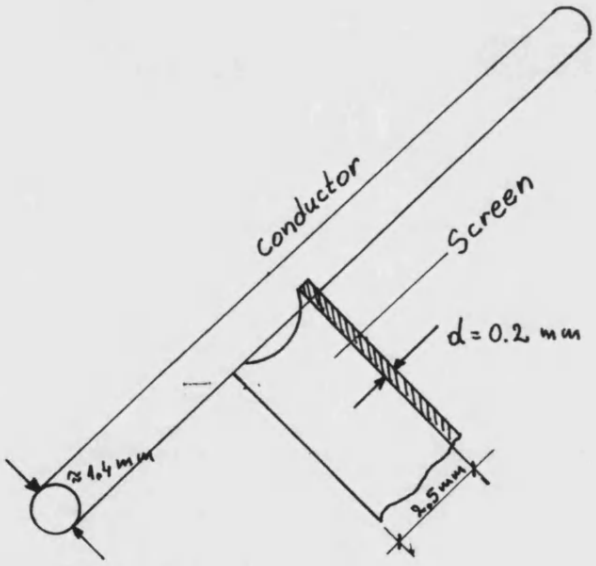

Figure 38– Influence of the mutual capacitance C_{KS}

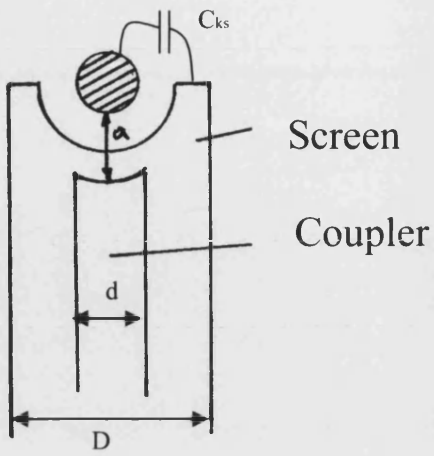

Figure 39 – Mutual capacitance C_{KS} : Conductor – Screen

The case shown in the figure above can be approximated with capacitance of the bushing as can be shown in the figure below:

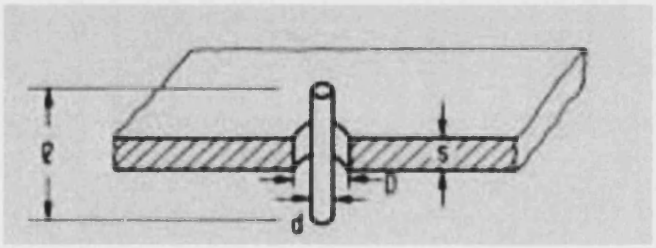

Figure 40: Capacitance of the bushing

l – length of the cylinder

d – cylinder diameter

D – bushing diameter

s – width

For $d \ll D$ and $l \approx S$:

$$C_{KS} \approx \frac{0{,}56 \times l}{\ln\left(\frac{2 \times D}{d}\right)} \qquad (pF;cm) \qquad [1, 2, 3]$$

Equation 21 – Capacitance between conductor and screen

In this researched case, half of the above shown capacitance value plays a role.

$D = 2.5mm$

$d = 14mm$

$l = 20mm$

$$C_{KS} \approx \frac{1}{2} \times \frac{0{,}56 \times 0{,}02}{\ln\left(\frac{2 \times 2{,}5}{1{,}4}\right)} \approx 0{,}0045 \ pF$$

Equation 22 – Calculation of C_{KS}

Regarding the calculation above, for the coupler shaped as a concentric cylinder segment C_{KS} is estimated to be:

$C_{KS} \approx 0.005pF$

For the coupler shaped as two parallel conductors C_{KS} is estimated to be:

$C_{KS} \approx 0.002pF$ Estimated according ref.[1]

5.5 The discussion about Value of C_{SG} – Mutual capacitance : Screen – Generator Coupler and C_{SM} – Mutual Capacitance : Sensor Coupler – Screen

Additional analysis of the symmetrical case where the left and the right side are the same will be done and the following equivalent scheme can be used:

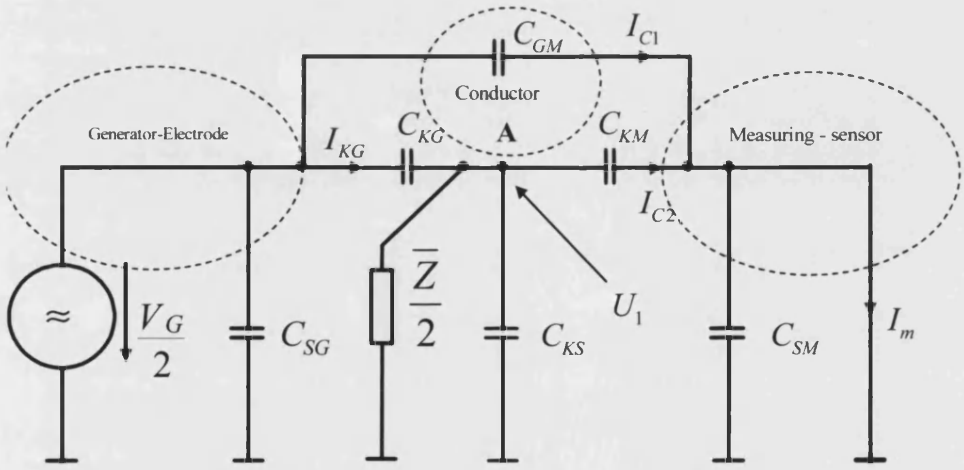

Figure 41 – Electrical equivalent circuit of the symetrical case

C_{KG}	Mutual Capacitance : Generator coupling electrode – Conductor
C_{KM}	Mutual Capacitance : Sensor – Conductor
C_{KS}	Mutual Capacitance : Screen – Conductor

C_{GM}	Mutual Capacitance: Sensor – Generator coupling electrode
C_{SG}	Mutual Capacitance: Screen – Generator coupling electrode
C_{SM}	Mutual Capacitance: Sensor – Screen
V_G	Generator – Voltage
I_m	Measured current
$\overline{Z}$	Contact Impedance
$C'_K = C_K / m$	Capacitance per meter length
V_{AB}	Measured voltage

The equivalent circuit above shows that C_{SG} is only the capacitance load from the generator and does not have any influence, although the generator must be capable of supplying the current. The generator must be a pure (ideal) voltage source, that is, with a very low resistance. With this specific construction of the generator, the value of the C_{SG} will not have any influence on the measurement. For this reason it will be not necessary to determine the value of C_{SG}.

Increasing the signal frequency will increase the current I_m and decrease the reactance $\left(X_C = \frac{1}{\omega C}\right)$ associated with the capacitance value of C_{SM} (Mutual capacitance : sensor coupler–

screen). There will be no voltage existing on the capacitance C_{SM} while the sensor coupler is producing the short circuit. This is one of the reasons why the measurement of the current is preferred over the measurement of the voltage. For this reason it will be not necessary to determine the value of C_{SM} - it has a very low influence on the current measurement.

The conclusion is that the C_{SM} and C_{SG} mutual capacitances may have a very significant capacitance but this will have very low influence on the current measurement.

5.6 The Determination of the Dependency of $I_m = f(Z)$

In the test case described in previous sections, it was explained that the current flowing in the measuring sensor must be determined. Using the electrical equivalent circuit shown in Figure 41, the following equations can be developed:

$$I_M = I_{C1} + I_{C2}$$

$$I_{C1} = \frac{V_G}{2} \times j\omega C_{GM}$$

$$I_{C2} = V_1 \times j\omega C_{KM}$$

$$V_1 = \frac{V_G}{2} - I_{KG} \times \frac{1}{j\omega C_{KG}}$$

$$I_{KG} = \frac{V_G}{2} \times \frac{1}{\frac{1}{j\omega C_{KM}} + \frac{1}{j\omega C_{KM} + j\omega C_{KS} + 2Y}}$$

$$\Rightarrow V_1 = \frac{V_G}{2} \times \left(1 - \frac{1}{j\omega C_{KG}} \times \frac{1}{\frac{1}{j\omega C_{KG}} + \frac{1}{j\omega C_{KM} + j\omega C_{KS} + 2Y}} \right) =$$

$$= \frac{V_G}{2} \times \left(\frac{1}{1 + \frac{j\omega C_{KG}}{j\omega C_{KM} + j\omega C_{KS} + 2Y}} \right)$$

This portion of the stray capacitance C_{GM} sensor – generator can be compensated as always kept as a constant. (Same shape and same geometry from the couplers)

$$\Rightarrow I_M = \frac{V_G}{2} \times \left\{ j\omega C_{GM} + j\omega C_{KM} \times \left(1 - \frac{j\omega C_{KM} + j\omega C_{KS} + 2Y}{j\omega C_{KM} + j\omega C_{KS} + 2Y + j\omega C_{KG}} \right) \right\} =$$

$$\Rightarrow \left\{ \left(1 - \frac{j\omega C_{KM} + j\omega C_{KS} + 2Y}{j\omega C_{KM} + j\omega C_{KS} + 2Y + j\omega C_{KG}} \right) \right\} = B$$

$$\Rightarrow B = \left\{ \left(\frac{j\omega C_{KM} + j\omega C_{KS} + 2Y + j\omega C_{KG} - j\omega C_{KM} - j\omega C_{KS} - 2Y}{j\omega C_{KM} + j\omega C_{KS} + 2Y + j\omega C_{KG}} \right) \right\} =$$

$$\Rightarrow B = \left\{ \left(\frac{j\omega C_{KG}}{j\omega C_{KM} + j\omega C_{KS} + 2Y + j\omega C_{KG}} \right) \right\} =$$

$$\Rightarrow I_M = \frac{V_G}{2} \times \left\{ j\omega C_{GM} + j\omega C_{KM} \times \left(\frac{j\omega C_{KG}}{j\omega C_{KM} + j\omega C_{KS} + 2Y + j\omega C_{KG}} \right) \right\} =$$

$$\Rightarrow I_M = \frac{V_G}{2} \times \left(j\omega C_{GM} + \left(\frac{j\omega C_{KM} \times j\omega C_{KG}}{j\omega C_{KM} + j\omega C_{KS} + 2Y + j\omega C_{KG}} \right) \right)$$

Equation 23 –Current I_m and dependency of the impedance Z

5.7 Summary about Capacitance Analyses and Mathematical Model

The target of previous research was to find dependency $I_m = f(Z)$. For the calculation of this dependency was necessary to determine all mutual capacitances :

- C_{KG} Generator coupler – Conductor
- C_{KM} Sensor – Conductor
- C_{KS} Screen –Conductor
- C_{GM} Capacitance between couplers

- C_{SG} Screen generator coupler
- C_{SM} Sensor – Screen

In order to find values of the required capacitances, different shapes of the couplers were investigated. In conclusion the average value between cylinder segment and two cylinder capacitors was estimated. Further values of the dissipation (stray) capacitances were calculated in order to achieve values needed to solve equity $I_m = f(Z)$.

The electrical equivalent circuit was constructed and dependency $I_m = f(Z)$ was calculated. This will be used as the input for further MATLAB simulations.

References Chapter 5

1. Dieter Nührmann " Das große Werkbuch Electronik ; Band 2" Franzis-Verlag München 1998

2. A. A. Zaky and R. Haveley " Fundamentals of Electromagnetic Fields Theory"George G. Harrap & Co. Ltd 182-184 High Holborn, London WC1V 7AX

3. Zahn Markus " Electromagnetic Field Theory" John Wiley Wiley & Sons, Inc.

Chapter 6

6. Practical Considerations

6.1 Introduction

In this chapter the frequency of the measurement signal will be considered first. Furthermore, different MATLAB simulations will be defined in order to focus on an optimal design for the hardware prototype.

Determination of the contact closed state or the contact open state will be possible by using this method.

The coupling capacitors are only estimations but it will be possible to measure the difference between closed and open contact states.

The conclusion in the Chapter 5 was that the current I_m should be measured (and not the voltage V_m).

6.2 Analysis of the Test Signal Frequency

One of the questions to be answered is which frequency will be used for the test signal? For practical measurements, the frequency must not be too high, because of influence of the

system, problems with screening, etc. (as explained in the Chapter 2 section 2.4) Additional problem with high frequency will be the construction of the generator. The generator must be able to carry the capacitive load from the couplers and cables. This will be more problematic for the higher frequency. This means from the point of view of experience, that probably frequencies below 10 MHz will be used. The big problem that can arise is the resonance effect; if the frequency is too high then measurements will be not possible, as the generator electrodes can operate as antennae. Too low a frequency allows the influence of the power system disturbances and a big influence of the dissipation capacitance. With too low a frequency there are existing problems with mutual coupling as well.

From experience, the most realistic range for the frequency used is from 0.1 MHz to 5 MHz. This range will be investigated. The tool used for system simulation is MATLAB. With MATLAB, the influence of the frequency on the measurement results will be simulated but for the practical evaluation of the frequency, a real hardware model must be developed. Further on, the optimisation and the confirmation of the chosen frequency will be investigated by using a hardware model.

6.3 $I_m = f(z)$ Simulation with 1 MHz test signal – Variable contact resistance 0-10kΩ

Using this method, a quantitative estimation of the contact resistance using this method is practically impossible (see the MATLAB simulation in Figure below). From 0 – 1000 Ω the value of the capacitance (current) is almost constant. Starting at 10 kΩ, the influence on I_m can be measured.

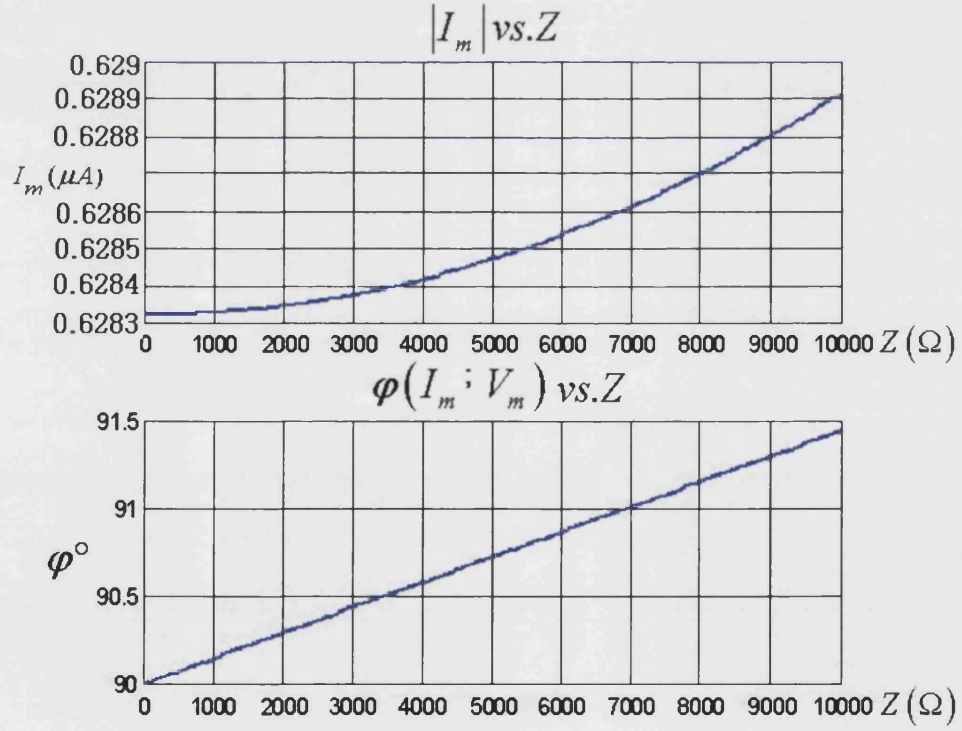

Figure 42: $I_m = f(z)$ – Simulation with 1MHz signal frequency and variable contact resistance 0 – 10kΩ

Quantity	Value	Comment
C_K	1 pF	1 cm length of the electrodes
C_{GM}	0.2 pF	Mutual capacitance: Sensor – Generator
C_{KM}	0.4 pF	Mutual capacitance: Sensor – Conductor
C_{KS}	0.005 pF	Mutual capacitance: Screen – Conductor
C_{KG}	0.4 pF	Mutual capacitance: Generator – Conductor
p	1 MHz	Signal frequency
*par*1	10 kΩ	Resistance Max. Value

Table 1: Values used in the MATLAB simulation (Appendix 7)

The current values from about 1μA/V generator voltage (at f=1MHz) should be easily measurable (see the MATLAB simulation in the figure Figure 42). The measurement must be frequency selective with a narrow frequency band (In this case, high accuracy will be possible).

The current at $Z=0$ is caused by dissipation capacitance and this can be almost compensated for, by using reference measurement. An evaluation from the phase angle may be able to give some results at small values of $Z \rightarrow 0$. Further it will be

very difficult to measure angle on such low values and this will be not main focus in this research.

6.4 $I_m = f(z)$ - Simulation with 1 MHz test signal-variable Contact Resistance 0-1MΩ

In this simulation the variation of the contact resistance from 0 - 1MΩ was investigated. The typical value of the broken contact resistance is a value greater then 1MΩ. As can be seen on the Figure 43, the current value for the case of changing contact resistance from solid to broken contact rises from about 0.6 to 1.2 μA This value difference can be measured and used as trigger criteria for the broken contact detection.

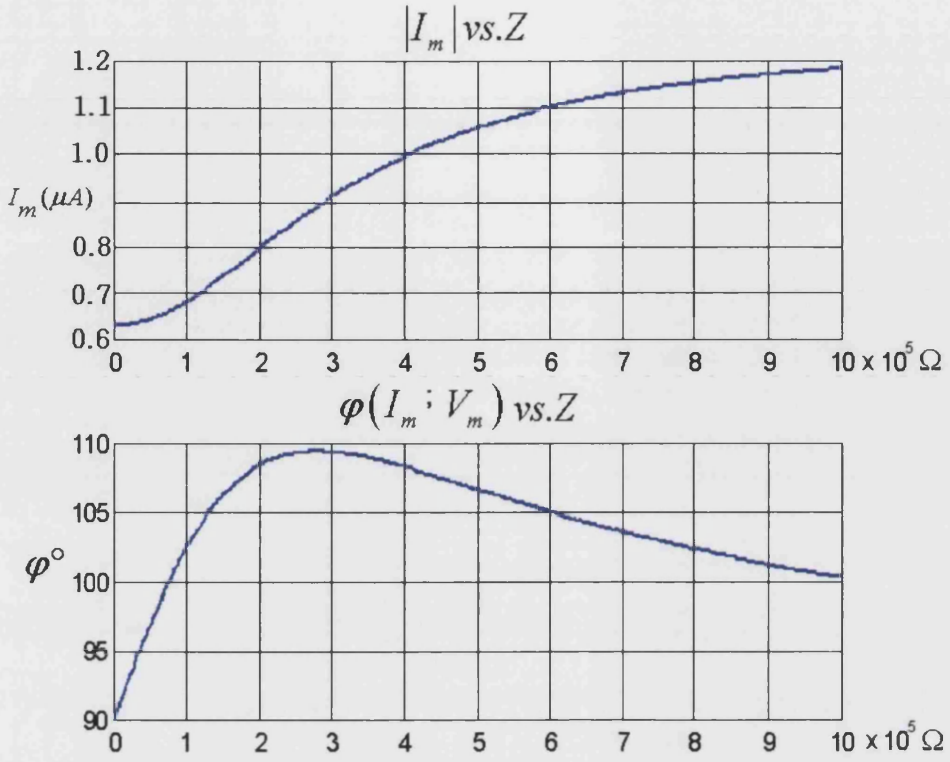

Figure 43 $I_m = f(z)$ – Simulation with 1 MHz test signal – Variable contact resistance 0–1MΩ

Quantity	Value	Comment
C_K	1 pF	1 cm length of the electrodes
C_{GM}	2 pF	Mutual capacitance: Sensor – Generator
C_{KM}	0.4 pF	Mutual capacitance: Sensor – Conductor
C_{KS}	0.005 pF	Mutual capacitance: Screen – Conductor
C_{KG}	0.4 pF	Mutual capacitance: Generator – Conductor
p	1 MHz	Signal frequency
*par*1	1 MΩ	Resistance Max. Value

Table 2: Values used in the MATLAB simulation (Appendix 8)

6.5 $I_m = f(z)$ Simulation with 1 MHz test signal – Variable contact resistance 0–1MΩ and reduced mutual capacitance C_{GM} sensor –generator couplers

In this simulation, the value of the mutual capacitance C_{GM} (sensor coupler–generator coupler) was reduced from 2 pF to 0.002 pF. As can be seen this decreases the measured current signal.

The simulation shows that by decreasing mutual capacitance C_{GM} (sensor coupler–generator coupler), the current gradient changes. Furthermore the mutual capacitance C_{GM} (sensor

coupler-generator coupler) will be constant (constant geometry of the measuring couplers) and for the later hardware prototype it will be possible to compensate this. The compensation will be used in the future hardware for reduction of the parasitic capacitances. Reduction of this value will increase measurement sensitivity.

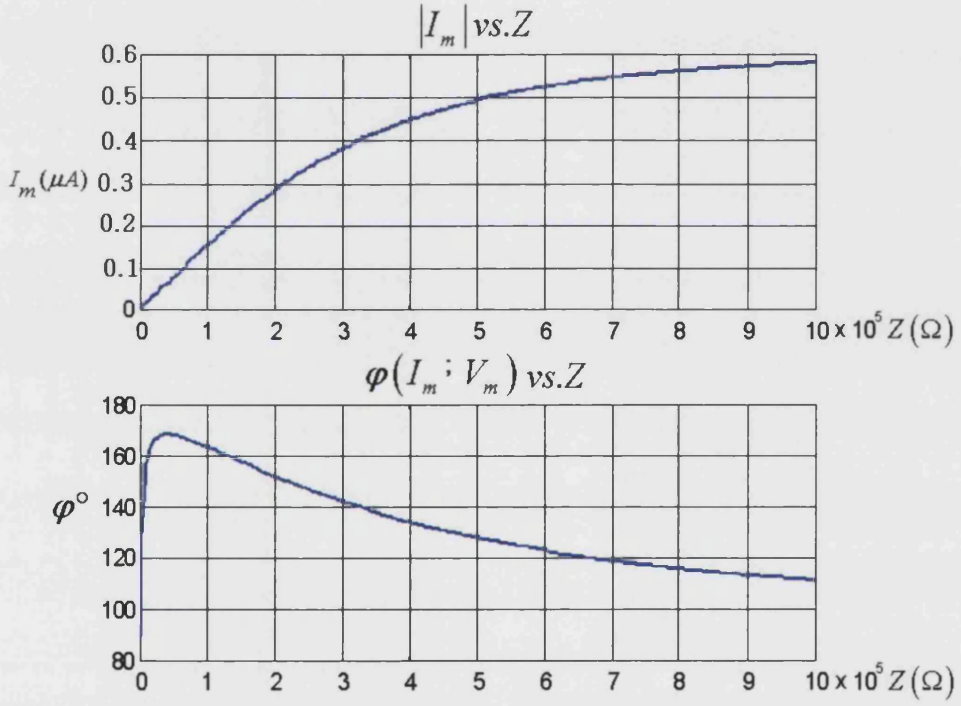

Figure 44 - Simulation with 1 MHz test signal - Variable contact resistance 0-1MΩ and reduced mutual capacitance C_{GM} sensor - generator couplers

Quantity	Value	Comment
C_K	1 pF	1 cm length of the electrodes
C_{GM}	0.002 pF	Mutual capacitance: Sensor – Generator
C_{KM}	0.4 pF	Mutual capacitance: Sensor – Conductor
C_{KS}	0.005 pF	Mutual capacitance: Screen – Conductor
C_{KG}	0.4 pF	Mutual capacitance: Generator – Conductor
p	1 MHz	Signal frequency
$par1$	1 MΩ	Resistance Max. Value

Table 3: Values used in the MATLAB simulation (Appendix 9)

6.6 $I_m = f(z)$ Simulation with 1 MHz test signal – Resistance 0–1MΩ and increased distance between generator couplers – conductor

Increasing the distance between generator couplers and conductor will cause the reduction of the mutual capacitance C_{KG}. In the following simulation the capacitance C_{KG} was varied.

In this simulation, it can be seen that increasing the distance between generator couplers and conductor (decreasing capacitance C_{KG}) will cause a decrease in the measured current

I_m. As can be seen on the graph with decreasing capacitance C_{KG} from 0.4 to 0.1 pF causes the decrease of the measured current from about 1.2 to 0.8 µA (corresponds to a change in distance between sensors and conductor of approximately 1mm to 3mm). This can have a very negative influence on the measuring method and must be taken into the consideration for later hardware development.

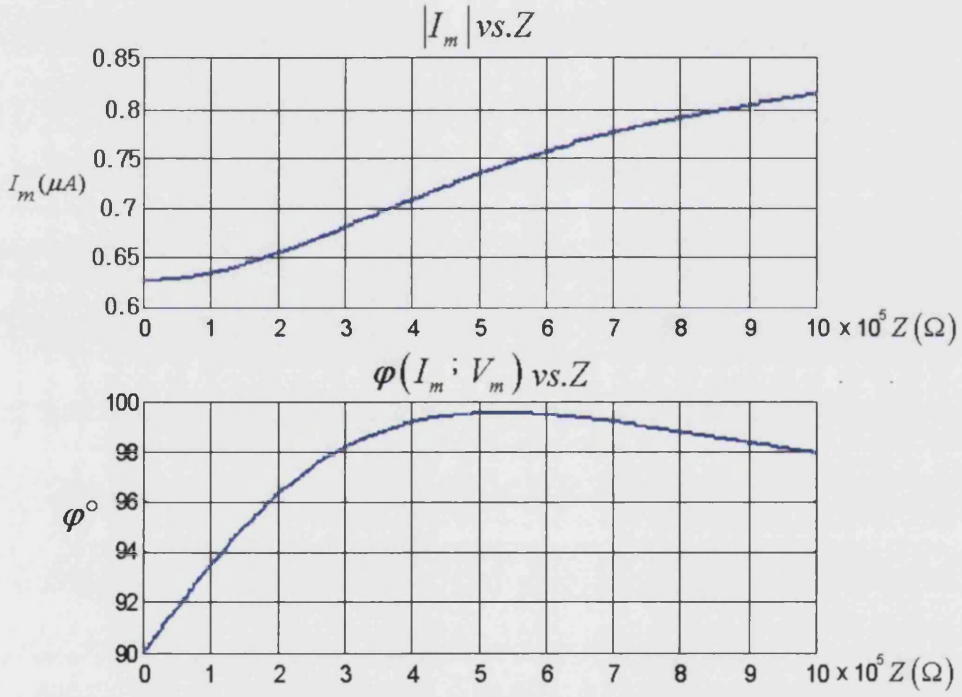

Figure 45 - Simulation with 1 MHz test signal - Variable contact resistance 0-1MΩ and reduced mutual capacitance C_{KG} generator couplers - conductor

Quantity	Value	Comment
C_K	1 pF	1 cm length of the electrodes
C_{GM}	0.2 pF	Mutual capacitance: Sensor – Generator
C_{KM}	0.4 pF	Mutual capacitance: Sensor – Conductor
C_{KS}	0.005 pF	Mutual capacitance: Screen – Conductor
C_{KG}	0.1 pF	Mutual capacitance: Generator – Conductor
p	1 MHz	Signal frequency
$par1$	1 MΩ	Resistance Max. Value

Table 4: Values used in the MATLAB simulation (Appendix 10)

6.7 $I_m = f(z)$ Simulation with 5 MHz test signal – Resistance 0–1MΩ

As can be seen in the Figure 46, raising the frequency produces an increase in the current. $I_m = f(Vm)$. This can have a positive influence on the later hardware development and on the measuring quality.

At the same time, a higher signal frequency will cause problems with screening; the influence of resonance effects on other conductors, etc. It will be necessary to use a hardware prototype to research the influence of different signal

frequencies. The hardware will have a possibility for generating the signal with variable frequencies, e.g., from 50 kHz to above 1MHz.

In the following figure simulation with signal frequency 5MHz is presented.

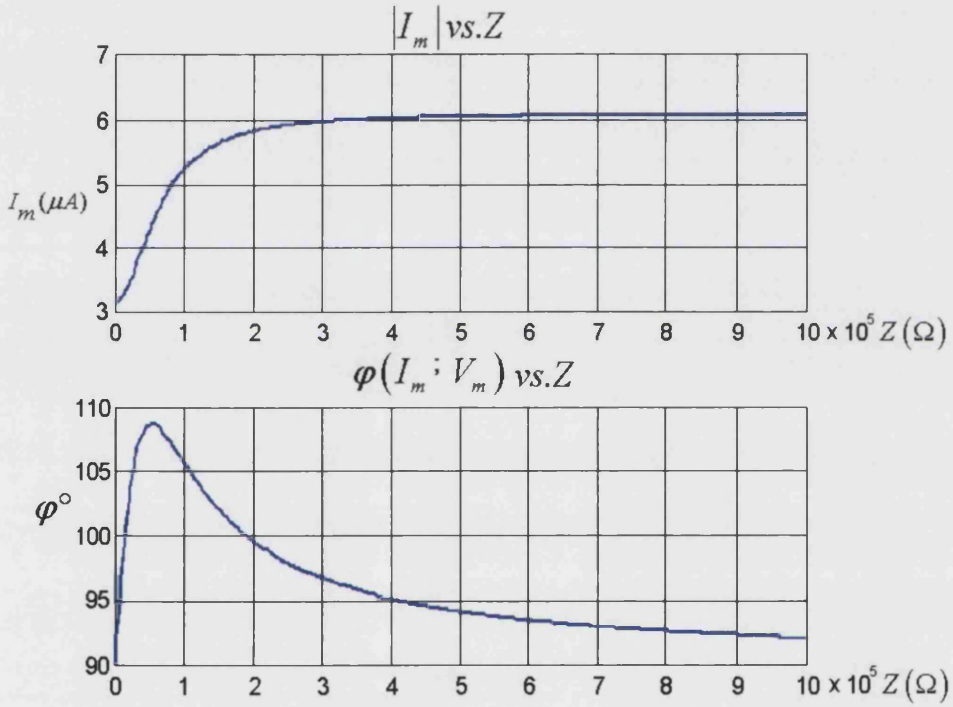

Figure 46 - $I_m = f(z)$ Simulation with 5 MHz test signal - Resistance 0-1MΩ

Quantity	Value	Comment
C_K	1 pF	1 cm length of the electrodes
C_{GM}	0.2 pF	Mutual capacitance: Sensor – Generator
C_{KM}	0.4 pF	Mutual capacitance: Sensor – Conductor
C_{KS}	0.05 pF	Mutual capacitance: Screen – Conductor
C_{KG}	0.1 pF	Mutual capacitance: Generator – Conductor
p	5 MHz	Signal frequency
*par*1	1 MΩ	Resistance Max. Value

Table 5: Values used in the MATLAB simulation (Appendix 11)

6.8 $I_m = f(z)$ Simulation with 1 MHz test signal – Variable contact resistance 0–1MΩ and large distance between sensor/generator couplers and conductor

This simulation shows that the large distance between the couplers and the conductor's current gradient is almost zero and that an evaluation is not possible. Furthermore while developing and testing the hardware the influence of the distance between couplers and conductor on the measurement prototype must be investigated. Some minimum required distance from couplers to the conductor should be evaluated.

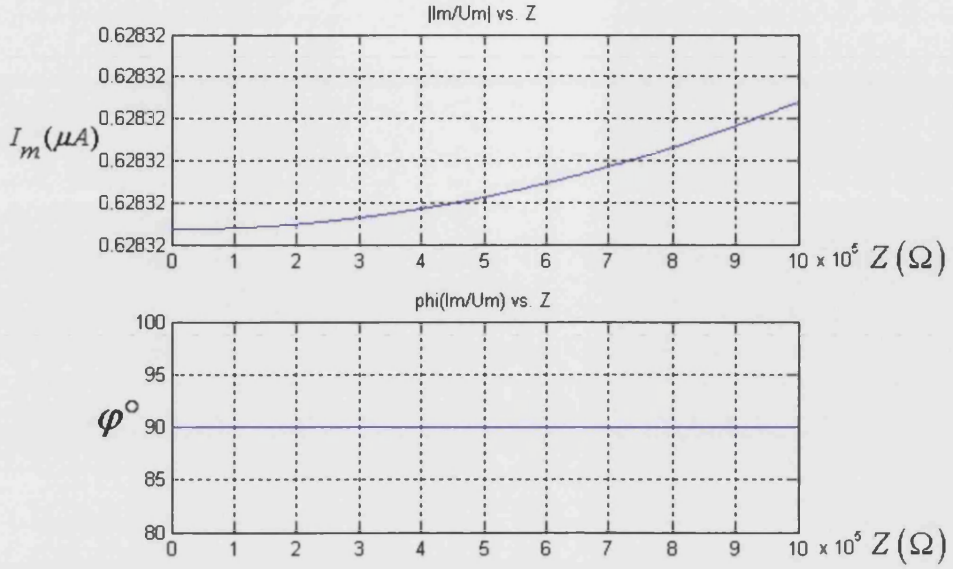

Figure 47 - Simulation with 1 MHz test signal – variable contact Resistance 0-1MΩ and large distance between sensor/generator couplers and conductor

Quantity	Value	Comment
C_K	1 pF	1 cm length of the electrodes
C_{GM}	0.2 pF	Mutual capacitance: Sensor – Generator
C_{KM}	0.00001 pF	Mutual capacitance: Sensor – Conductor
C_{KS}	0.05 pF	Mutual capacitance: Screen – Conductor
C_{KG}	0.00001 pF	Mutual capacitance: Generator – Conductor
p	1 MHz	Signal frequency
*par*1	1 MΩ	Resistance Max. Value

Table 6: Values used in the MATLAB simulation (Appendix 12)

6.9 $I_m = f(z)$ Simulation with 5 MHz test signal – Resistance 0–1MΩ and large distance between sensor/generator couplers and conductor

This simulation shows the same results with a frequency of 1MHz – 5MHz signal, that with a large distance between the couplers and the conductors, the current gradient is almost zero and an evaluation is also not possible. For the development of the future hardware it is important that large distances have a big influence on the measuring method. The increase of the signal frequency can not improve the method to be more accurate with the large distance between couplers and conductor.

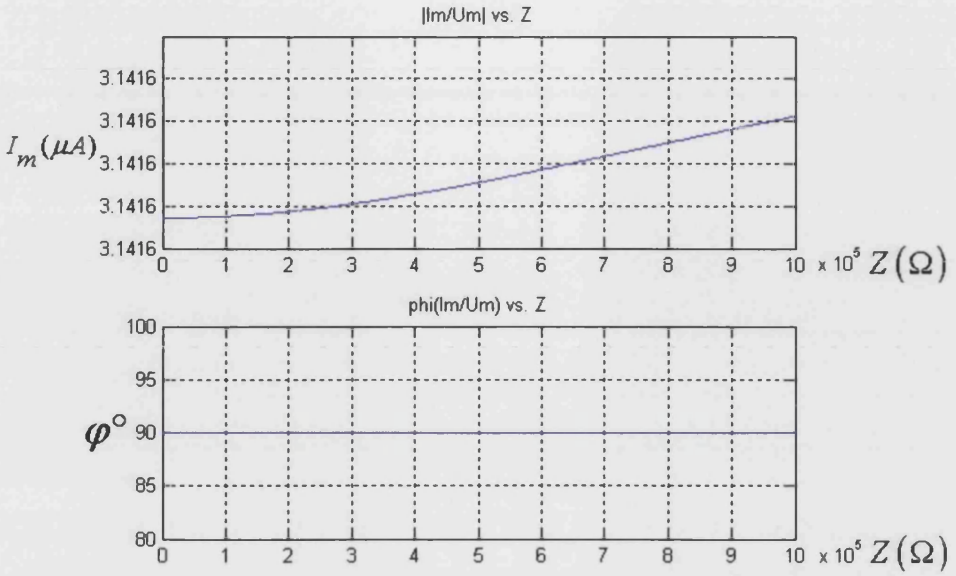

Figure 48 - Simulation with 5 MHz test signal - Variable contact resistance 0-1MΩ and large distance between sensor/generator couplers and conductor

Quantity	Value	Comment
C_K	1 pF	1 cm length of the electrodes
C_{GM}	0.2 pF	Mutual capacitance: Sensor - Generator
C_{KM}	0.00001 pF	Mutual capacitance: Sensor - Conductor
C_{KS}	0.05 pF	Mutual capacitance: Screen - Conductor
C_{KG}	0.00001 pF	Mutual capacitance: Generator - Conductor
p	5 MHz	Signal frequency
*par*1	1 MΩ	Resistance Max. Value

Table 7: Values used in the MATLAB simulation (Appendix 13)

6.10 Simulation of Solid Contact Z=1 mΩ v. C_{KG}/C_{KM}

In the following simulations it is assumed that $C_{KG} = C_{KM}$, and that these values are variable. As can be seen the influence of distance "a" between the sensors and the electrodes to the conductor is very low if $Z = 0$ (solid contact). The current gradient is almost equal to zero. A zero current gradient will be further used for detection of the solid contact.

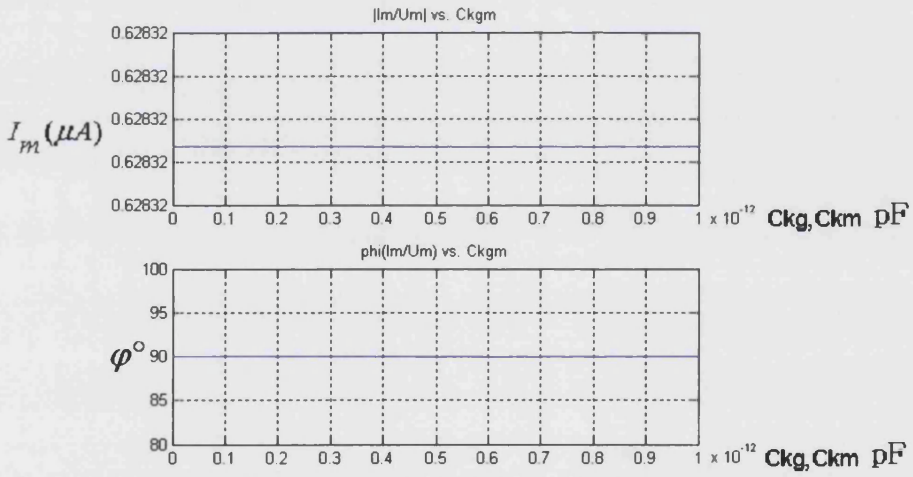

Figure 49 - Simulation of Solid Contact $Z = 1m\Omega$ vs. $C_{KG}; C_{KM}$

Quantity	Value	Comment
C_K	1 pF	1 cm length of the electrodes
Z	0.001 Ω	Contact resistance
C_{GM}	0.02 pF	Mutual capacitance: Sensor – Generator
C_{KS}	0.05 pF	Mutual capacitance: Screen – Conductor
p	5 MHz	Signal frequency
*par*1	1 MΩ	Resistance Max. Value

Table 8: Values used in the MATLAB simulation (Appendix 14)

$$C_{KM} = C_{KG} = \text{var}$$

6.11 Simulation of the broken Contact $Z = 1$ MΩ v. C_{KG} / C_{KM}

The following investigation will simulate broken contact. In the case of broken contacts, the impedance increases to infinity ($Z \to \infty$), the voltage on contacts increases to generator voltage, which increases the measured current I_m if the sensors are closer to the conductor. This will be used as trigger to detect broken terminal contact. In the hardware model described later, the value of the current will be measured.

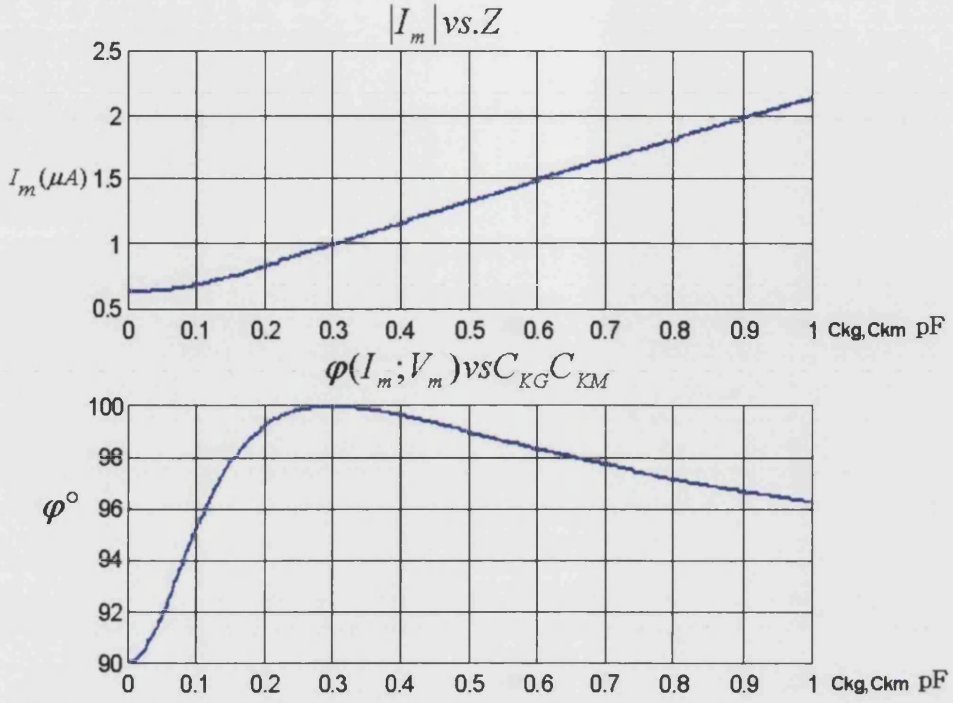

Figure 50 – Simulation of the broken Contact $Z = 1M\Omega$ v. C_{KG} / C_{KM}

Quantity	Value	Comment
C_K	1 pF	1 cm length of the electrodes
Z	1 MΩ	Contact resistance
C_{GM}	0.02 pF	Mutual capacitance: Sensor – Generator
C_{KS}	0.05 pF	Mutual capacitance: Screen – Conductor
p	5 MHz	Signal frequency
$par1$	1 MΩ	Resistance Max. Value

Table 9: Values used in the MATLAB simulation (Appendix 15)

$$C_{KM} = C_{KG} = \text{var}$$

6.12 Summary about Practical Considerations and Simulations

The purpose of this chapter was to evaluate testing methods and give some conclusions for the future hardware development.

At the beginning of chapter 6 the pre-selection of the measuring signal frequency was explained. Further the comparison of the measured results with 1 and 5 MHz signal frequency showed that both results are accurate enough and that the lower frequency can be used. By using lower frequency it can be expected that no big disturbances will occur within measurement hardware.

According to practical considerations about frequency, the measuring signal frequency will be somewhere between 0.1 and 1 MHz.

One of the most important conclusions about this chapter is that the measuring method is not able to measure contact resistance lower then 1000 Ω. The application is therefore focused on the detection of broken or weak contacts.

Simulation of the variable distance "a" (couplers-conductor) showed that this quantity has a very big influence on the measuring results and that must be investigated with future

hardware prototype. Further investigations with variable dissipation capacitance were performed. The influence of the dissipation capacitance can be compensated later within the hardware.

The difference between solid and broken contact was clearly detected and displayed. The simulation shows that the measurement method, which is the task of this thesis, can be used for the detection of broken contacts.

Chapter 7

7. Experimental Hardware

7.1 Introduction

For further investigation, it will be necessary to build experimental hardware, and use it for research and confirmation of the theoretical statements. The hardware must be simple but also must be capable of making very accurate measurements.

In this chapter the basic idea about hardware construction will be described.

7.2 Basic Hardware Scheme

The experimental hardware will be a combination of a high-frequency generator and the very narrow band accurate measurement. The hardware will be connected with the test object via couplers, which will inject a signal via capacitive coupling, and will sense the gradient (peak) of the current (as

has been shown in the section 3.3.3, Figure 24). The following figure shows the basic hardware scheme:

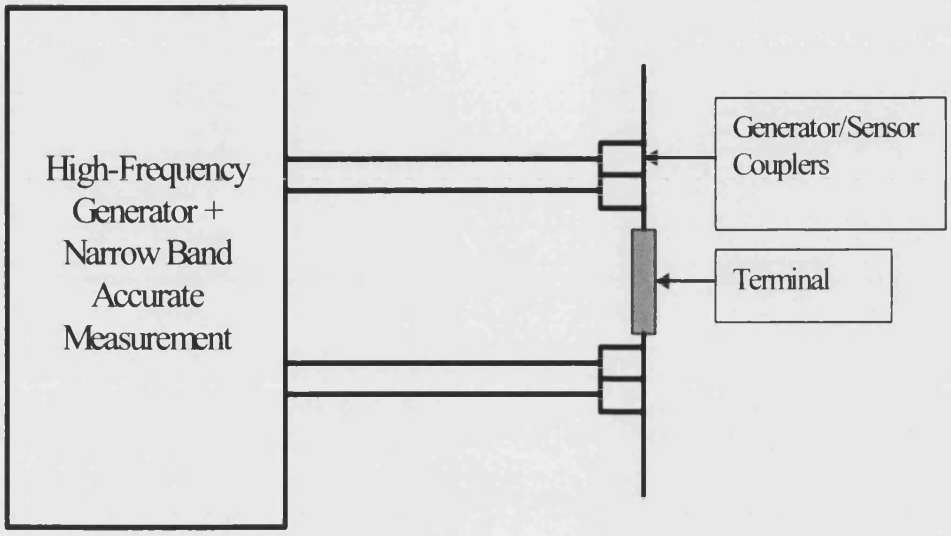

Figure 51 –Basic Hardware Scheme

7.3 Influence of the practical problems on the coupler shape and signal frequency selection

One of the biggest problems is the influence of conductors that are too close to each other, i.e. neighbouring conductors (see Figure 52). In the research later on in this thesis, it will be investigated whether this influence can be reduced with a

special form of electrodes (couplers), and with optimized selection of the corresponding measuring signal frequency.

In the next Figure 52, terminal number 7 is broken on the displayed terminal block example. With the method described above and a high frequency signal injected on terminal 7 (on the left and the right conductors), voltage U_M will exist on the broken terminal 7 and the current I_M induced from this voltage can be measured. If the influence of the next bay conductors can not be compensated the current will flow trough the neighbours conductor and determination of the state of the terminal 7 using this method will not be possible.

Conversely, if the mutual capacitance coupling will influence the conductors in the next bay, they will create parallel short-circuits and the detection of the broken contacts using this method will not be possible (Current I_M will flow through close neighbours conductors and not through measurement circuit).

Using a special shape for the electrodes, optimized signal frequency (frequency must not be too high, < 1MHz) and a specific screening of the couplers as shown in the previous

analyses, influence of the close parallel conductors can be reduced.

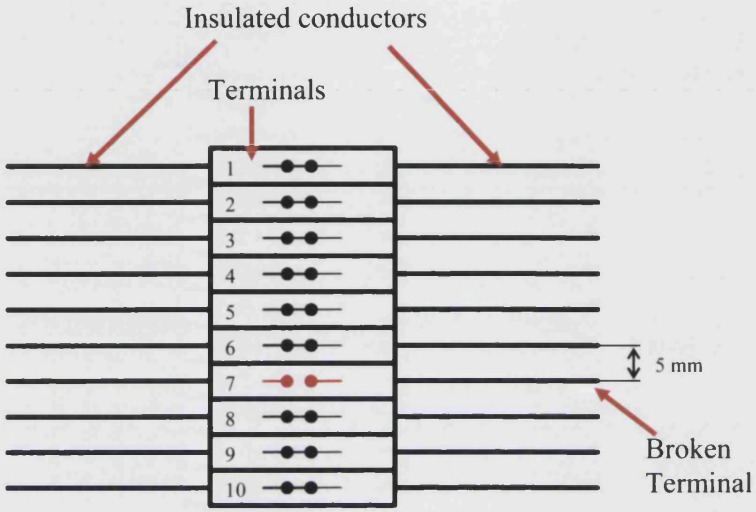

Figure 52 - Influence of next bay conductors on measurement

The described problem with neighbouring conductors can be reduced with selection of the couplers with better capacitive coupling. As investigated before, the cylinder segment couplers shows significantly better capacitive coupling compared to the cylinder coupler. For the hardware model, the electrodes (couplers) will be made as cylinder segment capacitors. Additional screening of the couplers will be needed.

A signal frequency set too high will easily penetrate through the insulation into the neighbouring conductors and will make detection (measuring) very difficult. This should be taken into account for selection of signal frequency.

Further problems can be caused by the background metal plate which is used for mounting the terminals (see next figure).

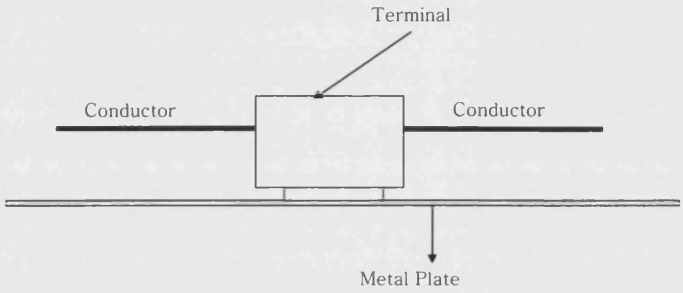

Figure 53: Influence of the metal plate

The metal plate will cause a similar effect as described for the closely placed neighboring conductors. Electromagnetic fields will penetrate through the metal plate and will make detection of the broken contact more difficult. The influence of the stray capacitance will be significant. To allow detection of the broken and closed terminal contact, the experimental hardware must have very accurate and sensitive measurement.

7.4 Couplers

In Figure 54 construction of the couplers is shown. The shape of the couplers is a cylinder segment made out of aluminium with pitch angle of approximately 180°. In the Chapter 4, Section: 4.3.1 Concentric Cylinder Segment Capacitor and influence of the Coupler Pitch Angle, the influence of the pitch angle on the capacitive coupling was explained. For the practical realisation of the couplers it was recommended to use a pitch angle close to180°.

The couplers are insulated from the screen by varnish and separated from each other by the screen as can be seen in the Figure 54.

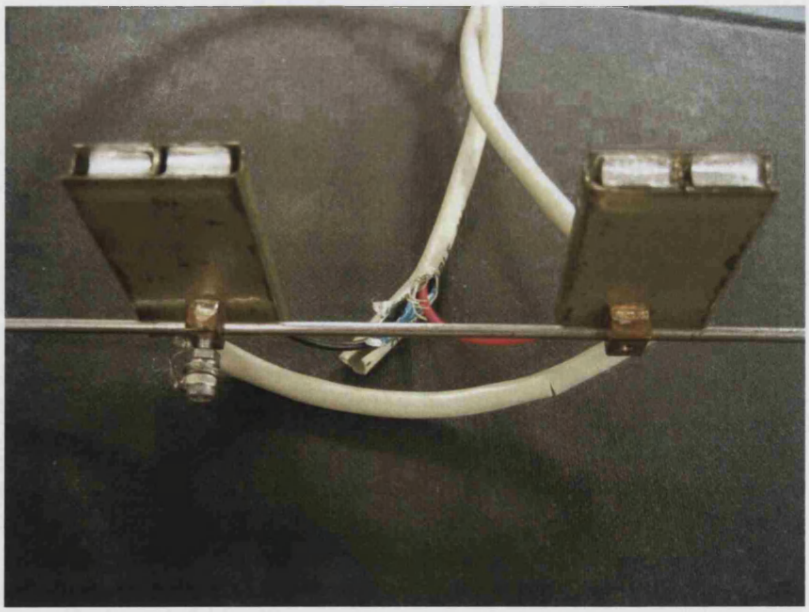

Figure 54 – Construction of the couplers

To allow better capacitive coupling and lower stray capacitances (dissipation) in addition to the screen between sensors the screen also encloses the couplers (As shown in the Figure 54).

Such construction of the couplers with combination of corresponding signal frequency will allow good capacitive coupling where the majority of the electromagnetic field will penetrate through the conductor under measurement. The stray capacitance caused by close neighboring conductors and metal plate will be reduced and minimized.

7.5 System Hardware

The following hardware scheme will be used for the hardware design:

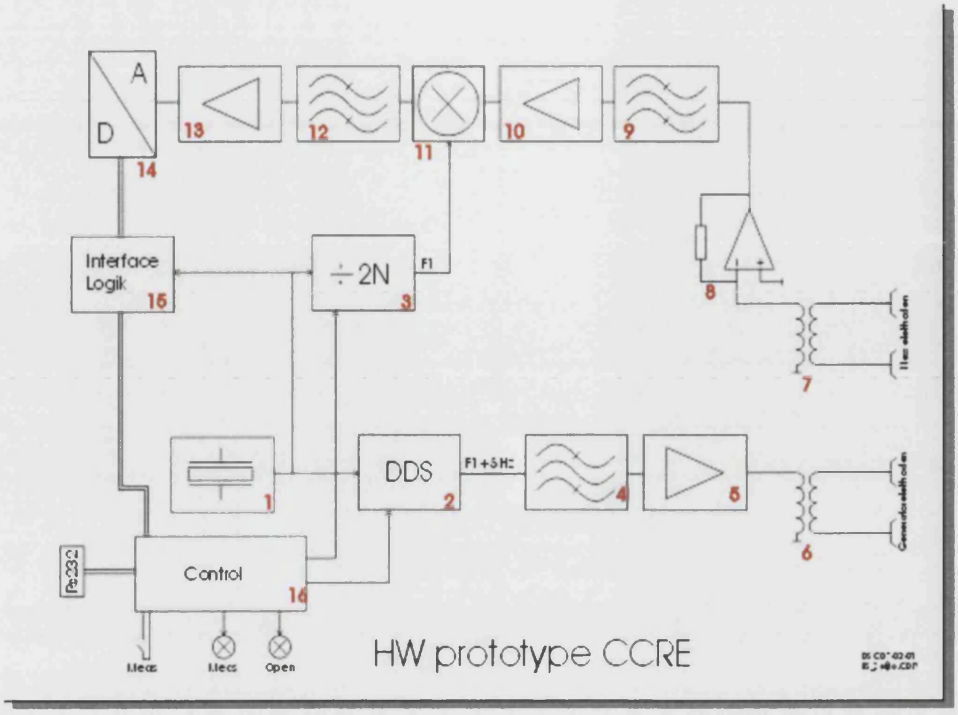

Figure 55 - Scheme of the hardware system

1. Quartz Crystal - Internal frequency oscillator (Mother clock type 20 MHz).
2. DDS - Direct Digital Synthesis. [1]
3. Programmable divisor
4. Band-pass-filter
5. Amplifier
6. Generator electrodes
7. Measuring sensors
8. Voltage/Current converter

9. Band pass filter
10. Amplifier
11. Mixer
12. High Q Band pass filter
13. Amplifier
14. A/D converter
15. Interface logic
16. Control

The quartz crystal (1) (mother clock type 20 MHz) will generate a signal with a reference clock frequency ($F_{REF\_CLK} = 20MHz$) and then deliver it to the DDS (2) and the programmable divisor (3).

The DDS can create a very clear accurate sine signal. The frequency can be very accurate to the value of 1μHz [1]. In the range from 100 kHz to 1 MHz, the frequency of DDS is very accurate.

1. With the DDS, a sine signal will be created. The output frequency from DDS (2) will be adjusted to $F_1 + F_{offset}$. (offset frequency will be approximately 5 Hz)

(See explanation about offset frequency after description of the basic hardware functionality)

$$F_{DDS\_OUT} = \frac{M(F_{REF\_CLK})}{2^n} \qquad [1]$$

Equation 24: DDS Output frequency

F_{DDS_OUT} - The output frequency of the DDS

M - The binary tuning word

F_{REF_CLK} - The internal clock frequency

n - The length in bits of the phase accumulator

The length of the phase accumulator (N) is the length of the tuning word which determines the degree of frequency tuning resolution of the DDS implementation.

The DDS output frequency will be adjusted at $F_{DDS\_OUT} = F_1 + F_{offset}$ i.e. 200005 Hz where 5 Hz is the offset frequency.

2. After the DDS, the High Q Band pass filter will help with the generation of the clear sine signal. The DDS output normally has some distortions. These distortions are system-dependent and a function of the sampling theorem.[1,2]

3. After amplification of the signal with transformer (6), the output voltage will be raised to about 50 V.

4. With current transformer (7), the current signal will be transformed, and afterwards will be converted using current/voltage converter (8).

5. The Band pass filter will suppress unwanted 50 Hz component and amplifier (10) will amplify the signal.

6. The signal with frequency $F_1 + F_{offset}$ (i.e. 200005 Hz) will come to the mixer(11).

7. The Mixer is supplied with a square wave signal with frequency F_1, produced from the programmable divisor.[2]

$$F_1 = \frac{F_{REF\_CLK}}{MDIV + 1}$$

Equation 25: The output frequency of the programmable divisor

F_1 - The output frequency of the programmable divisor

$MDIV$ - Division ratio (adjustable from 10 - 100)

For the above example:

$$F_1 = \frac{200000000Hz}{99+1} = 200000Hz$$

NOTE: The resulting frequency after the mixer will be:

$$F_{RESULTING} = F_{DDS\_OUT} - F_1 = F_1 + F_{OFFSET} - F_1 = F_{OFFSET}$$

Equation 26: Resulting frequency after mixer

For the above example:

$$F_{RESULTING} = 200000Hz - 200005Hz = 5Hz$$

The programmable divisor frequency must be selected so that the resulting frequency after the mixer is within the following values (band pass filter 1-10Hz):

$1 < F_{RESULTING} < 10Hz$.

8. Only a F_{offset} (approximately 5 Hz) signal is the output from the mixer.

9. This signal will be filtered (band pass filter1 – 10 Hz)

10. After amplification, the signal is converted to a digital signal via an ADC.

11. The ADC can be realised as a low-sampling rate, high-resolution converter (with about a 100 kHz sampling rate).

12. Through some interface logic the ADC is connected to the controller.

13. In the controller, the measurement results are evaluated.

14. A PC will be connected via RS 232.

Hardware design show in the Figure 55 - Scheme of the hardware system must have the following properties:

- Ability to accurate generate the high frequency voltage signal which will be used for capacitive coupling.
- Ability to accurate measure very low level current signals (range of 1 μA))
- Ability to filter out system disturbances (almost 50 Hz and corresponding harmonics)
- Simple and low cost hardware solution
- Recording capability for research purpose

Two contradictory facts are facing the application problem:

1. A high frequency signal is needed for better capacitive coupling and induction of the higher measurement current.
2. A lower frequency signal is needed for more accurate, sensitive and easier current measurement.

One of the innovative solutions in the presented hardware design is special filtering of the measured signal using the offset frequency F_{offset} (typically about 5Hz).

One of the application problems is the very strong disturbances of the system and the very weak measuring signal. A premium idea to solve these problems is to use a signal generated with frequency $F_{DDS\_OUT} = F_1 + F_{offset}$ where the offset frequency is about 5 Hz. For the capacitive coupling at such a frequency signal will be used. High sensitivity and accuracy of the measurement will be achieved after deducting this signal to measure only signal with offset frequency (very narrow band measurement). Such measuring of the almost DC signal (about 5 Hz) can be made very accurate and high sensitivity of the measurement can be achieved. Such method will be able to detect currents which are in the range of 1 μA/V. Such sensitivity will be needed to detect the difference between solid and broken contacts and also be able to detect weak contact "with help of mechanical vibrations".

As can be seen in the Figure 55 two separate circuits are used for generation of the signal and for measurement sensing. This requirement is explained in the Chapter 2; section 3.2.4.

The following innovations have been developed in the hardware design:

- Two separate circuits (allow measuring of the parallel conductors)
- Special filtering of the signal with offset frequency
- Very accurate generation and measurement of the low level signal
- Using high frequency for capacitive coupling
- Using about 5 Hz for accurate measurement (almost DC)
- filtering of the power signal disturbances
- low cost hardware

With this hardware, it will be possible to investigate the influence of different coupler geometry and different test signal frequencies. The feasibility of the entire method under practical conditions will be investigated.

7.6 Mechanical Vibration generator

One of the biggest practical problems in electrical substations is weak contacts at the secondary terminals. Weak contacts in the control and especially in the current circuits can be very dangerous.

Using the method of capacitance coupling described above, it will be possible to detect solid or broken closed or open only.

For weak contact the idea is to use mechanical vibrations (superimposing) to cause weak contacts to change state from open to closed and to detect this change by measuring the current change. This idea will be investigated using above-described hardware, improved with a vibration feature. This will be a topic for further research and will be a complementary part of the PhD thesis.

The mechanical vibrations will be researched using simple mechanical movement of the conductors or using separate vibration generators.

The frequency of the superimposed mechanical vibrations is a topic that must be investigated. The vibrations will be used to transfer mechanical energy into the electrical contact and so provoke movement. While moving the electrical contact, the

current will change from zero current to a pick-up current, which can be recorded and used as trigger criteria for electrical contact evaluation.

7.6.1 Basic Hardware Scheme with Mechanical Vibration Generator

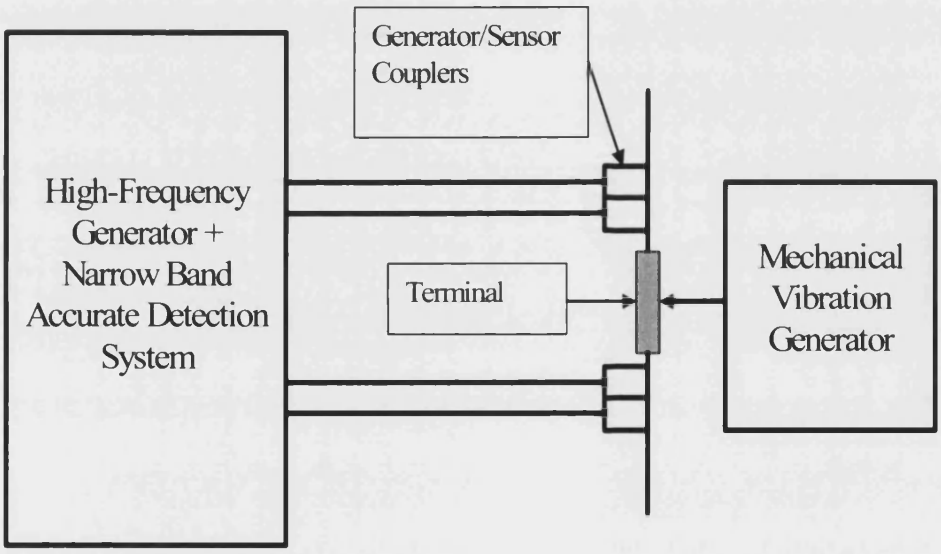

Figure 56 - Basic Hardware Scheme with Mechanical Vibration Generator

The method used in this research must satisfy certain conditions regarding practicability and usage of the test device:

- Low cost
- Small (handhold) size

- Simple to use

The method for injecting mechanical vibrations into the contacts will be by the use of mechanical pressure through sensors. In this case no extra mechanical vibration generator must be used. Specific mechanical construction (catch clamps) of the sensors will allow mechanical movement of the conductors.

7.7 Summary about Hardware

In Chapter 7 the general hardware design was explained. Requirements for the hardware design are to make a low-cost, light-weight portable device which can be used for research and investigation of the measuring principle. The hardware will be a combination of the high-frequency generator and the very narrow band accurate measurement which is connected to the test object via capacitive coupler. The explanation about selected capacitive coupler construction was clarified.

Figure 55 - Scheme of the hardware system shows the basic hardware design which incorporates the following inventions and functions:

- Separate circuits for signal generation measurement that will allow detection of the broken contact detection as explained before.
- Very accurate and sensitive current measurement with innovative filtering method using offset frequency
- Simple hardware design idea
- Flexible solution for research purpose

A further idea about connecting the mechanical vibration generator to the tested terminal to provoke weak contact moving was presented (see Figure 56).

References Chapter 7

1. A Technical Tutorial on Digital Signal Synthesis; Analog Devices 2003; Norwood Massachussetts;

2. Mixed Signal and DSP Design Techniques; Walter Kester; ISBN 0-916550-23-0; www.analog.com/Analog_Root/statistic/pdf/dataConverters/MixedSignal_Outline.pdf; Accessed on 01.03.2004

Chapter 8

8. Experimental Hardware Prototype

A prototype was developed based on hardware described in Chapter 7, section 7.5.

The experimental hardware which will be used for research in this thesis, must have some advanced and flexible features. These capabilities will be not necessarily be part of a later comercial product.

The experimental hardware must have the following capability:

- Recording capability with possibility to record measuring signals
- Online measurement of the current peak
- Adjustable parameters regarding:
    - o Signal Frequency
    - o Sampling length
    - o Offset frequency
    - o Decimation factor

- PC interface

In this chapter, the construction of the experimental hardware will be explained. Further, the problems with the first developed hardware prototype, and the functional improvements required, will be discussed.

8.1 Hardware Prototype – Technical Specification and Explanations

The basic technical specification of the experimental hardware prototype is displayed in the following table:

External Power supply	220 V ; 50 Hz
Internal Power supply	+/- 5V
Acquisition length	10 – 10000 Samples
Narrow band filtering	1 – 10 Hz
Default offset frequency	5 Hz
Signal frequency (DDS-frequency)	Adjustable 0 – 3 MHz ; Accuracy 0.5 Hz
Quartz sampling rate	20 MHz
ADC converter sampling rate	100 kHz
Current measurement sensitivity	≈10 nA
PC communication	RS232 (57600 Baud, 8 Bit, No parity, 1 Stop bit
Controlling Software	Tera Term Pro V2.3

Table 10: Technical specification – Hardware

The following figure shows the developed hardware module.

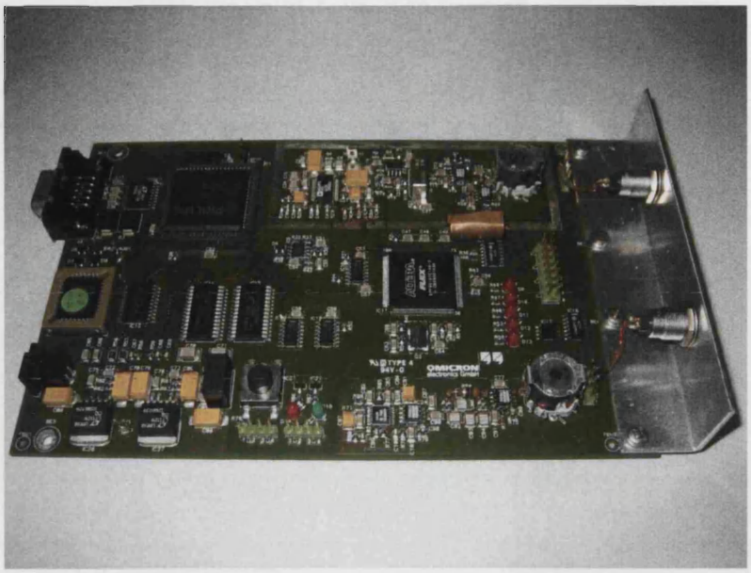

Figure 57-Basic module of the hardware prototype

The communication with the module works via the common serial RS232 interface (57600 Baud, 8 Bit, no parity, 1 stop bit) by means of a terminal program Tera Term Pro V2.3.

The software controls the selection of the adjustable parameters and gives information about the current status of the device. In the following figure the user interface for adjusting variable parameters of the device can be seen:

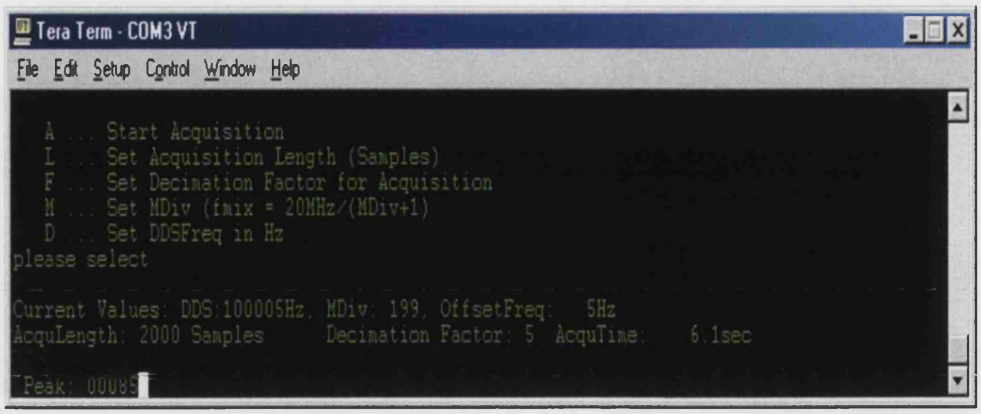

Figure 58 – User interface for the experimental hardware prototype

A….: Starts acquisition. Pressing the onboard key will trigger the start of the recording. The acquired samples are stored in onboard memory. After the finalisation of the acquisition the samples are sent out to the RS232 as ASCII text and can be recorded and stored to a file. The results are analysed using Excel.

L….: Adjusts the length of the acquisition in samples. The resulting duration of the recorded signal (in seconds) depends also on the setting of the decimation factor F and the setting of the sampling frequency (Range 10 – 10000 Samples)

F…..: Sets decimation factor F. With F set to 3 only every 3rd sample from the detector goes to memory. This decreases virtually the sampling frequency by a factor of three.

M…..: Divider factor adjusts the oscillator frequency for the mixer in the RX-path. The oscillator frequency can be derived according to Chapter 7, section 7.5, Equation 25: $F_1 = \frac{F_{REF\_CLK}}{M+1}$

Example:. M=199 leads to a oscillator frequency at the mixer input of 100kHz. ($F_1 = \frac{20MHz}{199+1} = 100kHz$)

D…..: Sets the DDS frequency in Hz (This is the generator frequency of the signal in the TX-path).

The actual settings and the actual measured value of the peak detector are displayed.

Peak: Peak shows peak value of the current measured by test device. This can be monitored online while measuring. The value of the peak will detect difference between close and open

contact. The peak value is very important for the measurement method and further explanation is provided:

EXPLANATION ABOUT PEAK: The current of the receiver electrodes is converted to a voltage and amplified in the first state. Further the voltage signal is forwarded to the mixer which is fed by an oscillator having a small frequency offset relative to the frequency of the receiving signal (i.e. 200 kHz +5Hz). The signal component at the frequency difference (offset in the example 5 Hz) is filtered and amplified before it is AC-coupled to a sigma delta AD-converter running at a sampling frequency of approximately 1 kHz. The AC coupling has the advantage of removing all offsets in the signal path. The sigma delta converter itself contains a high pass filter for the digital domain (cut-off below approximately 1 Hz). The sampled signal is the forwarded to a micro controller which handles memory allocation for capture of transient signals, rectifies the sampled signal and measures the "peak" value over period of approximately 100 ms. The peak value is displayed via RS232 on a terminal. The scaling between the displayed peak value and the real current through receiver electrodes will be experimentally derived. For the capture of transient signals it is possible to set a decimation factor which

enables a longer acquisition time at the expense of a less accurate sampling of the signal.

8.1.1 Testing of the first hardware prototype

After completion of the first prototype, several tests were performed to test the basic capability of the hardware module. All tests were performed using an oscillator frequency of 100 kHz; the offset frequency was 5 Hz.

The following measurements with the experimental hardware have been performed:

- **Measurement 1.** : Without connected couplers:
  - o Detector shows a peak value of 138 (See figure below, value in the left bottom corner)

Figure 59: Current peak measurement without connected sensors – first hardware prototype

- **Measurement 2.** : Couplers are connected at the solid terminal contact. (See figure below)

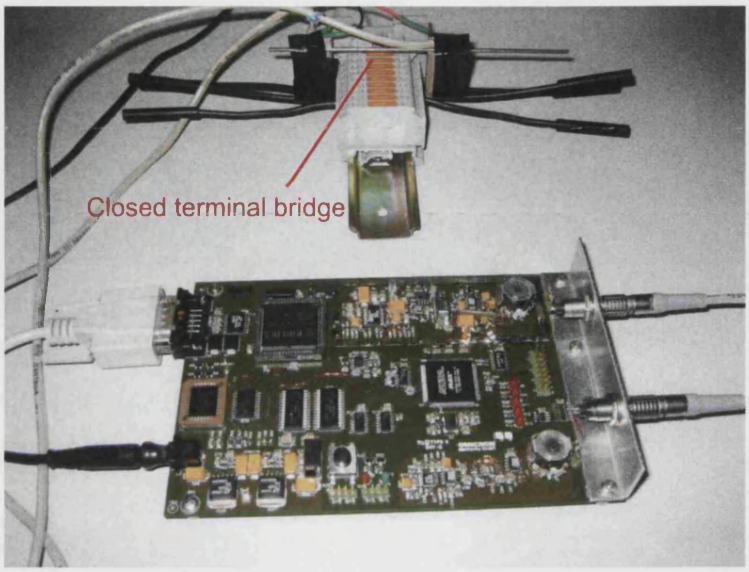

Figure 60: Measurement of the solid terminal contact with Closed terminal bridge

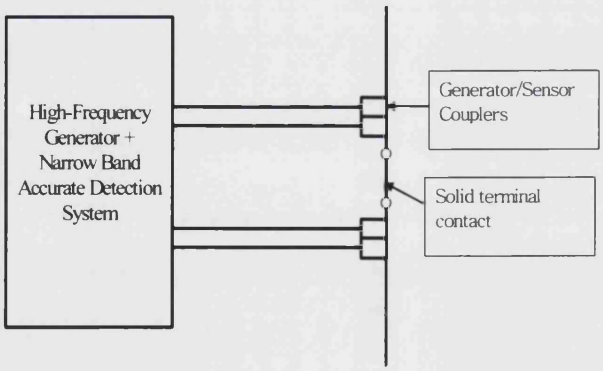

Figure 61: Measurement 2 – close terminal bridge – solid contact

o Detector shows a peak value of approximately 324 (See figure below, value in the left bottom corner)

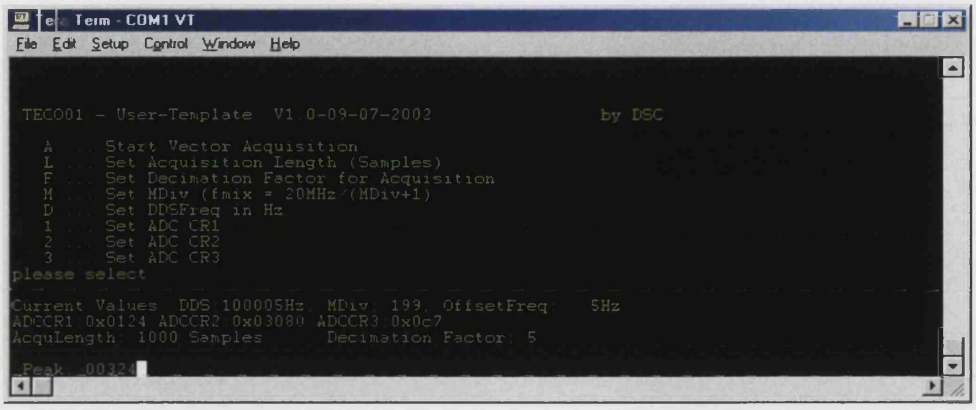

Figure 62: Current peak measurement with connected sensors to solid terminal contact

- Measurement 3.: Couplers are connected to the broken terminal contact (Opened terminal bridge see figure below).

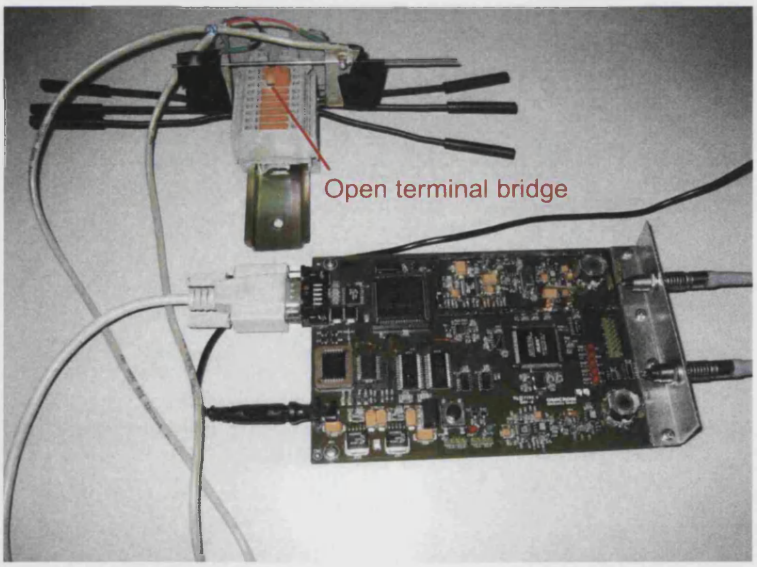

Figure 63: Measurement of the broken terminal contact with opened terminal bridge

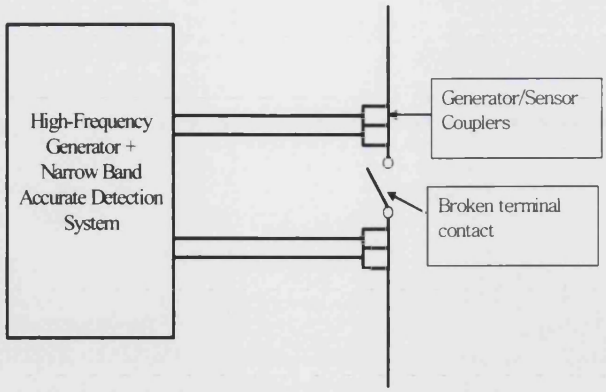

Figure 64: Measurement 3 – Open terminal bridge – broken contact

o Detector shows a peak value of 417 (See Figure 65, value in the left bottom corner)

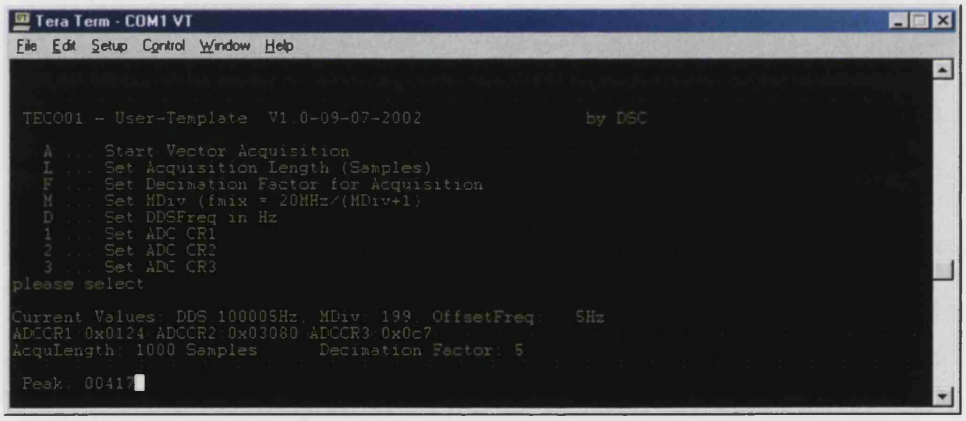

Figure 65: Current peak measurement with sensors connected to the broken (open) terminal contact–First hardware prototype

8.1.2 Summary about measurement with first hardware prototype

Measuring Nr.	Measuring Case	Peak Current Value
1	Without Couplers	138
2	Solid terminal contact	324
3	Broken terminal contact	417

Table 11: Mesurement of the first hardware prototype

As can be seen from table 11, the delta peak value (as explained below) between measurements of the solid terminal contact and broken terminal contact is 93.

$$\Delta = (PeakBrokenContact - PeakSolidContact) = 417 - 324 = 93$$

Equation 27: Delta peak value with first hardware prototype

Sensitivity of the measurement can be calculated as :

$$Msensitivity = \frac{PeakBrokenContact}{PeakSolidContact} = \frac{417}{324} \approx 1.3$$

Equation 28: Hardware measurment sensitivity

This value is very important for the feature test device. This value is main criteria which will be used to detect difference between solid and broken contact.

The result of the measurements with the first hardware prototype has not been satisfactory. Especially the delta peak value between current peak on solid and broken contact (measurement sensitivity) was too low and the peak value detected without connected test object was too high.

8.1.3 Problems with the First Hardware Prototype

The following problems have been detected with first hardware prototype:

- Stability problem of TX amplifier
- Direct coupling of TX path with RX path
- Undefined offset/bias behaviour of the first state in the RX path
- Passband frequency of TX-filter too low- approximately. 1MHz

- High virtual measured peak current without connected couplers
- Delta peak value too small between open and close contact (low measurement sensitivity)

In the following measurements (see Table 12 and Figure 66) with different signal frequencies and disconnected couplers the above described problems can be seen. Without connected couplers the measurement will measure virtual current (peak) caused by direct coupling between TX and RX path.
Measurements without connected couplers were made to evaluate capacitive coupling between TX and RX path of the hardware. A frequency sweep from 50 kHz to about 4 MHz has been done and results can be seen in the table below.

DDS Frequency (Hz)	MDiv	Signal frequency before mixer	Signal frequency After mixer	Peak value without sensors
50005	399	50000	5,000	125
60065	332	60060,06006	4,940	140
69935	285	69930,06993	4,930	145
80005	249	80000	5,000	180
90095	221	90090,09009	4,910	155
100005	199	100000	5,000	50
109895	181	109890,1099	4,890	135
119766	166	119760,479	5,521	125
129875	153	129870,1299	4,870	110
139865	142	139860,1399	4,860	100
150381	132	150375,9398	5,060	85
160005	124	160000	5,000	65
169497	117	169491,5254	5,475	45
180185	110	180180,1802	4,820	30
190482	104	190476,1905	5,810	35
200005	99	200000	5,000	55
210532	94	210526,3158	5,684	85
219786	90	219780,2198	5,780	125
229890	86	229885,0575	4,943	275
240969	82	240963,8554	5,145	540
250005	79	250000	5,000	270
298513	66	298507,4627	5,537	55
444450	44	444444,4444	5,556	150
500005	39	500000	5,000	175
555561	35	555555,5556	5,444	200
606066	32	606060,6061	5,394	230
689660	28	689655,1724	4,828	280
800005	24	800000	5,000	320
909096	21	909090,9091	5,091	480
1000005	19	1000000	5,000	360
1176476	16	1176470,588	5,412	350
1538467	12	1538461,538	5,462	242
1818187	10	1818181,818	5,182	15
2000005	9	2000000	5,000	15
2500005	7	2500000	5,000	25
2857148	6	2857142,857	5,143	30
3333338	5	3333333,333	4,667	27
4000005	4	4000000	5,000	26

Table 12: Measurement of the peak value without connected sensors with frequency sweep between 50kHz and 4 MHz

Graphical representation of the measurement results can be seen in the figure below.

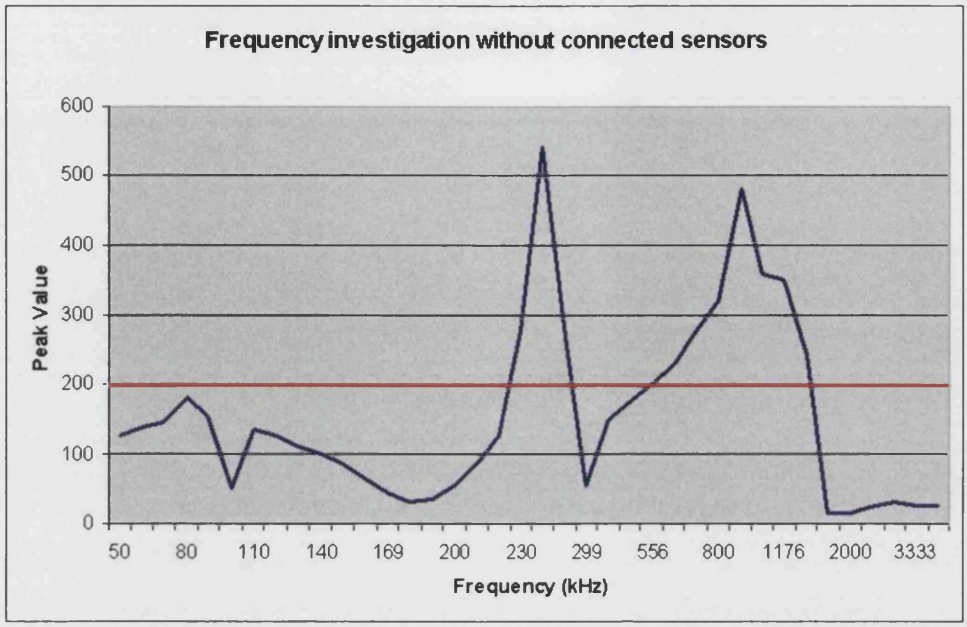

Figure 66: Capacitive coupling and dissipation of the hardware prototype without connected sensors

As can be seen from the graph above some frequencies are showing high peak value i.e. 220 - 250 kHz or 690 kHz- 1.2 MHz. The reason is resonant effects at specific frequencies and direct coupling between TX and RX path.

The problem of the pass band filter frequency of 1 MHz can be seen that all peak values above 1.2 MHz are cut-off. Frequencies in the range from 100 to 200 kHz are showing relative low capacitive dissipation without connected couplers.

8.1.4 Improvements of the hardware prototype

To improve the hardware behaviour and correct the above described problems, the following hardware improvements have been made:

- Stability problem of TX amplifier:

  Additional decoupling, in the TX amplifier output to the TX coil was added to decouple reactive load. This prevents the amplifier from oscillating.

- Direct coupling of TX path with RX path

  One of the main problems of the first hardware prototype was a coupling from the TX- (high signal level) to the RX-path (high sensitivity, small level). The dominant part of this coupling occurs across the common power supply +/-5V. A strict separation of the power supplies between TX- and RX-path is essential and will help to achieve better results.

  Additionally, additional shielding of the RX paths has been provided. Furthermore, improvement of the decoupling circuits, especially from the power supply has been made.

Unfortunately, the shielding of the RX-path had not showed positive effects. The coupling problem becomes smaller, but is still present.

- Undefined offset/bias behaviour of the first state in the RX path

  To solve this problem an additional regulation circuit for proper adjustments of the bias values was provided. The oscillator signal level, which is feeding the mixer, was improved.

- The passband frequency of the TX-filter was changed from approximately 1MHz to. 4.5MHz

- High virtual measured peak current without connected couplers

  Direct coupling of TX path with RX path produce a virtual peak current, as displayed in the previous section, which has a peak of 138 without connected capacitance couplers. The shielding of the RX-path did not show positive effects.

  Further the mathematical calibration of this value will be investigated.

- Delta peak value too small between open and close contact (low measurement sensitivity)

There are several reasons for the small delta peak measuring level between open and close contacts:

- High virtual current without connected conductors
- Weak capacitive coupling between conductor and couplers
- Stray capacitances too high
- Problems in the hardware construction (described above)

Weak capacitive coupling and high stray capacitances are mostly caused by the construction of the capacitive couplers. In the following section the improvement of the couplers will be explained.

8.1.4.1 Problems with couplers

Different positions of the coupler relative to the conductor during measurement have been investigated.

Measurements were made with different sensor positions relative to the conductor (geometry influence) See Figure 67.

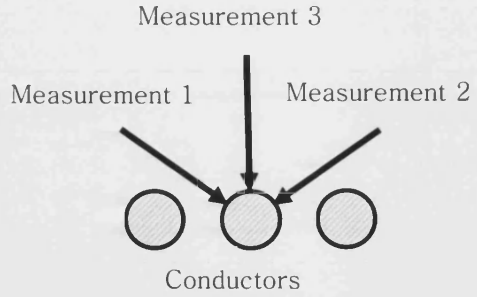

Figure 67: Position of the sensors for average measurement

Further in the table below, the measurement of the average peak value (with different couplers position) with the broken contact and average peak value with the solid contact has been presented.

	Measurem. Broken Contact:				Measurem. Solid Contact:					
DDS Freq. (Hz)	1	2	3	Average:	1	2	3	Average:	Delta - Peak value	Sensitivity factor
100005	350	660	620	543	220	280	340	280	263	1,9

Table 13: Influence of the coupler position on the peak measurement

As can be seen different values are measured, dependent on the coupler position to the conductors.

The main reason for such phenomena (different measurement results which are depending on the coupler relative position to

the conductor) is the non-optimal construction of the capacitive couplers (Sensors and electrodes). The general screening problem on the capacitive couplers was detected. The dissipation (stray) capacitance was very high, which is the main cause of the coupler positions affecting the measuring values.

The following weak points in the coupler construction are pointed out:

1. Non-optimal screening of the measurement cables
    - o High frequency signals and very sensitive measurements are influenced by the stray radiation (non-optimal screened generator and measurement cables) and the measurement was very dependent of the coupler position.

2. Weak varnish insulation between couplers and their screen
    - o Weak varnish insulation does not produce good capacitive coupling. Additionally, several times short circuits between the couplers and corresponding screen occurred during measurement.

3. Non-optimal connections between cables screens and conductor screens

   o Connection of all screens (cable screens and coupler screens) to one potential was not performed properly. This had an influence on the disturbances in the measurement signals.

In the figure below are pointed, weak points in the construction of the couplers:

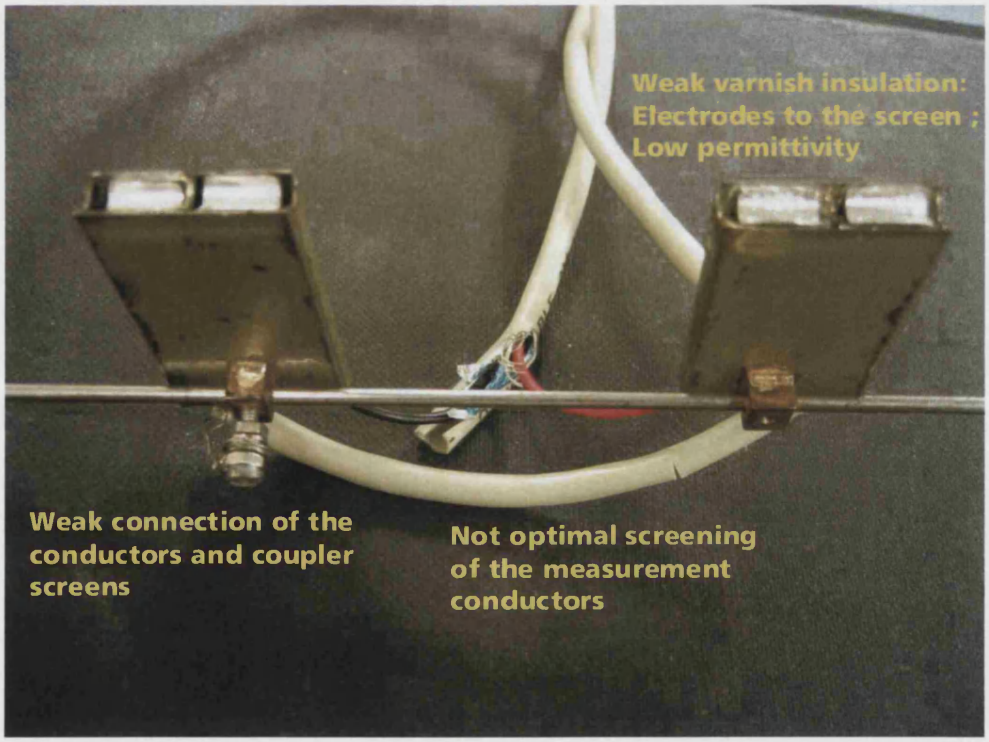

Figure 68: Problems with couplers

8.1.4.2 Couplers improvement

The following improvements were made in the construction of the couplers:

- All connecting cables have been screened properly. (see picture in the next figure)
- Weak varnish insulation has been exchanged with insulation transparent film. This will improve permittivity and will prevent short circuits between couplers and screen.
- The cable screens and coupler screens are connected together to the same potential. (see picture in Figure 69)

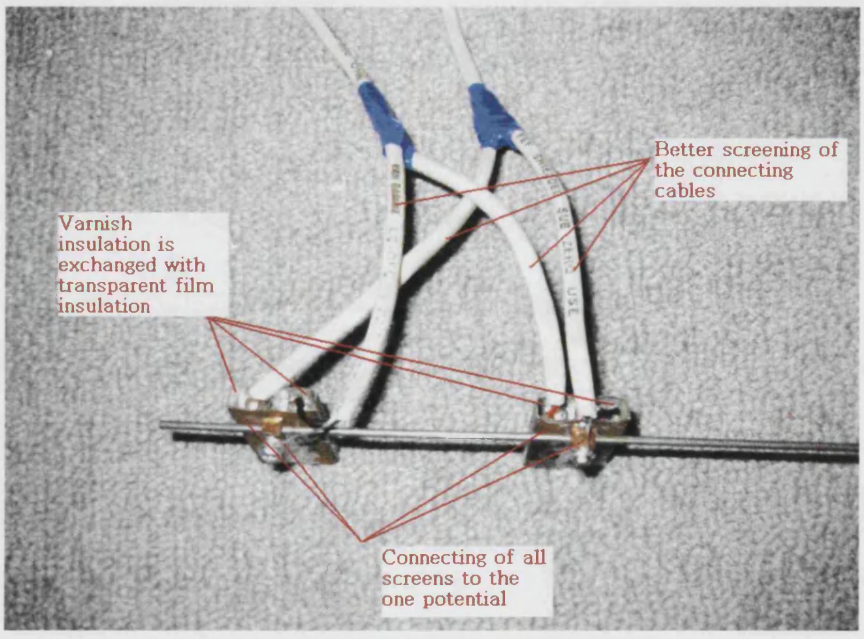

Figure 69: Coupler improvements

The described improvements of the couplers will have the following influences on the measurement method:

- better capacitive coupling will cause larger current (easier measurement)
- lower stray (dissipation) capacitance will force more accurate and sensitive measurement
- low influence of the coupler position on the measurement will cause more stable measurement results

8.1.4.3 Compensation of the stray capacitances

The current which is measured without couplers connected to the test object is caused by the following reasons:

- Direct coupling of TX path with RX path in the hardware:
- Stray capacitances (dissipation) between
    - o generator and sensing couplers
    - o couplers and screen

As has been described in the section 8.1.4, the shielding of the RX-path had not showed positive effects. The direct coupling problem between TX and RX path, becomes smaller, but still present.

In the section 8.1.4 the idea about mathematical calibration of the current caused by effects presented above was given. The value of the peak which is measured without couplers connected to the test object (measurement with couplers in the air) will be subtracted from the peak values measured by open and close contacts.

New entries in the user interface menu are developed:

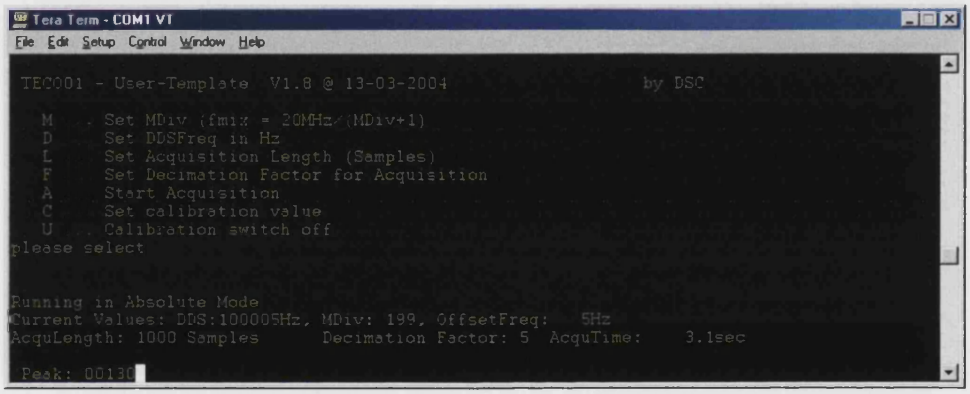

Figure 70: New user interface

C - Switch to calibration mode and uses the current peak value as the calibration offset. Current peak is subtracted from the actual peak and displayed as corrected peak value

U - Switch back to the normal mode

EXAMPLE:

- Measurement frequency 200005 Hz
- Measured peak value - contact open - 1680

- Measured peak value – contact closed – 840
- $\Delta = (PeakBrokenContact - PeakSolidContact) = 1680 - 840 = 840$
- $Msensitivity = \frac{PeakBrokenContact}{PeakSolidContact} = \frac{1680}{840} = 2.00$
- Coupler removed from conductor and calibration performed-> CP calibration offset = 940
- Coupler again connected to the conductor
- Measured peak value – contact open – 920 (with calibration on)
- Measured peak value – contact closed – 3 (with calibration on)
- $\Delta = (PeakBrokenContact - PeakSolidContact) = 920 - 3 = 917$
- $Msensitivity = \frac{PeakBrokenContact}{PeakSolidContact} = \frac{920}{3} = 306.6$

As can be seen in the example above, using the calibration does not have big influence on the delta peak value but the measuring sensitivity is greatly increased.

Hardware prototype has two modes of measurement:

1. Online peak monitoring mode via PC user interface

2. Acquisition mode which saves recorded signal for later post processing.

The described calibration mode can be activated in the online peak monitoring mode only, and it does not affect the acquisition (recording) mode.

8.1.5 Testing of the improved hardware prototype

After the completing the described improvements, the hardware performance was tested and the results showed a level construction for further research.

Similar to the first hardware prototype, all tests were performed at an ADC oscillator frequency of 100 kHz, offset frequency 5 Hz

The same tests as for the first hardware prototype were performed:

- **Measurement 1.** : Couplers are not connected:
    - o Detector shows a value of approximately 114

The peak level (due to dissipation) without connected sensors dropped, in comparison with the old hardware, from appr.138 on appr.114. The reason for such a small drop (improvement) is still due to coupling present between the TX and RX path.

Peak level without connected couplers should be zero and hardware improvement did not showed satisfactory results.

To compensate for this effect, the calibration described in the section 8.1.4.3 is performed. The peak value without connected couplers (virtual peak) can be calibrated (compensated) yielding a new value of 4, see figure below:

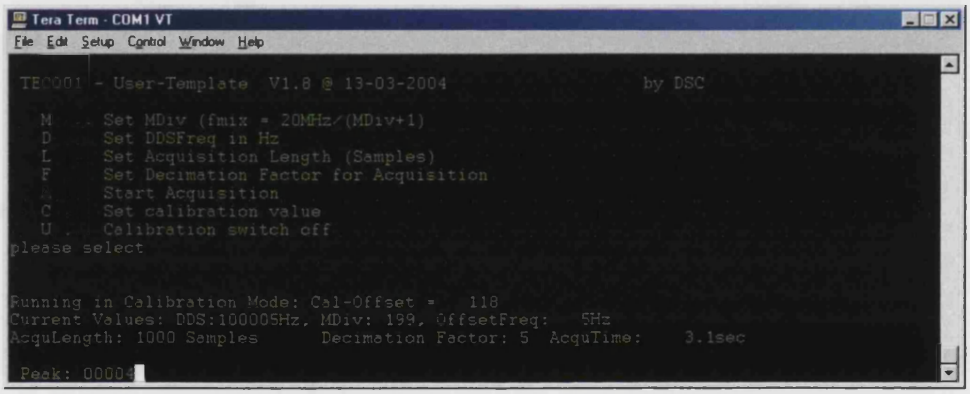

Figure 71: Calibration mode

- **Measuring 2.** : Couplers are connected to a solid terminal contact (See Figure 60: Measurement of the solid terminal contact with Closed terminal bridge)
    - o Detector shows a value of approximately 300

- **Measurement 3.**: Couplers are connected to the broken terminal contact (Opened terminal bridge see Figure 63:

Measurement of the broken terminal contact with opened terminal bridge).

- Detector shows a peak value of approximately 680

8.1.6 Summary about measuring with improved hardware prototype

Measuring Nr.	Measuring Case	Peak Current Value
1	Without Sensors	114
2	Solid terminal contact	300
3	Broken terminal contact	680

Table 14:Measuring of the first hardware prototype

As can be seen from Table 14, the delta peak value between measurement at solid terminal contact and broken terminal contact is approximately 380.

$$\Delta = (PeakBrokenContact - PeakSolidContact) = 680 - 300 = 380$$

Equation 29: Delta peak value with improved hardware prototype

The sensitivity of the measurement can be calculated as:

$$Msensitivity = \frac{PeakBrokenContact}{PeakSolidContact} = \frac{680}{300} \approx 2.7$$

Equation 30: Hardware measuring sensitivity –Improved hardware

The sensitivity of the device improved significantly in comparison with the first hardware prototype.

In the following table can be seen comparisons between measurements made with the first and improved hardware prototypes.

Case	First HW	Improved HW
Without Sensors	134	114
Solid Contact	328	300
Broken Contact	417	680
Delta	93	380
Sensitivity	1.3	2.7

Table 15:Comparison of the first and improved hardware prototype

A real improvement of the hardware can be seen when the calibration function is used. The difference between the solid

and broken contact states is easily distinguished, as shown in the Table 16:

Case	Improved HW	Improved HW with calibration ON
Without Sensors	114	0
Solid Contact	300	10
Broken Contact	680	370
Delta	380	360
Sensitivity	2.7	36.0

Table 16: Impact of calibration function

8.1.7 Conclusions about Hardware Prototype.

The major task for developing hardware prototype is to help research and investigation of the new testing method for electrical contacts evaluation described in this thesis.

This hardware prototype is research hardware only. For later commercial product design many parts must be changed and simplified. Further research will be defined in the conclusion of the direction and requirements on the future product development. The features, e.g. recording of the signal for example, will not be needed in the commercial product at all.

A satisfactory level of the hardware performance was achieved, although the problem of coupling between TX and RX path was not solved completely. Future hardware improvements might be possible by some averaging algorithms which can be done in the FPGA (hardware-solution) or in the micro-controller (software-solution).

8.2 Evaluation of the Theoretical Investigations with developed hardware

In this section the hardware prototype will be used for evaluation of the mathematical and MATLAB simulations described in the Chapter 6.

The MATLAB simulations are functions $\mathrm{Im} = f(\overline{Z})$ which describes the current flow through the contact impedance capacitivelly coupled to the sensor:

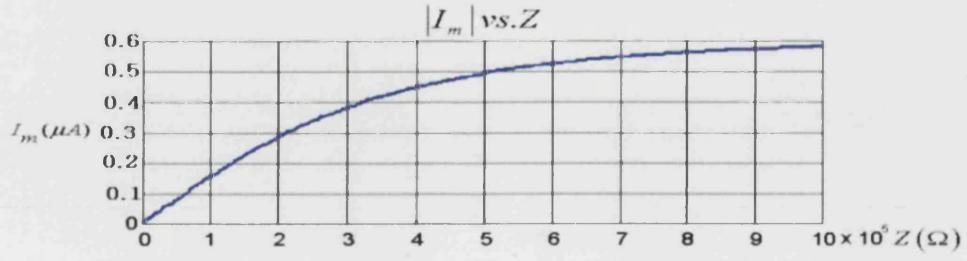

Figure 72: MATLAB Simulation at $1MHz$ and $1M\Omega$

The hardware prototype measures the current peak value scaled to the TX voltage only and not the current Im. As was explained in the section 8.1, the peak value is measured as the peak of the average digital value of the voltage signal after AD converter. In the following section the relationship between current Im and peak value will be made. For this calculation the couplers capacitance must be known or measured. In our experiment the couplers will be simulated with defined known capacitances.

The following experimental setup was used:

- Generator is coupled with capacitors 4 x 1pF (2 x 2 in series) and approximately 15 cm twisted pair wire.
- Sensor is coupled with capacitors 4 x 1pF (2 x 2 in series) and approximately 15 cm twisted pair wire.
- Signal frequency 200005 Hz

In Figure 73 experimental simulation setting is presented:

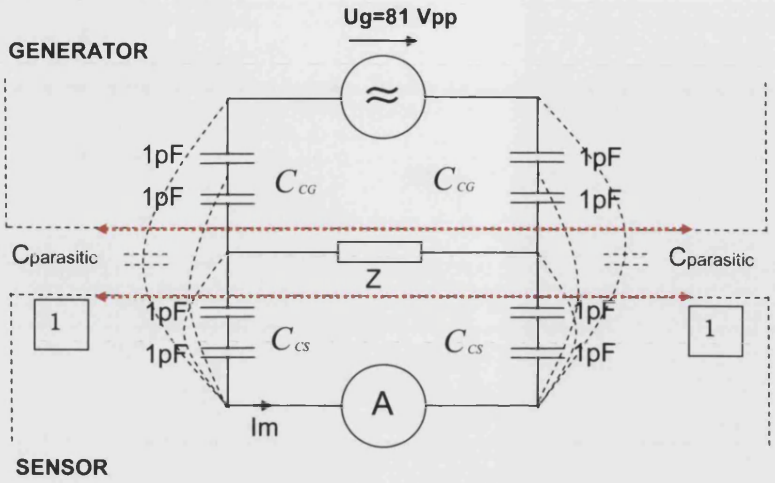

Figure 73: Experiment setup – Evaluataion of the theoretical investigation

C_{CS} – Coupling capacitances – measurement

C_{CG} – Coupling capacitances – generator

Z – Contact impedance

- Measurement 1 – Simulation of the parasitic coupling of the measurement setup (couplers in the air):

  Coupling capacitances from the sensors C_{CS} are disconnected (showed in the figure above with line 1). I_M is caused by parasitic capacitances only.

$$I_{M1} = U_G j\omega C_{PARASITIC} / 2$$

  Detector shows current peak value of: 1205

- Measurement 2: Simulation of the measurement of an open contact ($Z = \infty$)

  Coupling capacitance from sensors and generators are connected (simulation with chip capacitors 0.5 pF)

  $$I_{M2} = U_G j\omega(C_{PARASITIC}/2 + C_C)$$

  $$C_C = \frac{1}{8} pF$$

  Detector shows current peak value of: 6530

- Measurement 3: Simulation of the measurement of a closed contact ($Z = 0$)

  Coupling capacitance from measuring sensors and generators are connected (simulation with chip capacitors 0.5 pF)

  Detector shows peak value of: 120

  Following calculations can be made:

  Measurement 1: $I_{M1} = I_{PARASITIC}$ $U_{PEAK} = 1205$

  Measurement 2: $I_{M2} = I_{PARASITIC} + I_{SENSOR}$ $U_{PEAK} = 6530$

  $I_{SENSOR} = U_G j\omega C_C$

  $C_C = \frac{1}{8} pF$

  $f = 200kHz$

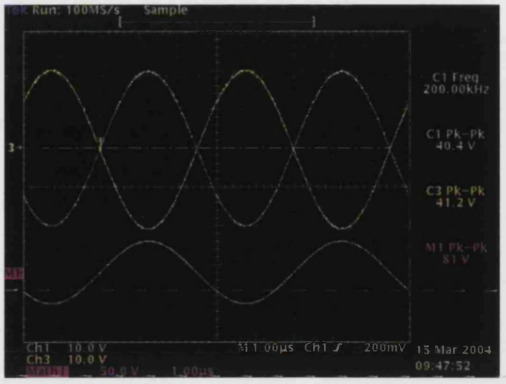

Figure 74: Measurement of the TX – Voltage

$U_G = 81Vpp$ (peak-peak value) see figure above

$I_{SENSOR} = U_G j\omega C_C = 12.7\mu A$

$I_{SENSOR} \cong U_{PEAK} = 6530 - 1205 = 5325$

$\Rightarrow 12.7\mu A$ corresponds to the peak of 5325

$$\boxed{Peak\_1000 \Leftrightarrow 2.4\mu A}$$

With this relationship the peak value can be related to the current.

This corresponds to the used signal frequency of 200 kHz. The peak value to the measuring current function is linear with frequency.

Measurements with different value of the contact resistance can be seen in Figure 75:

R (kOhm)	Upeak @ 100kHz	Upeak @ 200kHz
1	280	290
5,11	280	330
21,2	290	400
100	350	1030
1000	1300	5130
10000	2485	6530

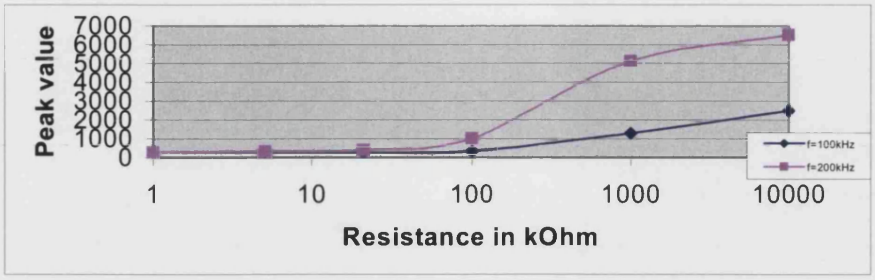

Figure 75: Simulation of the contact resistance vs. I_M

In the simulations shown in the Figure 72: MATLAB Simulation at $1MHz$ and $1M\Omega$,current is scaled to the TX-voltage from 1V. The simulated current at $1MHz$ and $1M\Omega$ is $0.6\mu A$.

If the scaling in the simulation will be changed to the 81Vpp (from 1Vpp) the current Im will be:

$$0.6\frac{\mu A}{V}\times 81V = 48.6\mu A$$

This value is valid at 1MHz. Our measurement with hardware is made with a signal frequency of 200 kHz. Recalculation from 1MHz to the 200 kHz will give:

$$I_{MATLAB} = 48.6\mu A \times \frac{200kHz}{1MHz} = 9.72\mu A \text{ at 200 kHz}$$

$$I_{MEASURED} = 12.7\mu A \text{ at 200 kHz}$$

The values which are calculated/measured are very close to each other (9.72 and 12.7μA) and after presenting in the logarithmic scale can be seen that the trends and curve slope are exact comparable. (see figure below)

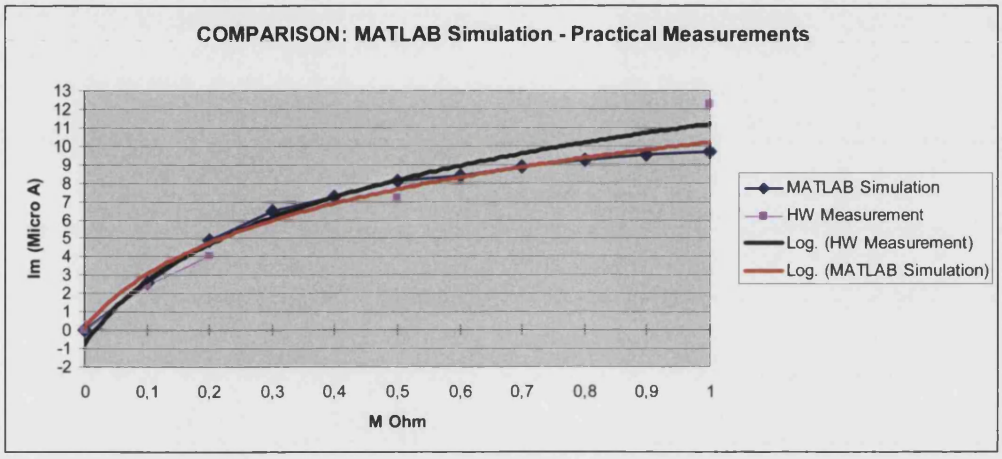

Figure 76: Comarison of MATLAB Simulation with practical measurements

In conclusion, it can be stated that theoretical investigations made earlier in this thesis have been proved to be correct with the experimental hardware.

8.3 Summary of the Chapter 8 – Hardware prototype

In Chapter 8 the construction and development of the hardware prototype according to the scheme shown in the Figure 55, was performed. First, the hardware prototype was described and its behaviour was tested. Detected problems with the first hardware prototype have been listed. Furthermore the improvements made on the hardware module were presented. Additional measurements and tests with improved hardware have been performed. Comparison between first and improved hardware have been presented and explained.

Theoretical investigations of the test method has been evaluated with hardware prototype.

The performance level of the hardware behaviour was not 100% but however all measurements were accurate.

Chapter 9

9. Experimental Work

9.1 Introduction

The major task of the experimental work was to evaluate the research idea. The principle for detecting broken and solid contacts, embodied in the improved hardware prototype described in the Chapter 8, will be used. The phenomena of broken (faulty) and solid contact must be detected using the described hardware prototype. Additional investigations about the test signal frequency must be performed. The test signal frequency which allows optimal coupling and measured results must be investigated for later use.

A real model of the test object (different types of substation terminals and conductors) was constructed as shown in Figure 77:

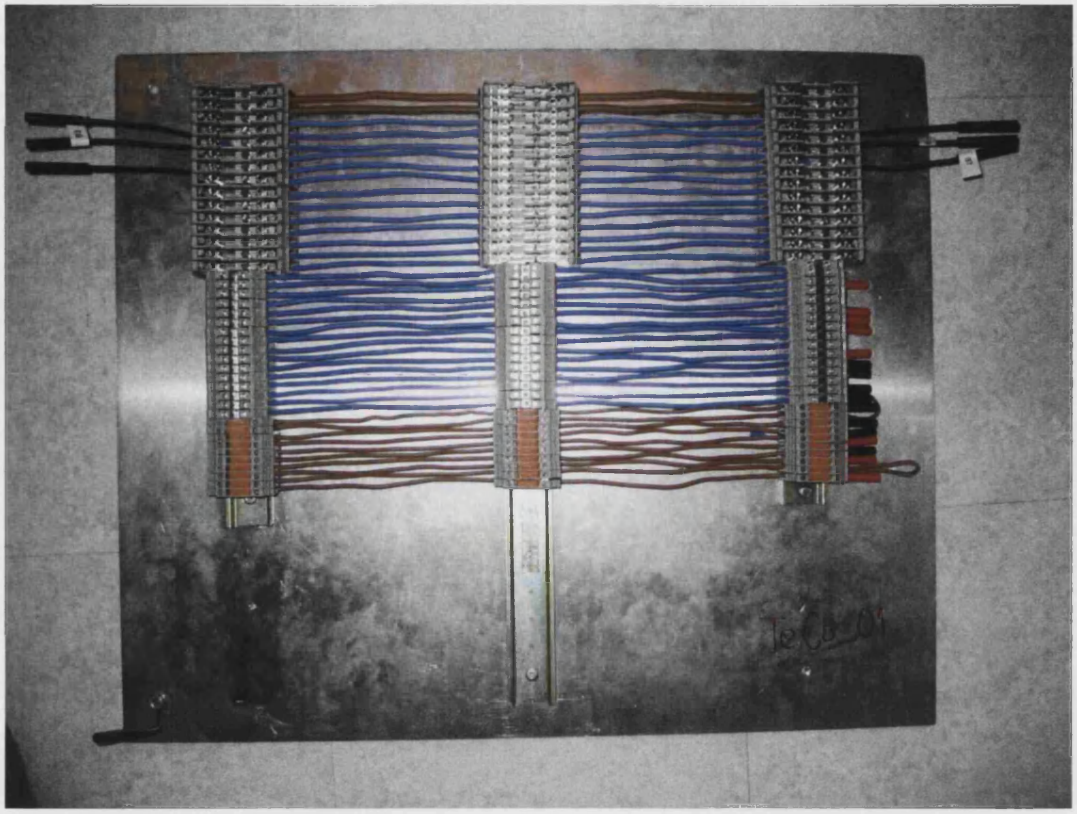

Figure 77: Real model of the test object

Following topics must be done inside of experimental work:

- Investigation and selection of the test signal frequency
- Influence of the background metal plate
- Influence of the neighbouring conductors
- Influence of the parallel load
- Investigation of the influence of superimposed vibrations
- Detection of the weak contact
- Successful detection of unknown broken and solid contact on the real test object model

9.2 Frequency Investigations

In this section, the signal frequency to be used in the measurement method will be investigated.

9.2.1 Measuring without connected couplers

In the Figure 78 measurements without connected couplers will be performed. The reason for this is to investigate eventual capacitive dissipation coupling inside of the experimental hardware. The peak value as the function of the signal frequency is presented. (Table with measurements see Appendix 16)

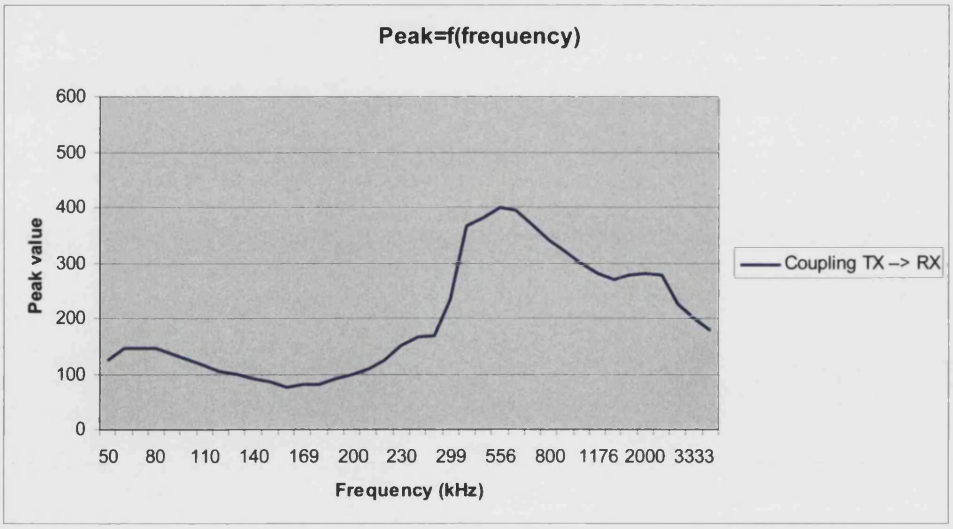

Figure 78: Variation of peak value with frequency

As can be seen in the figure above the problem of the coupling between TX and RX path is still present but the measuring results are satisfactory. The lowest value is measured for frequencies in the range from 100 and 300 kHz and out of this range the selection of the used frequency will be chosen.

9.2.2 Measuring of the transition between open and close contact in terms of frequency

For the measurement of the transition between broken and solid contact, a special terminal with a bridge was used. A broken terminal contact will be simulated with opened bridge and a solid terminal contact will be simulated with a closed terminal bridge (see figure below).

Figure 79: Open terminal bridge – Simulation of broken contact

Figure 80: Closed terminal bridge – Simulation of solid contact

The table below presents the measurement results. The value of the peak for broken contact and solid contact, are displayed as delta peak value with sensitivity factor.

$$\Delta = \left(PeakBrokenContact - PeakSolidContact \right)$$

$$Msensitivity = \frac{PeakBrokenContact}{PeakSolidContact}$$

	Uncalibrated					Calibrated				
DDS Freq. (Hz)	PV: air	Peak: Broken	PV: Solid	DPV	SF*500	PV: air	PV: Broken	PV: Solid	DPV	SF
50005	160	200	165	35	606,06	0	45	1	44	45,0
60065	185	270	195	75	692,31	0	75	10	65	7,5
69935	205	330	230	100	717,39	0	125	25	100	5,0
80005	229	425	270	155	787,04	5	135	15	120	9,0
90095	277	470	310	160	758,06	0	200	20	180	10,0
100005	325	570	340	230	838,24	0	295	20	275	14,8
109895	385	720	410	310	878,05	0	330	30	300	11,0
119766	431	880	490	390	897,96	10	430	30	400	14,3
129875	478	1015	550	465	922,73	5	520	35	485	14,9
139865	553	1155	580	575	995,69	10	640	45	595	14,2
150381	587	1275	620	655	1028,23	10	740	40	700	18,5
160005	652	1350	670	680	1007,46	0	700	35	665	20,0
169497	685	1420	640	780	1109,38	0	680	30	650	22,7
180185	724	1700	690	1010	1231,88	0	1000	25	975	40,0
190482	779	1800	620	1180	1451,61	0	1090	5	1085	218,0
200005	807	1950	750	1200	1300,00	0	970	5	965	194,0
210532	1002	1850	780	1070	1185,90	15	920	5	915	184,0
219786	875	1770	780	990	1134,62	10	880	5	875	176,0
229890	957	1800	730	1070	1232,88	10	670	5	665	134,0
240969	1020	1720	880	840	977,27	0	1160	5	1155	232,0
250005	985	2200	930	1270	1182,80	15	770	5	765	154,0
298513	1039	1700	780	920	1089,74	0	800	5	795	160,0
444450	813	1390	630	760	1103,17	0	550	5	545	110,0
500005	627	1150	580	570	991,38	0	400	5	395	80,0
555561	567	856	520	336	823,08	5	250	5	245	50,0
606066	513	650	450	200	722,22	0	195	5	190	39,0
689660	421	550	380	170	723,68	5	235	5	230	47,0
800005	383	495	330	165	750,00	3	130	5	125	26,0
909096	317	380	290	90	655,17	5	35	5	30	7,0
1000005	299	315	280	35	562,50	0	20	5	15	4,0
1176476	276	275	265	10	518,87	1	15	1	14	15,0
1538467	251	252	252	0	500,00	1	1	1	0	1,0
1818187	251	248	248	0	500,00	0	1	1	0	1,0
2000005	251	260	260	0	500,00	0	1	1	0	1,0
2500005	234	275	244	31	563,52	0	10	1	9	10,0
2857148	200	225	206	19	546,12	0	34	10	24	3,4
3333338	218	237	223	14	531,39	0	25	8	17	3,1
4000005	174	193	189	4	510,58	0	22	10	12	2,2

Table 17: Frequency investigation – open close transition – Delta peak – Sensitivity

PV – Peak Value

DPV – Delta Peak Value

SF – Sensitivity Factor (is scaled by 500)

Out of the previous table following dependencies can be presented:

- Delta Peak – DP=f(frequency) – see following Figure 81
- Sensitivity Factor – SF=f(frequency) – see Figure 82

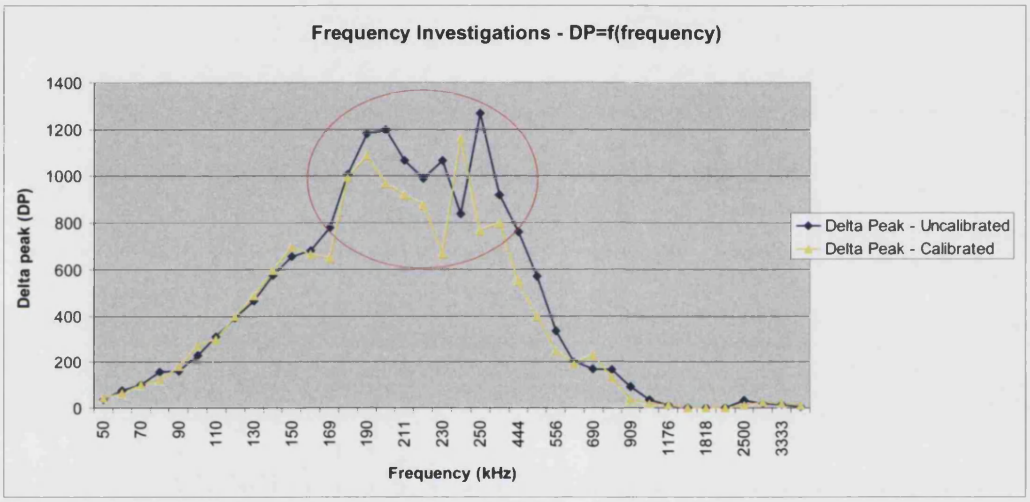

Figure 81: Frequency investigation – Optimal frequency range – Delta Peak (DP)

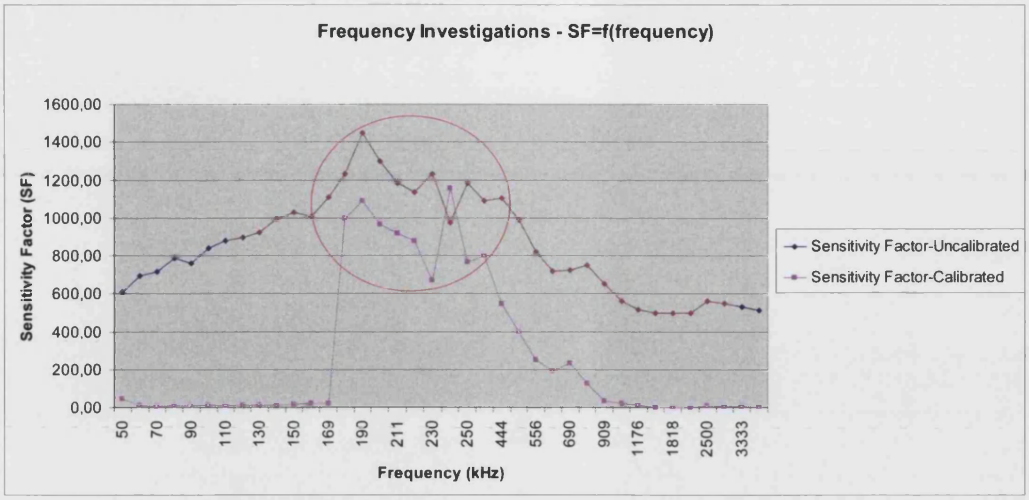

Figure 82: Frequency investigation – Optimal frequency range – Sensitivity Factor (SF – scaled by 500)

Through previous investigations the additional problem of high capacitive loads was detected. The generator capability is unable to supply loads for the frequencies above approximately 400 kHz – 500 kHz. Recordings of the voltage signal before and after amplifier (driver) show the following waveforms:

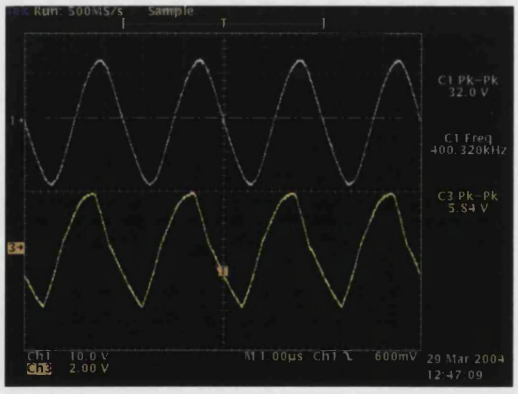

Figure 83: Generator output at 400 kHz

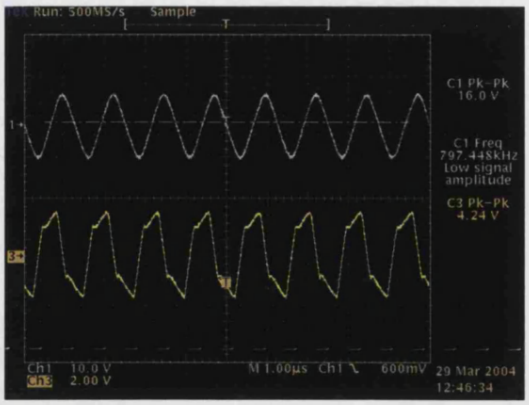

Figure 84: Generator output at 800 kHz

From simple theory, the voltage at the detector should be directly proportional to the frequency. But with the existing hardware the supply cannot deliver a constant output level at higher frequencies that decrease the detectable value. The generator is overstressed at high frequencies – a better supply is required for frequencies above 400 kHz.

Optimum frequency is very dependant on the parameters of the hardware: for the actual hardware frequencies above 400 kHz are not appropriate for this investigation. The previous research and literature research have show that the signal frequency to be used in this method must not be too high due to the radiation phenomena and problems of neighbouring connectors. It was stated that the optimal signal frequency should be placed somewhere around 200 kHz. For this reason

the hardware capabilities are satisfactory and additional hardware improvement is not necessary.

The optimal frequency will be selected as the frequency which gives best capacitive coupling, largest delta peak value (DP) and best sensitivity factor (SF). In the Figure 81 and Figure 82 the optimal frequency range is labelled and in Figure 85 summary of these can be presented.

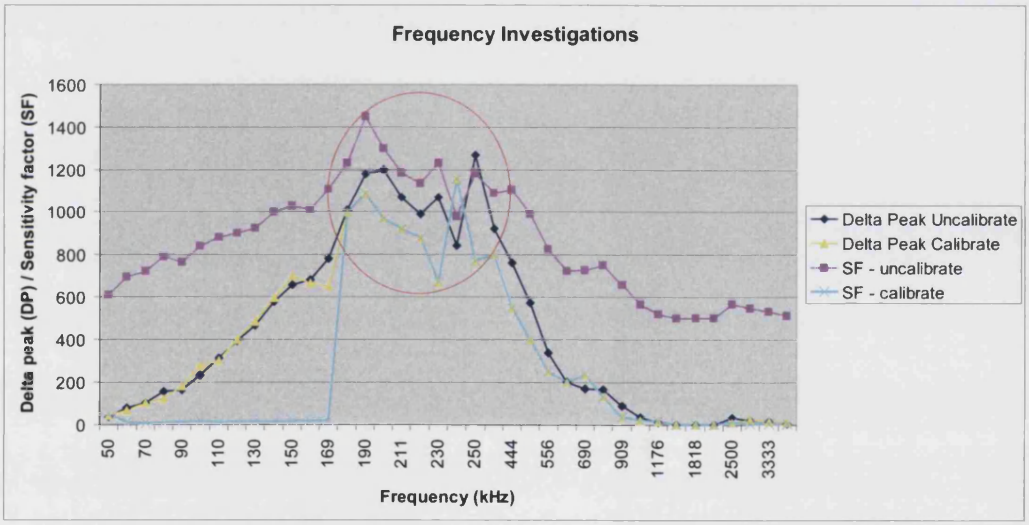

Figure 85: Optimal frequency range (SF scaled by 500)

As can be seen in the figure above, the optimal frequency will be out of the range from approximately 190 until 300 kHz. In Figure 86 more detailed presentation of the interesting frequency range is presented:

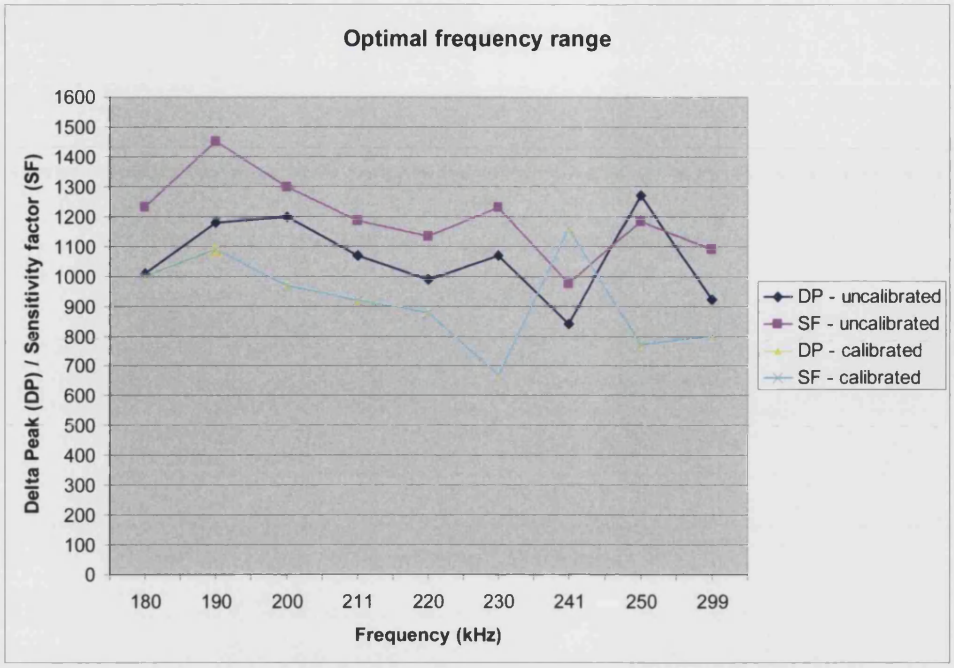

Figure 86 : Optimal frequency range

All frequencies in the range presented in the figure above can be used for the measuring method which is topic of this thesis. Detection of the open and close contact states is possible within all frequencies in this range and optimal frequency will be selected according to following criteria:

- lowest influence of the neighboring conductors
- best capacitive coupling
- lowest influence of the parallel load
- most stabile measurement results
- best response to measurement with combined vibrations

9.2.3 Measuring of the transition between open and close contact by using of optimal frequency range and recording mode

In following section the optimal frequency range between 180 – 300 kHz will be additional investigated. Usability of the test method will be definitely proved.

The following measurements will use the recording mode. Acquisition length will be approximately 3 s. Solid and broken contact will be simulated with terminals shown in the Figure 79 and Figure 80 (terminals with bridge).

MEASUREMENT : Signal frequency approximately 250 kHz

In the following figure can be seen that the transition between open and close contact was clearly recorded:

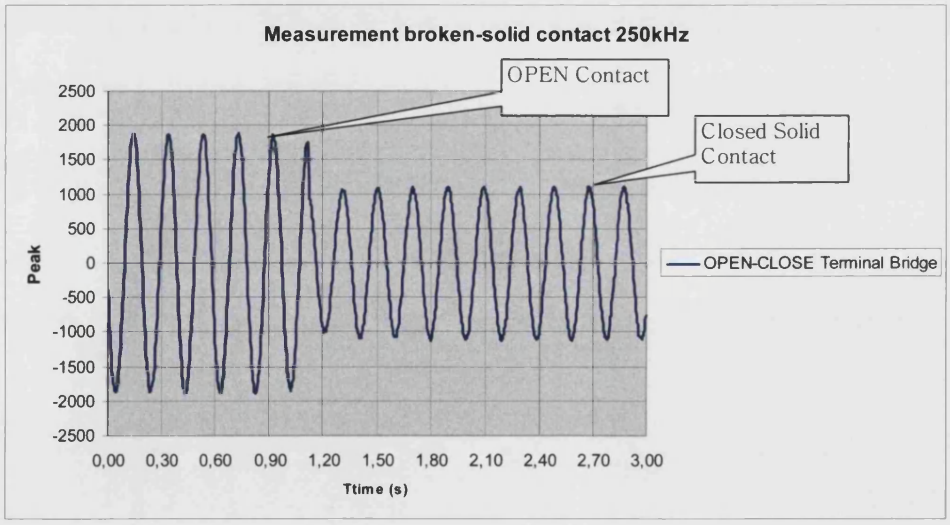

Figure 87: Measurement broken-solid contact at 250 kHz

Measurements with other frequencies within the optimal range between 180 and 300 kHz showed similarly good results as the measurement with 250 kHz presented in the Figure 87. The following table presents the results of the peak value detected, using the recording mode, with solid and broken contact states:

Recording Mode			
Test frequency kHz	Peak Value Solid Contact	Peak Value Broken Contact	Delta Peak value
180	1450	870	580
190	1620	845	775
200	1670	940	730
210	1659	880	779
220	1780	980	800
230	1720	1040	680
240	1930	1080	850
250	1870	1015	855
290	1850	1050	800
300	1850	1150	700

Table 18: Measurement results in the recording mode

As can be seen, all measurements show very clear and satisfactory results. Some frequencies show little better results compared to others (i.e. at 250 kHz) but all results are good and the detection of the broken and solid contact is definitely possible with all frequencies within this range.

Further the influence of the back metal plate will be investigated by using frequency within the optimal range. This will be used as additional criteria for the frequency selection.

9.3 Influence of the background metal plate on the measurement method

As explained in the Chapter 7 , section 7.3, the background metal plate could have an influence on the measuring results and on the measurement method.

The following figure shows measurements of the delta peak value with all the frequencies within the optimal range. The influence of the background metal plate on the delta peak value can be seen.

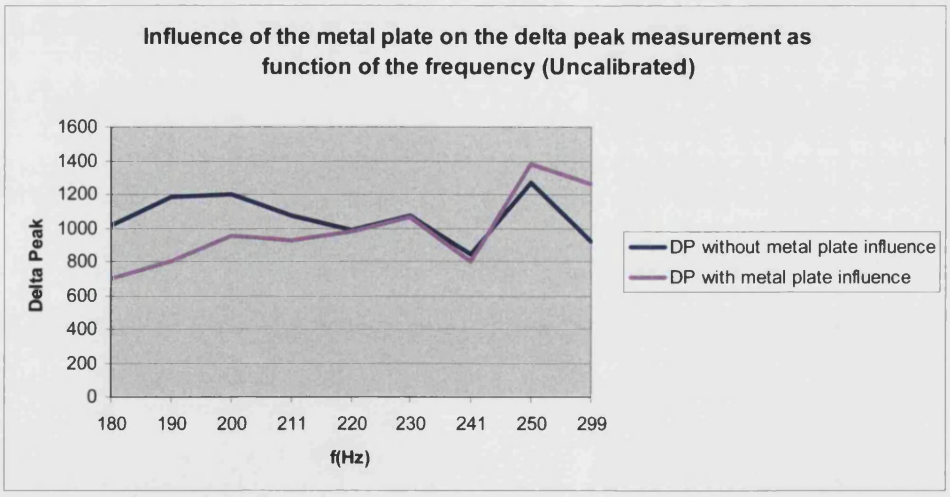

Figure 88: Influence of the metal plate

Some lower delta peak values have been measured for the frequency range 180-220 kHz. Frequencies from 220 - 250

kHz do not show any influence of the back metal plate: successful detection of the broken - solid contact with the presence of the earthed metal plate was possible.

The optimal frequency for the measurement method will be selected as 250 kHz. This frequency showed highest delta peak value and the lowest influence of the back metal plate.

In the figure below recording of the broken - solid contact transition with metal plate influence at 250 kHz test signal, has been shown.

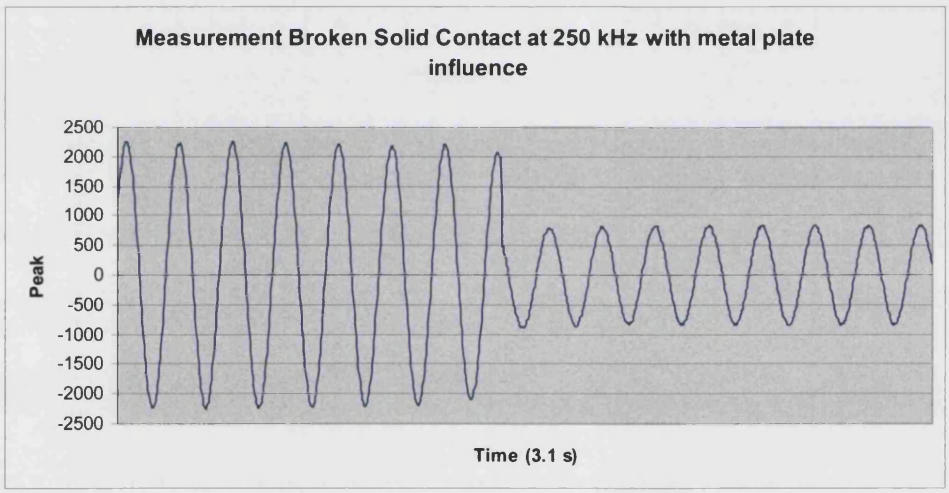

Figure 89: Broken-Solid Contact with metal plate influence

Figure 89 shows that there is no influence of the metal plate on this recording. The solid and broken states of the contact were clearly detected.

The method has shown good performance in a standard application.

9.4 Influence of the parallel close neighbour conductors

The possible influence of the neighbouring conductors has been explained in the Chapter 7; section 7.3, Figure 52. The practical measurements using real test object model shown in Figure 77 has shown that no relevant influence of the next bay conductors is present. The coupler form and optimal selected test signal frequency allow very accurate measurement of the broken and solid contact transition without influence of the neighbouring conductors.

The results of the recording mode with 250 kHz and no influence of the next bay conductors can be seen in Figure 90.

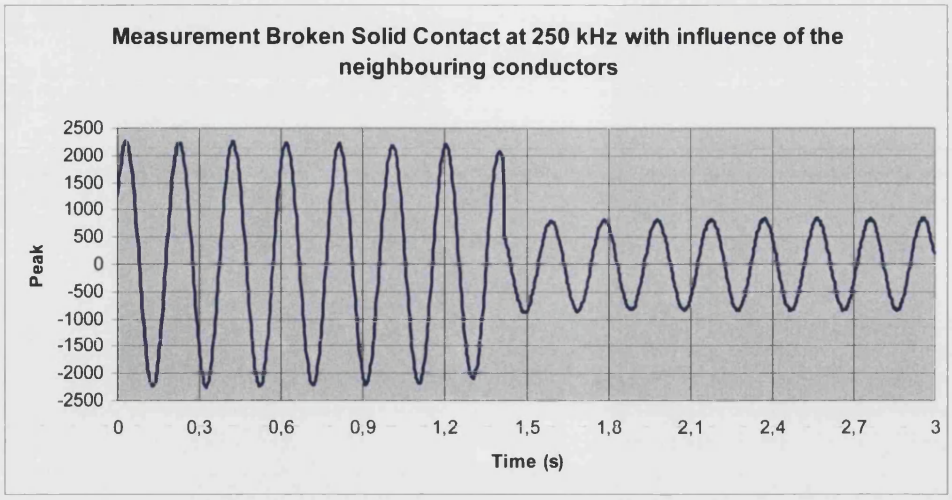

Figure 90: Broken-Solid contact and influence of the neighbouring conductors

It is clear from this figure that the method successfully detects broken and solid contact states in the presence of the neighbouring conductors.

9.5 Influence of the parallel load

In this section the performance of the method in the case of a parallel load will be investigated.

The parallel load case is shown in Figure 91:

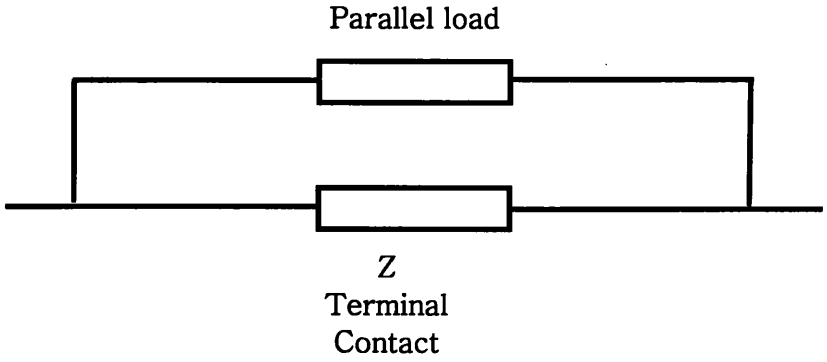

Figure 91: Parallel load

The influence of the parallel load will make the measurement method more difficult.

In the Chapter 8; section 8.2, Figure 75 the measurement of the peak in the function of the contact resistance has been presented. As can be seen in Figure 75, the parallel load with minimum 10 kΩ can be detected. In the large majority of the power system applications the parallel load will be inductive, reactive eg. relay coils, rather than resistive. Therefore it is more appropriate to consider an inductive load. In the following calculation the minimum inductance where the difference between open and close contacts can be just detected will be calculated.

$$X_L = \omega L$$

$$10k\Omega = 2 \times \pi \times f \times L$$

$$L = \frac{10 \times 10^3}{2 \times \pi \times f} = \frac{10 \times 10^3}{2 \times \pi \times 250 \times 10^3} = 6,37 mH$$

Practical cases in the application of the power systems have much higher value of the inductance as 6 mH.

The measurement with signal frequency of the 250 kHz brings the possibility of detecting open/close contacts in the presence of parallel loads. Measurement with signal frequency of 250 kHz in comparison with 50 Hz produces 5000 times higher reactance.

For the majority cases in practice, the influence of the parallel load does not play a big role. The conductors in the application which is topic of this thesis are not connected in a way where the parallel load can have a big influence. The majority of the terminals are connected outside and inside substation equipment without parallel load cases.

9.6 Experiments with different existing signals in the conductors

Conductors which are connected with terminals within secondary wiring systems carry different signals. The following values of the signals are typical for the power system secondary applications:

Typical Voltage Signals		
1	24	DC
2	48	DC
3	60	DC
4	110	DC
5	220	DC
6	110	60Hz
7	220	50Hz

Figure 92: Most typical cases of the substation signals

The following arrangement will be used to investigate the influence of the voltage or current signal in the measured conductor.

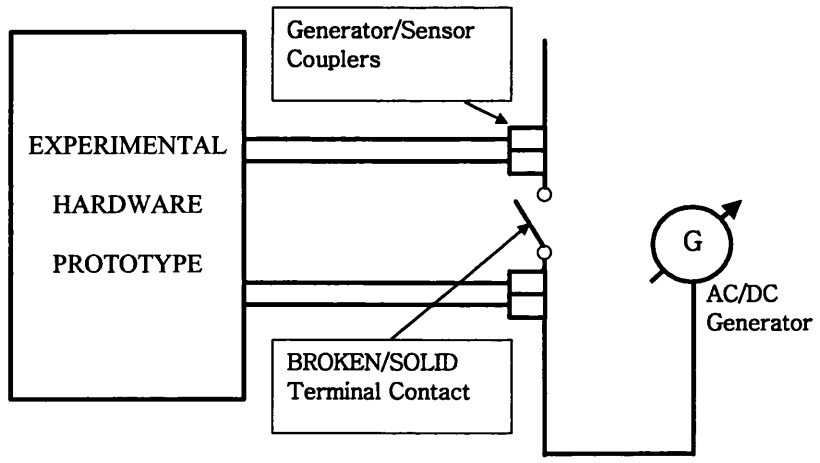

Figure 93: Measurement of the broken-solid contact with influence of the foreighn voltage signal

All measurements are made with the optimal selected signal frequency of 250 kHz. The results of the measurements are presented in the following table:

Foreign signal	non calibrated			calibrated		
	Peak value: Broken Contact	Peak value: Solid Contact	Delta Peak value	Peak value: Broken Contact	Peak value: Solid Contact	Delta Peak value
24 V DC	1800	880	920	730	0	730
48 V DC	1800	880	920	730	0	730
60 V DC	1800	880	920	730	0	730
110 V DC	1800	880	920	730	0	730
220 V DC	1800	880	920	730	0	730
220 V 50 Hz	1800	880	920	730	0	730
220 V 60 Hz	1800	880	920	730	0	730
110 V 50 Hz	1800	880	920	730	0	730
110 V 60 Hz	1800	880	920	730	0	730

Table 19: Measurement of the broken-solid contact with influenc of the existing signal in the conductor

As can be seen from the previous table there is no measurable influence of the existing voltage signal on the measurement results. Measurements with all existing values of the standard signals did not show any difference of the measured results. Test showed that detection of close circuits was not influenced by current flowing signal through secondary wiring.

9.7 Influence of different conductor cross-sections on the testing method

In the standard application of the power system substation different sized cross-sections of the secondary conductors are

used. Some typical cross section values are:1.5 mm², 2.5 mm², 4 mm², 6 mm², or 10 mm². These different conductors have different thickness of the insulation as well.

The size (cross-section) of the capacitive couplers should be adapted to the size (cross-section) of the measured conductor as shown in the next figure:

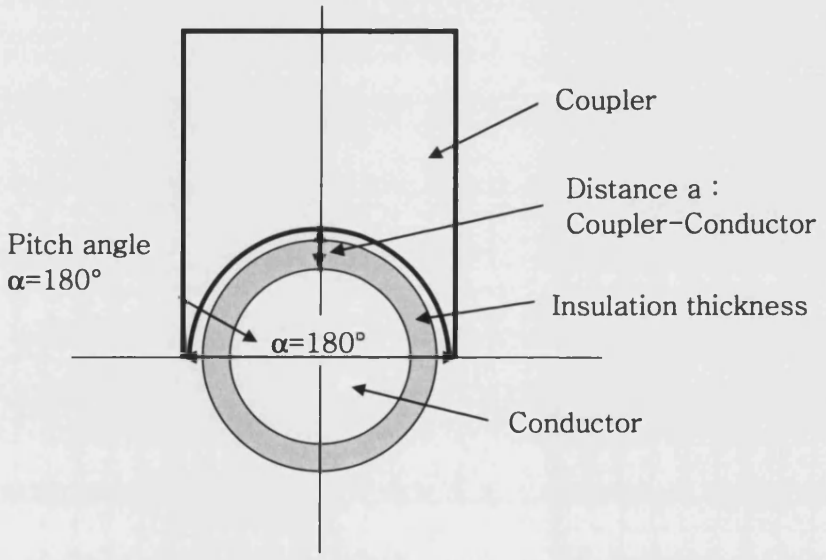

Figure 94: Couplers size adapted to the size of the conductor

In the Chapter 4; section 4.3.2; Figure 29, it was explained that capacitive coupling depends on the pitch angle α and distance "a" between coupler and conductor.

A smaller pitch angle α and greater distance "a" are influencing the capacitive coupling and can produce a lower peak value. The experimental hardware uses one coupler size only. This

size is made for conductors up to 2.5 mm². For the bigger cross-sections the experimental case can be shown in the next figure.

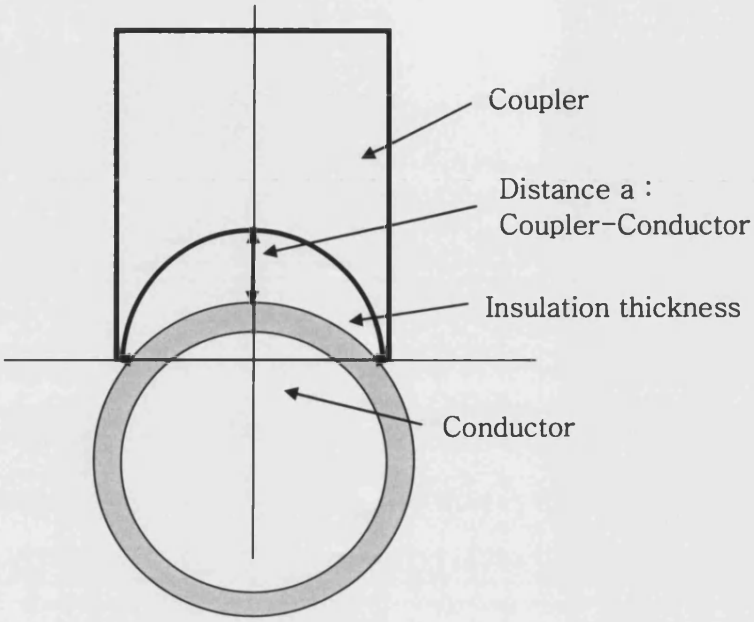

Figure 95: Coupler size is smaller then conductor

As can be seen in the figure above, the pitch angle is reduced. An additional consequence is that the distance "a" between the conductor and the greater cross-section couplers has increased as well. The result of such a case will be a lower measured peak value and a more difficult contact evaluation.

Further practical measurements on different conductor cross-sections have been made using measurement signal of 250 kHz:

Conductor cross-section in mm²	Peak Open	Peak Closed	Peak Compensated
1,50	2270	800	1470
2,50	1500	800	700
6,00	1050	820	230

Figure 96:Measurement on different conductor sizes

As can be seen a lower peak value has been measured with greater cross sections. A further improvement will be to use different coupler sizes for different conductor sizes. The optimal solution will be a coupler with adaptable size.

9.8 Weak contact investigations

9.8.1 Introduction

The weak contact is a very problematic type of terminal fault. Very difficult troubleshooting and large problems in the service are characterizing these phenomena.

As has been shown in the preceding sections, the invented measurement system is able to successfully detect broken and solid contact states. The premium idea for detection of the weak contacts with help of the superimposed mechanical vibrations was presented in the Chapter 7; section 7.6. . The main idea of this thesis is to find a simple and efficient way for

contact evaluation. The weak contact phenomena will be investigated by mechanical vibrating the measured conductors using an ultrasound generator.

9.8.2 Experiments with simple manual moving of the conductor

In the following measurement the recording mode of the experimental hardware will be used. The change of the faulty weak contact from solid to broken will be provoked by simple manual movement of the conductor.

The following figure presents a record of the solid contact measurement with manual movement of the conductor during measurement.

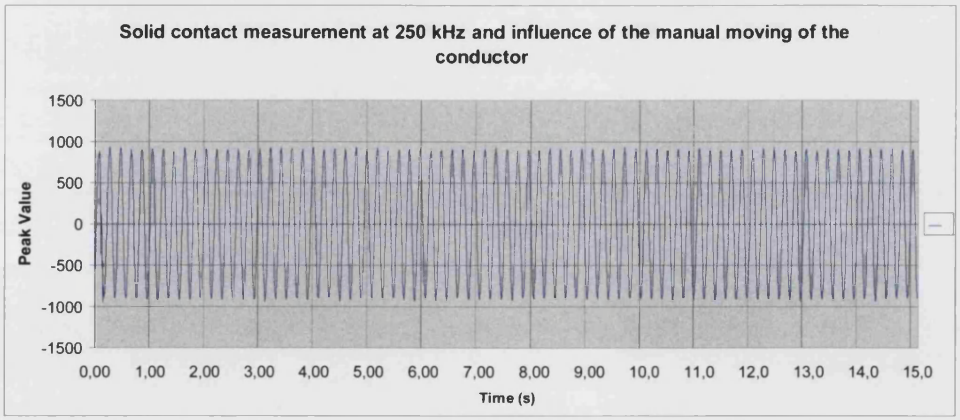

Figure 97: Influence of the manual moving of the conductor on the measurement of the solid contact

As can be seen there was no influence of the movement of the conductor on the measurement with solid contact. This was as expected.

In the next two figures the same experiment will be repeated with two measurement frequencies (250 and 200 kHz) but this time with weak contact (weakly tightened terminal screw):

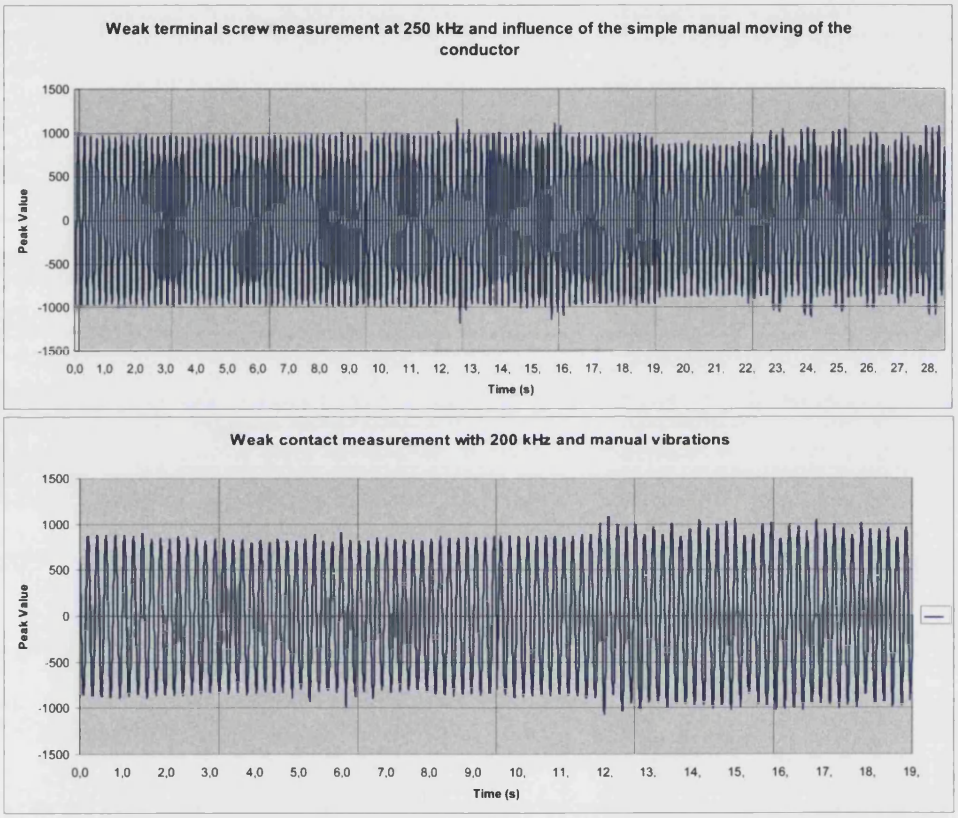

Figure 98: Influence of the manual moving of the conductor on the measurement of the weak contact

As can be seen the mechanical movement of the conductor has produced some nonlinearity and peaks in the recorded signal. These peaks are clearly measurable and visible in the

recording mode at both frequencies. The peaks above 1000 visible in the figures above are influenced by the change of the contact states from solid to broken due to mechanical movement (vibrations). As can be seen these peaks can be very clearly detected.

9.8.3 Experiments with superimposing of ultrasonic vibrations

In this section the idea of superimposing ultrasound mechanical vibrations will be investigated. Strong ultrasound vibrations will cause each weak contact to move and within the measuring method the detection of the weak contact should be possible.
In this section the ultrasonic generator will be used for production of the mechanical vibrations (see Figure 99).

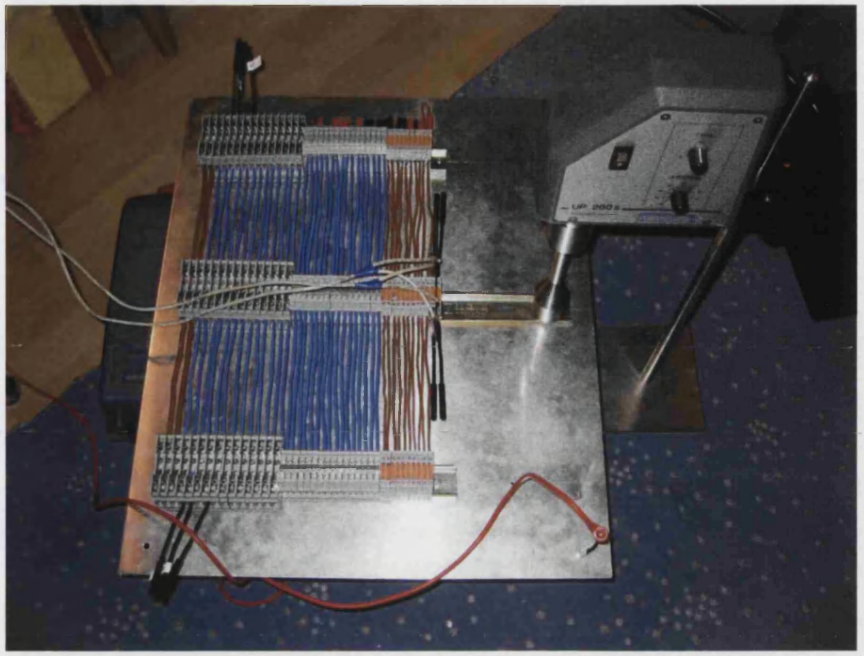

Figure 99: Ultrasound generator

Used ultrasound generator:

Power supply	230 V ±10%
Effective power output	200 W
Efficiency	>85%
Power control range	20% to 100%
Pulse ratio	10% to 100%
Operating frequency	24 kHz
Frequency control range	±1kHz
Max. power density	12 to 600 W/cm²
Max. amplitude	12 to 260µm

The following experiment will be to connect measurement couplers to the solid contact. Measurement of the solid contact states with impact of the mechanical ultrasound vibration did not show any peaks or nonlinearity. Recording of the

measurement with mechanical ultrasound vibrations and 250 kHz signal on the solid contact can be seen in the next figure:

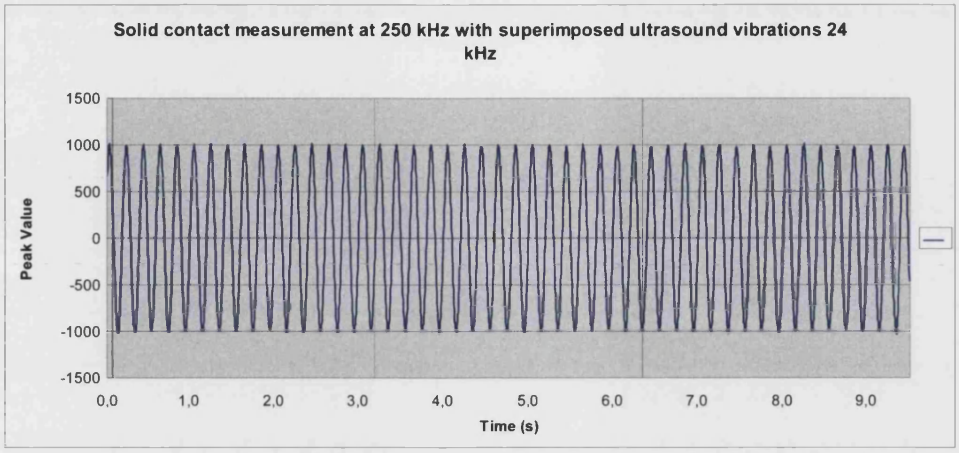

Figure 100: Solid contact measurement with superimposed ultrasound vibrations

The experiment was repeated with the very weak terminal screw (very weak contact).

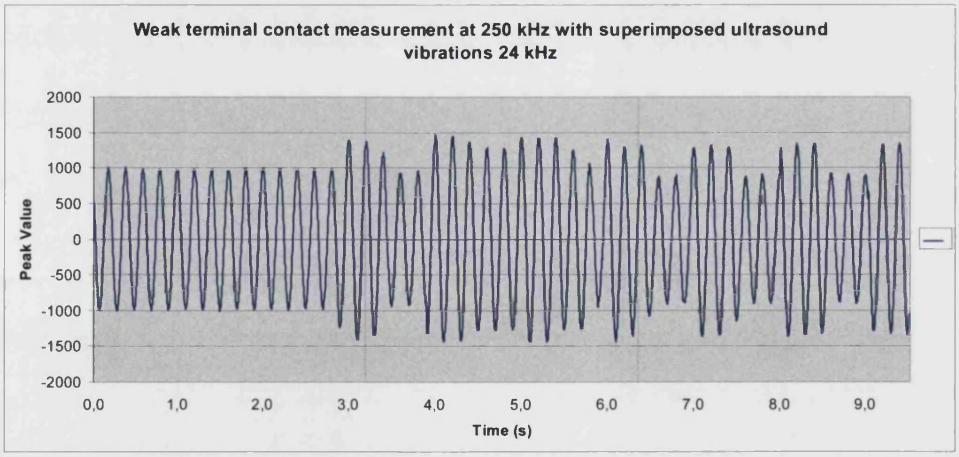

Figure 101: Measurement of the very weak contact with superimposed ultrasonic vibrations

The terminal screw in the next experiment was fixed tighter than the previous experiment. In this case the contact was still weak, but strong enough to allow good electrical contact. The measurement with a DC Ohmmeter did not discover any problems. In the next figure it can be seen that some peaks and nonlinearities are still visible in the recording:

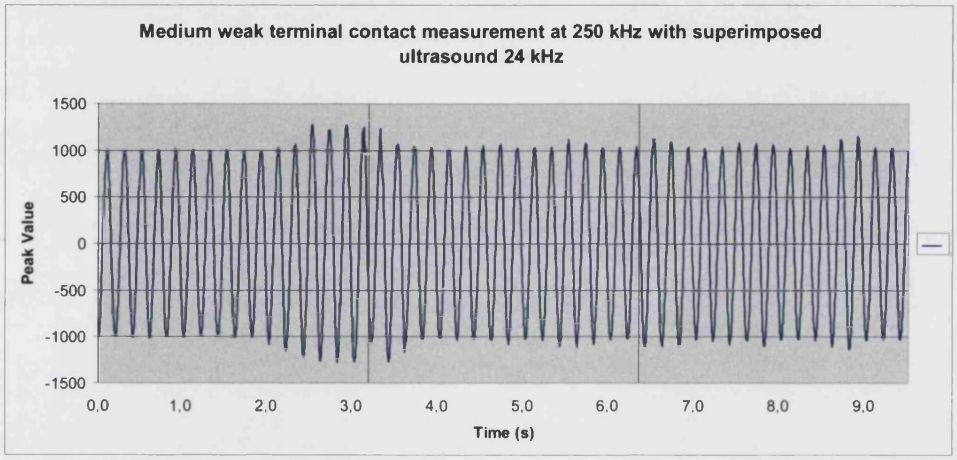

Figure 102: Measurement of the medium weak contact with ultrasonic vibrations

The weak contact was clearly detected and visible in the recording mode. The peak changing was visible in the online detection mode as well.

9.8.4 Conclusions about superimposing mechanical vibrations

In this section the idea about weak contact detection using a method of superimposed mechanical vibrations and detection of the current (peak) gradient has been proved. As was presented two different possibilities to provoke movement of the weak contact has been investigated:

- Simple manual movement of the conductor
- Superimposing of the ultrasound vibrations using ultrasound generator

The ultrasound method has shown stronger peaks and non linearity in the recorded signal compared with simple manual movement of the conductors. The recording mode has been used to record peaks and detect clearly changing in the peak value by changing of the contact states. The recording mode has been used to record peaks and detect clear changes in the peak value by changing of the contact states. The measuring of the weak contact was possible with using online measuring detector as well. The changing of the peak value was clearly visible in the online detector as well.

The measurement with the ultrasound generator is more complicated and more expensive compared to simple mechanical movement of the conductors. The more simple method of provoking weak contact using simple moving will be favoured.

In the future some special coupler construction will help to easily move conductors inside of the weak contacts (catch system).

9.9 Practical measurements on the real model

In this section the measurements on the real model shown in the Figure 77, will be performed. The results of these measurements are probably the most important measurements in this thesis. These results will show, following optimisation and investigation, the success of the measuring method invented in this thesis.

A real model with 42 terminals is used. Out of 42 terminals, 18 terminals have been set up as faulty, without taking care about exact number (location) of the faulty terminals. Several terminal faults have been simulated:

- Broken terminal
- Uncrimped wire tightened into terminal

- Weak terminal contact (weak terminal screw)

The following experiment will try to identify (locate) faulty terminals by using peak detection in calibrated mode. (peak value with coupler in the air is compensated). Simple mechanical movement of the conductors will be used to detect weak contact. The results of the measurements using method which is topic of this thesis will be proved with standard resistance (Ohmmeter method).

The results of the measurements are presented in the following table:

Term. Nr.	Calibrated Max.Peak	Terminal status	Checked with resistance method	Max. Resistance	Fault description
1	0	OK	OK	0,2 Ω	
2	0	OK	OK	0,2 Ω	
3	250	NOT OK	NOT OK	>10 kΩ	Insulation tighted
4	340	NOT OK	NOT OK	>10 kΩ	Insulation tighted
5	150	NOT OK	NOT OK	>10 kΩ	Weak Terminal Screew
6	380	NOT OK	NOT OK	>10 kΩ	Insulation tighted
7	0	OK	OK	0,2 Ω	
8	280	NOT OK	NOT OK	>10 kΩ	Broken terminal
9	0	OK	OK	0,2 Ω	
10	0	OK	OK	0,2 Ω	
11	200	NOT OK	NOT OK	>10 kΩ	Broken terminal
12	250	NOT OK	NOT OK	>10 kΩ	Broken terminal
13	180	NOT OK	NOT OK	>10 kΩ	Weak Terminal Screew
14	0	OK	OK	0,2 Ω	
15	0	OK	OK	0,2 Ω	
16	350	NOT OK	NOT OK	>10 kΩ	Insulation tighted
17	200	NOT OK	NOT OK	>10 kΩ	Weak Terminal Screew
18	0	OK	OK	0,2 Ω	
19	420	NOT OK	NOT OK	>10 kΩ	Insulation tighted
20	220	NOT OK	NOT OK	>10 kΩ	Insulation tighted
21	0	OK	OK	0,2 Ω	
22	0	OK	OK	0,2 Ω	
23	0	OK	OK	0,2 Ω	
24	0	OK	OK	0,2 Ω	
25	400	NOT OK	NOT OK	>10 kΩ	Broken terminal
26	0	OK	OK	0,2 Ω	
27	0	OK	OK	0,2 Ω	
28	0	OK	OK	0,2 Ω	
29	0	OK	OK	0,2 Ω	
30	0	OK	OK	0,2 Ω	
31	150	NOT OK	NOT OK	>10 kΩ	Weak Terminal Screew
32	120	NOT OK	NOT OK	>10 kΩ	Weak Terminal Screew
33	0	NOK	OK	0,2 Ω	
34	170	NOT OK	NOT OK	1,2 Ω	Weak contact
35	0	OK	OK	0,2 Ω	
36	0	OK	OK	0,2 Ω	
37	300	NOT OK	NOT OK	>10 kΩ	Insulation tighted
38	0	OK	OK	0,2 Ω	
39	0	OK	OK	0,2 Ω	
40	150	NOT OK	NOT OK	>10 kΩ	Weak Terminal Screew
41	0	OK	OK	0,2 Ω	
42	0	OK	OK	0,2 Ω	

Table 20: Measurements on the real model with faulty terminals

As can be seen in the previous table all faulty terminals have been successfully discovered. Checking with the classic

method has proved the results and traceability of the invented method. The weak contacts have been successful detected by using simple conductor movements.

The invented measurement method showed 100% measurement traceability.

9.10 Conclusions about experimental work

The major task of chapter 9 was to evaluate theoretical method and prove traceability and usability of invented measurement method.

In the beginning of the experimental investigations the selection of optimal test signal frequency was made. The frequency range from 180 – 300 kHz has been selected. Further the influence of the background metal plate was investigated. The frequency above 220 kHz did not show any influence and 250 kHz has been selected as the best test frequency with the developed experimental hardware. The experiment showed that no big influences are present from parallel load or from signals within the measured conductor.

Weak contacts have been successfully detected using superimposed mechanical vibrations. Two measurement

methods of superimposing vibrations using simple mechanical movement or using an ultrasound generator, have been presented. Both measurements had shown clear, measurable results. The ultrasound method presented better results but the method was more complicated and much more expensive. The results of the method using simple mechanical movement of the conductors has been favoured as more simple and still satisfactory accurate and traceable.

By end of the experimental work a measurement on the real terminal model with covered faulty terminals has been performed. The measurement had show very satisfactory results. The measurement method showed 100 % traceability.

Chapter 10

10. Further work and additional possible applications

10.1 Introduction

The further work arising from this thesis can be divided into two directions:

1. Further improvements of the measurement method invented in this thesis
2. Investigations on the use of the method in other applications

10.2 Further improvements of the measurement method

Further improvements of the measuring method invented in this thesis will target the development of a commercial product and will concentrate on the following topics:

- Improvement of the hardware measurement capability:
  - o Increasing power of the generator
  - o Solving problems with parasitic coupling between TX and RX path

- Improving of the filter capabilities and hardware measuring sensitivity
- Improvement of the couplers
- Development of the mechanical hardware

10.2.1 Improvements of the hardware capability

As described in the Chapter 8 , the developed hardware prototype had problems which could not be solved within the existing design. The following problems will be investigated and a solution will be redesigned in the future work:

- Parasitic coupling between RX and TX path
- Weak generator and driver capabilities with frequencies above 400 kHz
- Investigate simplification of the hardware for the future product

The parasitic coupling between RX and TX path is taking place via 5 V internal power supply. The solution, which will be topic of the investigation in the future work, will be the use of separate power supplies for TX and RX paths. Additional

shielding of the TX and RX path will be investigated. Further investigation must find a hardware design which will minimize capacitive coupling between TX and RX path. Future hardware improvements might be possible by using averaging algorithms which can be implemented in the FPGA (hardware-solution) or in the micro-controller (software-solution).

Weak capabilities of the signal generator and driver capability for the frequencies above 400 kHz have been detected as explained in Chapter 9, section 9.2.2. A high capacitive load made measurements above 400 kHz ineffective. Further work will investigate other possibilities for using a stronger driver and generator. For this purpose the hardware must be redesigned. The power supply must be changed from 5 to 10 V and another driver component must be used. Further work will investigate measurement capabilities by using signal frequency which is above 1 MHz (2 -5MHz). This frequency range will be better for other applications which are going to be investigated eg. circuit breaker applications due to improve capacitive coupling.

10.2.2 Improvement of the couplers

Improvement of the couplers will play a very important role for the future product development. The major problem of the couplers will be the mechanical construction.

As explained in the Chapter 9, section 9.7 , the cross-section of the conductors are playing a big role in the measurement results. Following topics in connection with coupler construction will be investigated:

- Increase of the capacitive coupling (increase of the pitch angle)
- Improvement of the coupler mechanical construction with:
    - o Adjustable distance between two couplers
    - o Adaptable coupler pitch according to the conductor cross-section
    - o Clamp-catch mechanism for catching coupler while moving because of weak contact detection
    - o More robust construction
- Short connection cables between couplers and test device because of the capacitive load reduction.

Fulfilling of all requirements listed above will be very challenging job in the future investigations.

10.2.3 Investigation of the hardware mechanic

The target of further investigations will be to improve the mechanical construction of the hardware with the goal of achieving a hand-held, small, simple test device for terminals evaluation. Within further work concerning the mechanical construction of the hardware the following problems must be solved:

- Small robust hand-held construction
- Couplers connected to the hardware without connection cable
- Battery supply
- Low cost
- Shielding against parasitic coupling

10.3 Usability within other applications

The measurement method invented in this thesis can be used outside of the described application, with some specific

modifications, in other additional applications. This will be target of the further work as well. The method can be used in all applications where some contact states (condition) must be measured where it is difficult or expensive to connect the test signal to the test object.

Further are listed two applications which can be investigated for future work:

- Power system circuit breaker applications
- Relay contact monitoring system

10.3.1 Power system circuit breaker applications

This will investigate if the method invented in this thesis can be used, with some modifications, for the following power system circuit breaker applications:

- Condition monitoring
- Measurement of the C-O (Close-Open) time
- Measurement of the contact travel speed
- Pole discrepancy supervision

Advantages of this method in comparison with other existing methods are:

- Low costs

- Simple application to existing CB without monitoring
- Measurement is possible under primary voltage conditions (under nominal service) or without any voltage
- Possible versions as a permanent monitoring system or as a portable test device.

The figure below shows an example of how the measurement system invented in this thesis can be fitted to an existing circuit breaker.

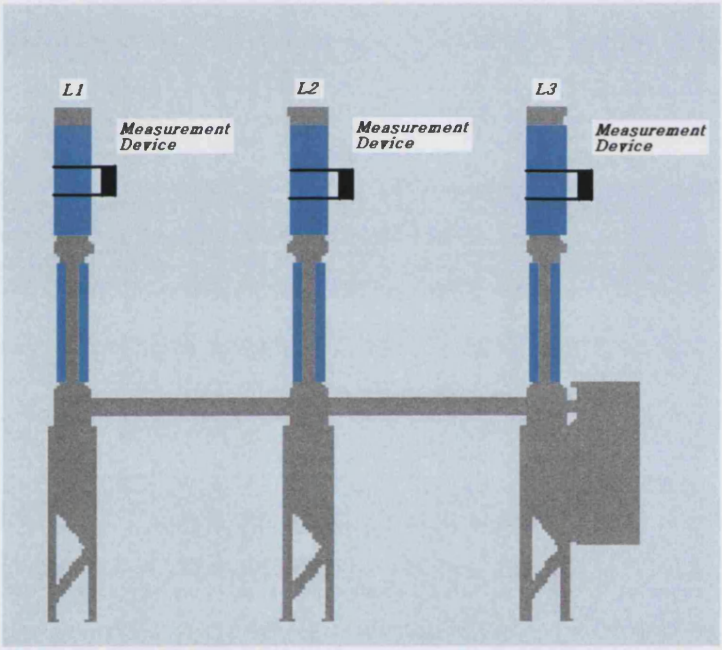

Figure 103: Example of the circuit breaker application

The following properties of the measurement system must be fulfilled:

- Each Phase must have separate measurement hardware.

- Three measurement devices must be synchronised between each other. (time recording synchronization)
- Independent DC power supply without need for external wiring (i.e. photo-voltaic solar)
- Time accuracy better then 1 ms
- Wireless communication to the substation PC or SCADA

Circuit breakers are one of the most important elements in the power systems substations. An invention in this area which will allow simple condition monitoring, will be a significant asset.

10.3.2 Relay contact applications

The method invented in this thesis can be used with some modification for monitoring relay contacts - especially sealed relays. The following applications related to relay contacts could be investigated:

- Detection of the contact bouncing / glitch effects
- Measuring of contact opening and closing times

This application could be interesting for all applications where correct operation of the relay contact plays a big role. Such

applications are often used in the aerospace industry and within development departments and factory testing by manufacturers of different equipments. Additional measurement of the contact speed (opening and closing time) can be useful, especially for applications where connection of the classical resistance measurement plays a difficult role (i.e. sealed relays).

Further work will investigate which modifications will be necessary on the measurement system to allow successful implementation in relay contact applications.

Chapter 11

11 Conclusions

One of the most common sources of malfunction in power system substations is the secondary terminals. Troubleshooting work on secondary terminals during commissioning is a very difficult and labour intensive operation.

The testing method invented in this thesis shows very good theoretical and experimental results. A functional prototype was developed and has given excellent results for the detection of typical terminal contact states: solid, broken and weak.

The importance of secondary terminals was explained at the beginning of this thesis. In power system applications, secondary terminals play a very important role and allow the basic functionality of the system. The system is interconnected via secondary terminals. Typical faults of secondary terminals include internal failure within the terminal, human error during construction/commissioning of the substation, or environmentally influenced errors. Most typical terminal errors are due to broken or weak electrical contacts between two

conductors connected by the terminal. The measurement method developed in this thesis has focused on the detection of the following states of the terminal contacts:

- Broken electrical contact
- Weak electrical contact
- Solid electrical contact

The literature research of the contact phenomena has shown the complexity of contact physics. Analyses in many of the published papers about contact problems have described the difficulties of the simple contact evaluation.

Research on other existing measuring techniques has shown some standard existing methods (i.e. resistive methods) which are inappropriate in the application of secondary terminals. Some interesting publications which use high frequency capacitive coupling have been found in the patent literature. Besides the similarity in the use of the contactless capacitive coupling technique, the methods are not applicable for the measurement of secondary terminal contacts in power substations. The application which is the topic of this thesis was not complementary to any literature used as reference in this thesis. It is surprising how little has been published on this important topic. Therefore the contribution of this work to the

problems of electrical terminal contacts is unique and will hopefully be of use within this technical area.

The idea of using a high frequency signal, which is capacitively coupled to the measured object, and superimposed mechanical vibration was presented. The detection of the current gradient was selected as the threshold criteria for the detection of contact malfunction.

In order to develop the prototype which has to confirm the application of the idea, a wide theoretical investigation was performed. First of all the phenomena of capacitors and capacitive coupling was investigated. Several shapes of the capacitive couplers were calculated and the dependency of several variable factors were investigated. A capacitive coupler shaped as a cylindrical segment with a pitch angle of 180° was selected as being constructed in practice and acceptable in terms of measurement capabilities.

During theoretical investigations several mathematical calculations were carried out. The target of the mathematical research was to evaluate the dependency I=f(Z) which describes the current flow through the contact impedance. By using a high frequency signal capacitively coupled via a coupler shaped as a cylindrical segment, the dependency of the current

and contact impedance has been found. With the help of MATLAB, physics and mathematical simulations of the method were performed. The results of the MATLAB simulations were confirmation of the theoretical idea. The simulations showed the clear possibility to detect broken and solid contact states using this method.

The theoretical investigation using MATLAB simulations has created a solid background for the design of the hardware prototype. The idea of the hardware prototype which can fulfil requirements of the theoretical investigations and be useful within the described application was created. The hardware prototype contains several innovations. High measurement sensitivity, small hand-held size, low costs, recording possibility and variable signal frequency are some of the requirements of the hardware prototype.

The designed hardware prototype was constructed and during the first test several weaknesses were corrected. Problems with hardware and with the couplers were detected. After several improvements a satisfactory level of the experimental hardware was achieved.

The aim of the experimental research was to prove the invented method worked in practice. At the beginning of the

experimental research, the goal was to find the optimal signal frequency. After several tests, the optimal frequency, which is related to the particular experimental hardware, was selected as 250 kHz. Using this frequency several other phenomena were investigated. The problems of close neighbouring conductors and the presence of the background metal plate during measurement were successfully solved by selection of the correct measuring signal frequency (250 kHz) and a coupler pitch angle of 180°. Problems of parallel loads do not play a big role within secondary terminal applications and the voltage level on the secondary wiring was shown to have no influence on the measurement results.

Using measurement of the peak value of the measured signal, it was possible to detect the open and closed states of the contact.

The theoretical investigations and MATLAB simulations were proved and confirmed using the hardware. A close agreement between the results of the simulations and real measurements was observed.

The idea of superimposing mechanical vibrations for provoking the weak contact to move, and therefore to allow measurement

of the current gradient while opening and closing, showed good results. The current gradient within weak contacts was clearly measured during superimposition of mechanical vibrations. Two separate possibilities for producing mechanical vibrations were used: manual movement of the conductors in the terminals and the use of an ultrasound generator at 24 kHz. Both methods gave positive results of the measurements and clearly measurable current peaks during mechanical movement of weak contacts. The target of the research was to find a simple and low cost method. Therefore, the simple method of the manual movement was preferred. At the conclusion of the experimental work detection on a realistic terminal model was performed. All typical contact malfunctions were successfully detected, thus confirming the application of the invented method for the troubleshooting of secondary power substation terminals.

Theoretically the invented method can be used, with some modifications, for any contact application. Several applications are possible and the most important can be listed as: power systems circuit breakers, relay contacts, primary contacts, cable joints etc. Further work will investigate application of the measurement method in other applications. Monitoring

applications is very beneficial and attractive presently and it is in this direction that further work will most likely be concentrated.

Appendix

Appendix 1- MATLAB simulation C'=f(a) Concentric cylinder segment capacitor with 45°pitch angle and variable distance a

```
function calccapcylpa45()
%Estimation of concentrical cylindar segment capacitor with 45°pitch angle
e0 = 8.8542*10^(-12);
ri = 1.38*10^(-3)/2;  % diameter of the inside conductors 1.5mm2 cross-
section
%Cylinder
umschl = 45/360;   % pitch angle 45°
ra = linspace(1.5*ri,6*ri,200);
czy = umschl*(2*pi*e0)./log(ra/ri);%equiation 3
czy2 = umschl*100*0.241*10^-12./log10(ra/ri);%equiation 2
%hold on


figure(1);
plot(ra-ri,czy,'r',ra-ri,czy2,'b'); grid on;
title('C-Cyl vs. a ');
```

Appendix 2- MATLAB simulation for Concentrically cylinder capacitor with variable pitch angle and distance a

```
function calccapcylpav2()
%Estimation of different capacitors

e0 = 8.8542*10^(-12);
ri = 1.38*10^(-3)/2;  % radius of the inside conductors 1.5mm2 cross-
section
ra = linspace(1.5*ri,6*ri,200);
%Cylinder
umschlall=[45:45:360];
czyall(length(umschlall):length(ra))=0;
for k=1:length(umschlall)

umschl = umschlall(k);   % pitch angle
czy = (umschl/360)*(2*pi*e0)./log(ra/ri);
czy2 = umschl*100*0.241*10^-12./log10(ra/ri);
hold on
czyall(k,:)=czy;


end
figure(1);
```

```
plot(ra-ri,czyall','b'); grid on;
title('C-Cyl as function from distance ');
```

Appendix 3- MATLAB simulation C'=f(α;a) Concentric Cylinder Segment Capacitor and Influence of variable Pitch Angle and Distance "a"

```
function calccap_umschl()
%capacitance estimation

e0 = 8.8542*10^(-12);
ri = 1.38*10^(-3)/2;  % durchmesser innenleiter für 1.5mm2 querschnitt
NPTS = 200;
umschl_all = [];
umschl_all = [45:45:360];
ra = linspace(1.5*ri,6*ri,NPTS);

Czyall (1:length(umschl_all),1:NPTS) = 0;
for par = 1:length(umschl_all)
    umschl = umschl_all(par)
    %Cylindar
    %umschl = 45/360;   % umschlingungswinkel
    czy = umschl*(2*pi*e0)./log(ra/ri);
    czy2 = umschl*100*0.241*10^-12./log10(ra/ri);
    % two conductors
    r2 = 1*ri;
    dist = linspace(0,5*ri,200);
    cp = (2*pi*e0)./log(4*(dist+ r2+ ri).*(dist+ r2+ ri)/(ri*r2));
    cp2 = 100*0.241*10^(-12)./log10(4*(dist+ r2+ ri).*(dist+ r2+ ri)/(ri*r2));
    % kopplung leiter vertikal über Erde
    figure(1);
    plot(dist,cp,'r',dist,cp2,'b'); grid on;
  title('C-2Coductor as function from distance');
  %hold on
    figure(2);
    plot(ra-ri,czy,'r',ra-ri,czy2,'b'); grid on;
    title('C-Zyl as function from distance ');

  hold on
  Czyall(par,:) = czy;
    pause(0.01);
end  % end for p
[Y,X] = meshgrid(umschl_all,ra-ri);
figure(99); mesh(X,Y,Czyall');
xlabel('distance "a"'); ylabel('embrace angle'); zlabel('Capacitance'); grid on;
title('C-Zyl as Fkt v. distance "a" and embrace angle');

% zylindrische anordnung, variation von umschlingungswinkel
% Czyall enthält alle Cokppelc als fkt von umschlingungswinkel und ra
(abstand)
```

```
IMovUMall (1:length(umschl_all),1:NPTS) = 0;
for par = 1: length(umschl_all)
    Ck = Czyall(par,:)*0.01;  % länge aufnehmer = 1cm angenommen
    Cgm = 0.1*10^(-12);   % C Generator - Meßaufnehmer Elektrode
    %Ckm = 0.4*10^(-12);      % C Meßaufnehmer - Leiter
    Cks = 0.005*10^(-12); % C Schirm - Leiter
    %Ckg = 0.4*10^(-12);   % C Generator - Leiter
    Z = 1*10^6+ 1i*10^6;
    Ckm = Ck;
    Ckg = Ck;
    p = i*2*pi*5*10^6;      % frequenz;

    Im_ov_Um = 1/2*(p*Cgm +  p.*Ckm.*p.*Ckg./(p.*(Ckm +  Cks +  Ckg) +
2/Z));
  figure(3);
    subplot(2,1,1);
    plot (Ck,abs(Im_ov_Um),'b'); grid on; axis([0,5e-10,0,0.005]);
  title('|Im/Um|  vs. Ck (Ckm = Ckg)');
  hold on
    subplot(2,1,2);
    plot (Ck,angle(Im_ov_Um)*180/pi,'b'); grid on;
  title('phi(Im/Um) vs. Ck (Ckm = Ckg) Z = 1e6');
  IMovUMall(par,:) = abs(Im_ov_Um);
  hold on
  pause(0.01);
  hold on
end
figure(98); mesh(X,Y,IMovUMall');
xlabel('Abstand ra-ri'); ylabel('Umschlingungswinkel in °');
zlabel('Meßstrom'); grid on;
title('Meßstrom als Fkt v. Abstand und Umschlingungswinkel');
```

Appendix 4- MATLAB simulation C'=f(a) Capacitance of two parallel conductors as function of distance a

```
function calccappl()
%Estimate of different capacitors

e0 = 8.8542*10^(-12);
ri = 1.38*10^(-3)/2;  % radius of the inside conductors 1.5mm2 cross-
section
% Two conductors;
r2 = 1*ri;
dist = linspace(0,5*ri,200);
cp = (2*pi*e0)./log(4*(dist+ r2+ ri).*(dist+ r2+ ri)/(ri*r2));
cp2 = 100*0.241*10^(-12)./log10(4*(dist+ r2+ ri).*(dist+ r2+ ri)/(ri*r2));
% coupling conductor over ground
figure(2);
plot(dist,cp,'r',dist,cp2,'b'); grid on;
```

```
title('C-2Coductor as function from distance');
```

Appendix 5- MATLAB simulation Comparison of the 2 parallel cylinder capacitor and the concentric cylinder segment

```
function calccap_umschl()%comparison of two different type couplers shape
%capacitance estimation
e0 = 8.8542*10^(-12);
ri = 1.38*10^(-3)/2;
NPTS = 200;
umschl_all = [];
umschl_all = [0:45:360];
ra = linspace(1.5*ri,6*ri,NPTS);

Czyall (1:length(umschl_all),1:NPTS) = 0;
for par = 1:length(umschl_all)
  umschl = umschl_all(par)
    czy = (umschl/360)*(2*pi*e0)./log(ra/ri);
    czy2 = (umschl/360)*100*0.241*10^-12./log10(ra/ri);
    % two conductors
    r2 = 1*ri;
    dist = linspace(0,5*ri,200);
    cp = (2*pi*e0)./log(4*(dist+ r2+ ri).*(dist+ r2+ ri)/(ri*r2));
    cp2 = 100*0.241*10^(-12)./log10(4*(dist+ r2+ ri).*(dist+ r2+ ri)/(ri*r2));

    figure(2);
    plot(ra-ri,czy,'r',ra-ri,czy2,'b'); grid on;
  plot(dist,cp,'r',dist,cp2,'b'); grid on;
  title('C-Cyl as function from distance ');

  hold on
  Czyall(par,:) = czy;
  pause(0.01);

end  % end for p
```

Appendix 6- MATLAB simulation; Average function of the capacitance

```
function calccapavr2()% average value from different coupler shapes
%Estimation of different capacitors
average=0;
e0 = 8.8542*10^(-12);
ri = 1.38*10^(-3)/2;  % diameter of the inside conductors 1.5mm2 cross-
section
%cylindar
umschl = 135/360;   % pitch angle

ra = linspace(1.5*ri,6*ri,200);
czy = umschl*(2*pi*e0)./log(ra/ri)%equiation 3
czy2 = umschl*100*0.241*10^-12./log10(ra/ri);%equiation 2
```

```
%hold on

% Two conductors;
r2 = 1*ri;
dist = linspace(0,5*ri,200);
cp = (2*pi*e0)./log(4*(dist+ r2+ ri).*(dist+ r2+ ri)/(ri*r2))
cp2 = 100*0.241*10^(-12)./log10(4*(dist+ r2+ ri).*(dist+ r2+ ri)/(ri*r2));
% couppling conducor over the earth
n_count= size(cp);

for t=1:1:200
  average(t)=(cp(t)+ czy(t))/2;
end
%hold on
figure(1);
plot(dist,cp2,'b',ra-ri,czy2,'gr',ra-ri); grid on;
title('C-2Coductor as function from distance');
```

Appendix 7- MATLAB simulation with 1MHz signal frequency and variable contact resistance 0 - 10kΩ

```
function z_testp(par1)%for running different Z set par1 on 10000 or
1000000
par1=10000
Npoints = 300;
Zref = linspace(1,par1,Npoints);

    Ck = 10^(-12);  %  1cm lenght of electrodes
    Cgm = 0.2*10^(-12);   % Mutual Capacitance: Sensor - Generator
coupling electrode
    Ckm = 0.4*10^(-12);   % Mutual Capacitance : Sensor  - Conductor
    Cks = 0.005*10^(-12); % Mutual Capacitance : Screen - Conductor
    Ckg = 0.4*10^(-12);   % Mutual Capacitance : Generator coupling
electrode - Conductor

        p = i*2*pi*1*10^6;      % frequency;

    Im_ov_Um = 1/2*(p*Cgm +  p.*Ckm.*p.*Ckg./(p.*(Ckm +  Cks +  Ckg) +
2./Zref));
  figure(3);
    subplot(2,1,1);
    plot (Zref,abs(Im_ov_Um),'b'); grid on; %axis([0,5e-10,0,0.005]);
  title('|Im/Um| vs. Z');
  %hold on
    subplot(2,1,2);
    plot (Zref,angle(Im_ov_Um)*180/pi,'b'); grid on;
  title('phi(Im/Um) vs. Z');
```

Appendix 8- MATLAB simulation with 1MHz signal frequency and variable contact resistance 0 - 1MΩ

```
function z_test1MOHM(par1)%simulation with 1MHz signal frequency and
variable contact resistance 0 - 1MW
```

```
par1=1000000
Npoints = 300;
Zref = linspace(1,par1,Npoints);

    Ck = 10^(-12);  %  1cm lenght of electrodes
    Cgm = 0.2*10^(-12);   % Mutual Capacitance: Sensor - Generator
coupling electrode
    Ckm = 0.4*10^(-12);   % Mutual Capacitance : Sensor  - Conductor
    Cks = 0.005*10^(-12); % Mutual Capacitance : Screen - Conductor
    Ckg = 0.4*10^(-12);   % Mutual Capacitance : Generator coupling
electrode - Conductor

    p = i*2*pi*1*10^6;      % frequency;

    Im_ov_Um = 1/2*(p*Cgm +  p.*Ckm.*p.*Ckg./(p.*(Ckm +  Cks +  Ckg) +
2./Zref));
  figure(3);
    subplot(2,1,1);
  plot (Zref,abs(Im_ov_Um),'b'); grid on;
  title('|Im/Um|  vs. Z');
  %hold on
    subplot(2,1,2);
    plot (Zref,angle(Im_ov_Um)*180/pi,'b'); grid on;
  title('phi(Im/Um) vs. Z');
```

Appendix 9 - MATLAB simulation Simulation with reduced mutual capacitance Cgm between sensor and gen. Couplers

```
function z_testCgm002(par1)%Simulation with reduced mutual capacitance
Cgm between sensor and gen. Couplers
%for running different Z set par1 on 10000 or 1000000
par1=1000000
Npoints = 300;
Zref = linspace(1,par1,Npoints);

    Ck = 10^(-12);  %  1cm lenght of electrodes
    Cgm = 0.002*10^(-12);   % Mutual Capacitance: Sensor - Generator
coupling electrode
    Ckm = 0.4*10^(-12);   % Mutual Capacitance : Sensor  - Conductor
    Cks = 0.005*10^(-12); % Mutual Capacitance : Screen - Conductor
    Ckg = 0.4*10^(-12);   % Mutual Capacitance : Generator coupling
electrode - Conductor
    %Z = Zref(par);
    p = i*2*pi*1*10^6;      % frequency;

    Im_ov_Um = 1/2*(p*Cgm +  p.*Ckm.*p.*Ckg./(p.*(Ckm +  Cks +  Ckg) +
2./Zref));
  figure(3);
    subplot(2,1,1);
    plot (Zref,abs(Im_ov_Um),'b'); grid on; %axis([0,5e-10,0,0.005]);
```

```
  title('|Im/Um| vs. Z');
  %hold on
    subplot(2,1,2);
    plot (Zref,angle(Im_ov_Um)*180/pi,'b'); grid on;
  title('phi(Im/Um) vs. Z');
```

Appendix 10- MATLAB simulation Simulation with reduced capacitance Ckg – increased distance between generator and conductor

```
function z_testCkg01(par1)%Simulation with reduced capacitance Ckg -
increased distance between generator and conductor
%for running different Z set par1 on 10000 or 1000000
par1=1000000
Npoints = 300;
Zref = linspace(1,par1,Npoints);


Ck = 10^(-12);  %  1cm lenght of couplers
Cgm = 0.2*10^(-12);   % Mutual Capacitance: Sensor - Generator coupling
electrode
Ckm = 0.4*10^(-12);   % Mutual Capacitance : Sensor  - Conductor
Cks = 0.005*10^(-12); % Mutual Capacitance : Screen - Conductor
Ckg = 0.1*10^(-12);   % Mutual Capacitance : Generator coupling electrode
- Conductor

    p = i*2*pi*1*10^6;      % frequency;

    Im_ov_Um = 1/2*(p*Cgm +  p.*Ckm.*p.*Ckg./(p.*(Ckm +  Cks +  Ckg) +
2./Zref));

  figure(3);
    subplot(2,1,1);
    plot (Zref,abs(Im_ov_Um),'b'); grid on; %axis([0,5e-10,0,0.005]);
  title('|Im/Um| vs. Z');
    subplot(2,1,2); plot (Zref,angle(Im_ov_Um)*180/pi,'b'); grid on;
title('phi(Im/Um) vs. Z');
```

Appendix 11- MATLAB simulation with signal frequency 5 MHz

```
function z_testCkg015MHz(par1)%Simulation with signal frequency 5 MHz
%for running different Z set par1 on 10000 or 1000000
par1=1000000
Npoints = 300;
Zref = linspace(1,par1,Npoints);

    Ck = 10^(-12);  %  1cm lenght of electrodes
    Cgm = 0.2*10^(-12);   % Mutual Capacitance: Sensor - Generator
coupling electrode
    Ckm = 0.4*10^(-12);   % Mutual Capacitance : Sensor  - Conductor
    Cks = 0.05*10^(-12); % Mutual Capacitance : Screen - Conductor
    Ckg = 0.4*10^(-12);   % Mutual Capacitance : Generator coupling
electrode - Conductor
```

```
    p = i*2*pi*5*10^6;      % frequency;

    Im_ov_Um = 1/2*(p*Cgm +  p.*Ckm.*p.*Ckg./(p.*(Ckm +  Cks +  Ckg) +
2./Zref));

  figure(3);
    subplot(2,1,1);
    plot (Zref,abs(Im_ov_Um),'b'); grid on; %axis([0,5e-10,0,0.005]);
  title('|Im/Um| vs. Z');
  %hold on
    subplot(2,1,2);
    plot (Zref,angle(Im_ov_Um)*180/pi,'b'); grid on;
  title('phi(Im/Um) vs. Z');
```

Appendix 12- MATLAB simulation with large distance between sensor/generator and conductor and 1MHz signal frequency

```
function z_testCkg000001(par1)%Simulation with large distance between
sensor/generator and conductor and 1MHz signal frequency
%for running different Z set par1 on 10000 or 1000000
par1=1000000
Npoints = 300;
Zref = linspace(1,par1,Npoints);

    Ck = 10^(-12);  %  1cm lenght of electrodes
    Cgm = 0.2*10^(-12);   % Mutual Capacitance: Sensor - Generator
coupling electrode
    Ckm = 0.00001*10^(-12); % Mutual Capacitance : Sensor  - Conductor
    Cks = 0.05*10^(-12); % Mutual Capacitance : Screen - Conductor
    Ckg = 0.00001*10^(-12);   % Mutual Capacitance : Generator coupling
electrode - Conductor
    %Z = Zref(par);
    p = i*2*pi*1*10^6;      % frequency;

    Im_ov_Um = 1/2*(p*Cgm +  p.*Ckm.*p.*Ckg./(p.*(Ckm +  Cks +  Ckg) +
2./Zref));

  figure(3);
    subplot(2,1,1);
    plot (Zref,abs(Im_ov_Um),'b'); grid on; %axis([0,5e-10,0,0.005]);
  title('|Im/Um| vs. Z');
  %hold on
    subplot(2,1,2);
    plot (Zref,angle(Im_ov_Um)*180/pi,'b'); grid on;
  title('phi(Im/Um) vs. Z');
```

Appendix 13- MATLAB simulation with large distance between sensor/generator and conductor and 5MHz signal frequency

```
function z_testCkg0000015MHZ(par1)%Simulation with large distance
between sensor/generator and conductor and 1MHz signal frequency
```

```
%for running different Z set par1 on 10000 or 1000000
par1=1000000
Npoints = 300;
Zref = linspace(1,par1,Npoints);

    Ck = 10^(-12);  %  1cm lenght of electrodes
    Cgm = 0.2*10^(-12);   % Mutual Capacitance: Sensor - Generator
coupling electrode
    Ckm = 0.00001*10^(-12); % Mutual Capacitance : Sensor  - Conductor
    Cks = 0.05*10^(-12); % Mutual Capacitance : Screen - Conductor
    Ckg = 0.00001*10^(-12);   % Mutual Capacitance : Generator coupling
electrode - Conductor
    %Z = Zref(par);
    p = i*2*pi*5*10^6;      % frequency;

    Im_ov_Um = 1/2*(p*Cgm +  p.*Ckm.*p.*Ckg./(p.*(Ckm +  Cks +  Ckg) +
2./Zref));

  figure(3);
    subplot(2,1,1);
    plot (Zref,abs(Im_ov_Um),'b'); grid on; %axis([0,5e-10,0,0.005]);
  title('|Im/Um| vs. Z');
  %hold on
    subplot(2,1,2);
    plot (Zref,angle(Im_ov_Um)*180/pi,'b'); grid on;
  title('phi(Im/Um) vs. Z');
```

Appendix 14- MATLAB simulation of solid contact Z=1 mOhm

```
function ckmg_testZ1mOhm(par1)
% par1 in pF!!!
par1=1
Npoints = 300;
Z = 0.01;
Cpar = linspace(0,par1*1e-12,Npoints);
    Ck = 10^(-12);  %  1cm lenght of electrodes
Ckm = Cpar;
  Cgm = 0.2*10^(-12);   % Mutual Capacitance: Sensor - Generator
coupling electrode
%   Ckm = 0.4*10^(-12);   % Mutual Capacitance : Sensor  - Conductor
    Cks = 0.05*10^(-12); % Mutual Capacitance : Screen - Conductor
%   Ckg = 0.1*10^(-12);   % Mutual Capacitance : Generator coupling
electrode - Conductor
Ckg = Cpar;

    p = i*2*pi*1*10^6;      % frequency;

    Im_ov_Um = 1/2*(p*Cgm +  p.*Ckm.*p.*Ckg./(p.*(Ckm +  Cks +  Ckg) +
2./Z));
  figure(3);
    subplot(2,1,1);
    plot (Cpar,abs(Im_ov_Um),'b'); grid on; %axis([0,5e-10,0,0.005]);
```

```
  title('|Im/Um| vs. Ckgm');
  %hold on
    subplot(2,1,2);
    plot (Cpar,angle(Im_ov_Um)*180/pi,'b'); grid on;
  title('phi(Im/Um) vs. Ckgm');
```

Appendix 15- MATLAB simulation of the broken contact Z=1Mohm

```
function ckmg1pF_test1MOhm(par1)%Simulation of the broken contact
Z=1Mohm
par1=1
Npoints = 300;
Z = 1e6;

Cpar = linspace(0,par1*1e-12,Npoints);
    Ck = 10^(-12);  %  1cm lenght of electrodes
Ckm = Cpar;
  Cgm = 0.2*10^(-12);   % Mutual Capacitance: Sensor - Generator
coupling electrode
%   Ckm = 0.4*10^(-12);   % Mutual Capacitance : Sensor  - Conductor
    Cks = 0.05*10^(-12); % Mutual Capacitance : Screen - Conductor
%   Ckg = 0.1*10^(-12);   % Mutual Capacitance : Generator coupling
electrode - Conductor
Ckg = Cpar;

    p = i*2*pi*1*10^6;      % frequency;

    Im_ov_Um = 1/2*(p*Cgm +  p.*Ckm.*p.*Ckg./(p.*(Ckm +  Cks +  Ckg) +
2./Z));
  figure(3);
    subplot(2,1,1);
    plot (Cpar,abs(Im_ov_Um),'b'); grid on; %axis([0,5e-10,0,0.005]);
  title('|Im/Um| vs. Ckgm');
  %hold on
    subplot(2,1,2);
    plot (Cpar,angle(Im_ov_Um)*180/pi,'b'); grid on;
  title('phi(Im/Um) vs. Ckgm');
```

Appendix 16 – Peak=f(f) for measurement without couplers

DDS Frequency (Hz)	MDiv 20MHz/(MDiv+ 1)	Signal frequency before mixer	Signal frequency After mixer	Peak value without sensors
50005	399	50000	5,000	125
60065	332	60060	4,940	145
69935	285	69930	4,930	145
80005	249	80000	5,000	145
90095	221	90090	4,910	135
100005	199	100000	5,000	125
109895	181	109890	4,890	115
119766	166	119760	5,521	105
129875	153	129870	4,870	100
139865	142	139860	4,860	90
150381	132	150376	5,060	85
160005	124	160000	5,000	75
169497	117	169492	5,475	80
180185	110	180180	4,820	80
190482	104	190476	5,810	90
200005	99	200000	5,000	100
210532	94	210526	5,684	110
219786	90	219780	5,780	125
229890	86	229885	4,943	150
240969	82	240964	5,145	165
250005	79	250000	5,000	170
298513	66	298507	5,537	235
444450	44	444444	5,556	365
500005	39	500000	5,000	382
555561	35	555556	5,444	400
606066	32	606061	5,394	395
689660	28	689655	4,828	370
800005	24	800000	5,000	340
909096	21	909091	5,091	320
1000005	19	1E+06	5,000	300
1176476	16	1E+06	5,412	280
1538467	12	2E+06	5,462	270
1818187	10	2E+06	5,182	277
2000005	9	2E+06	5,000	280
2500005	7	3E+06	5,000	277
2857148	6	3E+06	5,143	225
3333338	5	3E+06	4,667	200
4000005	4	4E+06	5,000	180